

In presenting the dissertation as a partial fulfillment of the requirements for an advanced degree from the Georgia Institute of Technology, I agree that the Library of the Institute shall make it available for inspection and circulation in accordance with its regulations governing materials of this type. I agree that permission to copy from, or to publish from, this dissertation may be granted by the professor under whose direction it was written, or, in his absence, by the Dean of the Graduate Division when such copying or publication is solely for scholarly purposes and does not involve potential financial gain. It is understood that any copying from, or publication of, this dissertation which involves potential financial gain will not be allowed without written permission.

7/25/68

MASS SPECTROMETRIC INVESTIGATION OF THE SYNTHESIS
AND MOLECULAR ENERGETICS OF
NITROGEN-OXYGEN-FLUORINE COMPOUNDS

A THESIS

Presented to

The Faculty of the Graduate Division

by

Paul Anthony Sessa

In Partial Fulfillment
of the Requirements for the Degree
Doctor of Philosophy in the
School of Chemical Engineering

Georgia Institute of Technology

December, 1970

MASS SPECTROMETRIC INVESTIGATION OF THE SYNTHESIS
AND MOLECULAR ENERGETICS OF
NITROGEN-OXYGEN-FLUORINE COMPOUNDS

Approved: _____

Chairman: _____

Date approved by Chairman: 12/16/70

ACKNOWLEDGMENTS

The author is grateful to Dr. Henry A. McGee, Jr., for his suggestion of the research problem and his interest and guidance as the work progressed. The suggestions and assistance given by my fellow graduate students, C. T. Kwon, P. Ganguli, and J. K. Holzhauer, are greatly appreciated. I am also indebted to Dr. W. T. Ziegler and Dr. T. F. Moran for their suggestions while serving on the reading committee.

A major part of this research was sponsored by the Air Force Office of Scientific Research through grant AF-AFOSR-1308-67 and the author is most grateful. I am also thankful to the Department of Health, Education, and Welfare for providing me with an NDEA Title IV Fellowship and to the Union Carbide Corporation for their financial assistance.

The encouragement, patience, and understanding of my wife, Marie, and the motivation inspired by my daughter, Jacqueline, are gratefully acknowledged. I would also like to thank my parents, Mr. and Mrs. Samuel P. Sessa, who made my education possible, and my wife's parents, Mr. and Mrs. Ralph Martino, for their encouragement and assistance while in Atlanta.

TABLE OF CONTENTS

	Page
ACKNOWLEDGMENTS	ii
LIST OF TABLES	vi
LIST OF ILLUSTRATIONS	ix
SUMMARY	x
Chapter	
I. INTRODUCTION	1
Brief History and Objectives	
Known N-O-F Compounds	
Nitrosyl Fluoride (ONF)	
Nitryl Fluoride (NO_2F)	
Fluorine Nitrate (NO_3F)	
Nitrosodifluoramine (ONNF_2)	
Trifluoramine Oxide (ONF_3)	
Unconfirmed and Postulated N-O-F Compounds	
II. APPARATUS AND EXPERIMENTAL TECHNIQUE	22
Mass Spectrometer	
Cryogenic Reactor and Analytical Facility	
Synthesis Techniques	
Positive and Negative Ion Mass Spectra	
Appearance Potential Measurements	
III. RESULTS AND DISCUSSION	40
Preparation of Known N-O-F Compounds	
Nitrosyl Fluoride (ONF)	
Nitryl Fluoride (NO_2F)	
Fluorine Nitrate (NO_3F)	
Nitrosodifluoramine (ONNF_2)	
Trifluoramine Oxide (ONF_3)	
Reactions With Dioxygen Difluoride (O_2F_2)	
$\text{O}_2\text{F}_2 + \text{NO}$	
$\text{O}_2\text{F}_2 + \text{NO}_2$	
$\text{O}_2\text{F}_2 + \text{N}_2\text{F}_4$	
$\text{O}_2\text{F}_2 + \text{NH}_3$	
Reactions With Tetrafluorohydrazine (N_2F_4)	
$\text{N}_2\text{F}_4 + \text{NO}_2$	

TABLE OF CONTENTS (Continued)

Chapter	Page
III. (Continued)	
$\text{N}_2\text{F}_4 + \text{O}_2$ $\text{N}_2\text{F}_4 + \text{O}_3$ $\text{N}_2\text{F}_4 + \text{NO}$ Reaction of NF_3 With F_2 Summary and Discussion of Reactions Studied Mass Spectra Positive Ions Negative Ions Appearance Potentials and Molecular Energetics Nitrosyl Fluoride (ONF) Nitryl Fluoride (NO_2F) Fluorine Nitrate (NO_3F) Nitrosodifluoramine (ONNF_2) Trifluoramine Oxide (ONF_3) Nitrodifluoramine (O_2NNF_3) Summary of Results from Appearance Potential Data Bond Dissociation Energies in N-O-F Species	
IV. CONCLUSIONS AND RECOMMENDATIONS	92
APPENDICES	
A. SUMMARY OF BEST LITERATURE VALUES FOR THERMODYNAMIC QUANTITIES OF N-O-F SPECIES	96
B. ELECTRONIC STRUCTURES OF N-O-F COMPOUNDS USING LINNETT'S DOUBLE QUARTET MODEL	104
Introduction ONF and ONF^- NO_2F NO_3F ONNF_2 ONF_3 , ONF_2^+ , and ONF_2 Radical O_2NNF_2 ONNF_2 Dimer and F_2NONNF_2 $\text{F}(\text{O}_2)_n\text{NO}$ and $\text{FO}(\text{O}_2)_n\text{NO}$ O_2NF_2 , F_2NONF_2 , $\text{F}_2\text{NO}_2\text{NF}_2$, and ONNFNFNO F_2NOF , $\text{FN}(\text{OF})_2$ and $\text{N}(\text{OF})_3$ $\text{F}_2\text{NO}_2\text{F}$, $\text{FN}(\text{O}_2\text{F})_2$, and $\text{N}(\text{O}_2\text{F})_3$ NF_5 and F_3NNF_3 Summary and Conclusions	

TABLE OF CONTENTS (Concluded)

	Page
APPENDICES (Continued)	
C. SELECTED IONIZATION EFFICIENCY DATA AND APPEARANCE POTENTIAL DETERMINATIONS BY EVD	139
D. MISCELLANEOUS DATA	151
NOMENCLATURE	158
BIBLIOGRAPHY	161
VITA	169

LIST OF TABLES

Table	Page
1. Mass Spectrum of ONF_3 by Electron Impact at 70 eV	14
2. Mass Spectrum of ONF_3 by Photon Impact	14
3. Properties of N-O-F Compounds	15
4. Families of Predicted N-O-F Compounds	19
5. Experimental Appearance Potential Techniques	34
6. Summary of Preparations of Previously Known N-O-F Compounds	55
7. Summary of Reactions with Dioxygen Difluoride (O_2F_2) . .	56
8. Summary of Reactions with Tetrafluorohydrazine (N_2F_4) . .	58
9. Positive Ion Mass Spectra of N-O-F Compounds	60
10. Negative Ion Mass Spectra of N-O-F Compounds	63
11. Vapor Pressures of N-O-F Compounds	64
12. Appearance Potentials of Nitrosyl Fluoride (ONF)	66
13. Appearance Potentials of Nitryl Fluoride (NO_2F)	69
14. Appearance Potentials of Fluorine Nitrate (NO_3F)	74
15. Appearance Potentials of Nitrosodifluoramine (ONNF_2) . .	79
16. Appearance Potentials of Nitrodifluoramine (O_2NNF_2) . .	83
17. Summary of Thermodynamic Quantities Derived from Appearance Potential Data	88
18. Bond Dissociation Energies at 298°K in N-O-F Species . .	90
19. Best Literature Values of Standard Heats of Formation . .	100
20. Best Literature Values of Ionization Potentials	102
21. Best Literature Values of Electron Affinities	103
22. Formal Charge Limitations	105

LIST OF TABLES (Continued)

Table		Page
23.	Formal Charges in ONF	107
24.	Formal Charges in ONF ⁻	110
25.	Formal Charges in NO ₂ F	111
26.	Formal Charges in NO ₃ F	113
27.	Formal Charges in ONNF ₂	115
28.	Formal Charges in ONF ₃	117
29.	Formal Charges in O ₂ NNF ₂	120
30.	Formal Charges in (RNO) ₂	121
31.	Formal Charges in F ₂ NONNF ₂	123
32.	Formal Charges in FO ₂ NO	125
33.	Formal Charges in FONO	126
34.	Formal Charges in FOO ₂ NO	127
35.	Formal Charges in O ₂ NF ₂	128
36.	Formal Charges in F ₂ NONF ₂	129
37.	Formal Charges in F ₂ NO ₂ NF ₂	130
38.	Formal Charges in ONNFNFNO	131
39.	Formal Charges in F ₂ NOF	132
40.	Formal Charges in FN(OF) ₂	133
41.	Formal Charges in N(OF) ₃	134
42.	Summary of Predicted Existences of Postulated N-O-F Species Based Upon Linnett's Double Quartet Model , . .	138
43.	Temperature Corresponding to Vapor Pressures of One Torr for Compounds Observed in N-O-F Experiments	152
44.	Positive Ion Mass Spectra of NO, NO ₂ , N ₂ O and N ₂ F ₂ . .	154
45.	Positive Ion Mass Spectra of NF ₃ , N ₂ F ₄ , OF ₂ and O ₂ F ₂ . .	155

LIST OF TABLES (Concluded)

Table	Page
46. Positive Ion Mass Spectra of SiF_4 and NH_3	156
47. Positive Ion Mass Spectra of SF_6 and CF_3Cl	157

LIST OF ILLUSTRATIONS

Figure	Page
1. Glass Electric Discharge Reactor	27
2. Metal Electric Discharge Reactor	28
3. Radio Frequency Discharge Reactor	29
4. Glass Capillary Pyrolysis Reactor	30
5. Calibration of Furnace Attachment for Pyrolysis Reactor .	31
6. Diagram of the Potential Energy Curves for the General Diatomic Species AB and AB^+ Comparing the Vertical and Adiabatic Ionization Potentials	37
7. Ionization Efficiency Data for NO_2F^+ from NO_2F with Argon as Standard	141
8. Ionization Efficiency Data for NO_2^+ from O_2NNF_2 with Argon as Standard	142
9. Appearance Potential Determination of NO_2F^+ from NO_2F and NO_2^+ from O_2NNF_2 By EVD	143
10. Ionization Efficiency Data for ONF_2^+ from ONF_3 with Argon as Standard	144
11. Ionization Efficiency Data for NO^+ from $ONNF_2$ with Argon as Standard	145
12. Appearance Potential Determination of ONF_2^+ from ONF_3 and NO^+ from $ONNF_2$ by EVD	146
13. Ionization Efficiency Data for NF^+ from $ONNF_2$ with Argon as Standard	147
14. Appearance Potential Determination of NF^+ from $ONNF_2$ by EVD	148
15. Ionization Efficiency Data for O^+ from NO_2F with Argon as Standard	149
16. Appearance Potential Determination of O^+ from NO_2F by EVD	150

SUMMARY

This thesis has been concerned with the mass spectrometric investigation of the synthesis and molecular energetics of nitrogen-oxygen-fluorine compounds. In the last ten or fifteen years a great amount of interest has been generated in the field of N-O-F compounds due to their possible use as high energy oxidizers. There are five previously known N-O-F compounds: nitrosyl fluoride (ONF), nitryl fluoride (NO_2F), fluorine nitrate (NO_3F), nitrosodifluoramine (ONNF_2), and trifluoramine oxide (ONF_3). However, the literature contains mass spectrometric data on only one of these, ONF_3 . The main objectives of this thesis were to prepare and identify the five known N-O-F compounds using the mass spectrometer, to attempt to prepare new N-O-F compounds, and to calculate heats of formation of N-O-F species from appearance potential data.

The five known N-O-F compounds were prepared according to methods published in the literature. Nitrosyl fluoride, nitryl fluoride and fluorine nitrate were prepared by reacting fluorine gas with nitric oxide (NO), sodium nitrite (NaNO_2), and potassium nitrate (KNO_3), respectively. Nitrosodifluoramine, an unstable purple substance, was prepared by passing a mixture of nitric oxide and tetrafluorohydrazine (N_2F_4) through a glass capillary at 310°C followed by a fast quench at -196°C . Trifluoramine oxide was most readily prepared by an electric discharge of nitrogen trifluoride (NF_3) with oxygen difluoride (OF_2) at -183 or -196°C .

The search for new N-O-F compounds was centered around the use of dioxygen difluoride (O_2F_2) as a potential source of OF or O_2F radicals

and tetrafluorohydrazine as a source of NF_2 radicals. The reactions of O_2F_2 with NO , NO_2 , N_2F_4 , and NH_3 produced no evidence for any new N-O-F compounds. The addition of NO or NO_2 to O_2F_2 at -183°C produced both ONF and NO_2F plus some side products. The addition of N_2F_4 to O_2F_2 at -183 to -155°C produced no reaction, but an electric discharge of this mixture at -155°C produced NF_3 , F_2 , N_2 , and O_2 . The addition of diluted NH_3 to O_2F_2 at -196°C produced a rapid reaction (with occasional flashes) to give NO_2 , HF and SiF_4 .

The reactions of N_2F_4 with NO_2 , O_2 , O_3 , and NO were studied. The room temperature addition of NO_2 to N_2F_4 caused decomposition to NF_3 and other stable products. However, the pyrolysis of N_2F_4 at 310°C and the subsequent addition of NO_2 with a fast quench at -196°C resulted in the formation of a previously unidentified compound, nitrodifluoramine (O_2NNF_2). This compound is a white solid at -196°C and decomposes slowly to N_2F_4 and NO_2 even at -130°C . The pyrolysis of N_2F_4 and O_2 at 310°C produced no reaction. The pyrolysis of N_2F_4 with subsequent quenching onto a thin film of O_3 at -196°C produced a vigorous reaction (once a violent explosion) to form all the known N-O-F compounds, but no evidence was obtained for any new compound. The trapping at -196°C of a room temperature mixture of N_2F_4 and NO produced small amounts of red-brown and purple solids. The purple substance was identified as ONNF_2 . However, the red-brown substance decomposed between -183 and -168°C before it could exert a sufficiently high vapor pressure to be detected in the mass spectrometer. Since the red-brown substance resulted from the reversible reaction of NO with either N_2F_4 or NF_2 , then the only likely possibilities were F_2NONNF_2 and $(\text{ONNF}_2)_2$. On the basis of the

discussion of the electronic structures of these molecules, the red-brown substance was attributed to F_2NONNF_2 .

The positive and approximate negative ion mass spectra were obtained for all six N-O-F compounds. These spectra were all uniquely different. Although the parent molecular ions were usually absent and most positive ions containing F were usually of low intensity, the identification of each compound was straightforward. The cryogenic inlet system of the mass spectrometer was essential in analyzing the unstable compounds ONNF_2 and O_2NNF_2 .

The temperatures at which the vapor pressures of ONNF_2 and O_2NNF_2 are one torr were estimated to be $-141 \pm 2^\circ\text{C}$ and $-123 \pm 2^\circ\text{C}$ by comparison with the known vapor pressures of 0.1-0.2 torr for ONF_3 , NO_2F , NO_3F , and ONF .

The appearance potentials were measured for most of the positive ions of the six N-O-F compounds. These were compared to the appearance potentials of the attributed ion-source processes calculated from the best literature values of heats of formation, ionization potentials and electron affinities. The experimental appearance potentials were of varying quality. In general, the high intensity ions resulted in good or excellent appearance potentials, whereas the low intensity ions gave poor or fair data. The molecular energetics of the N-O-F compounds were derived from those appearance potentials rated as either good or excellent.

The heat of formation of ONF was derived to be -0.90 ± 0.10 eV (compared to the literature value of -0.68 eV) from the $A(\text{NO}^+)_{\text{exptl.}}$ of 8.33 eV which was attributed to the process



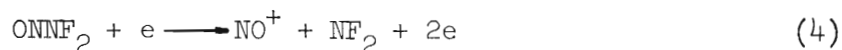
The heat of formation of NO_2F was derived to be -1.46 ± 0.12 eV (compared to the literature value of -1.12 eV) from $A(\text{NO}_2^+)_{\text{exptl.}}$ of 13.49 eV, which was attributed to



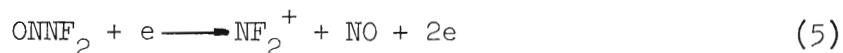
The heat of formation of OF was derived to be $+1.40 \pm 0.10$ eV (compared to the literature values of $+1.26$ eV) from $A(\text{NO}_2^+)_{\text{exptl.}}$ of 12.62 eV which was attributed to



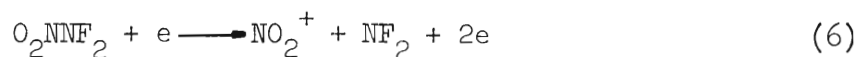
The heat of formation of ONNF_2 was derived to be $+0.49 \pm 0.13$ eV (compared to the literature value of $+0.82$ eV) from $A(\text{NO}^+)_{\text{exptl.}}$ of 10.08 and $A(\text{NF}_2^+)_{\text{exptl.}}$ of 12.81 eV which were attributed to the following respective processes



and

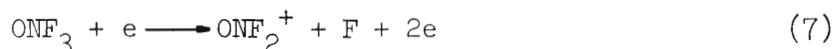


The heat of formation of the new compound O_2NNF_2 was derived to be 0.00 ± 0.11 eV from $A(\text{NO}_2^+)_{\text{exptl.}}$ of 11.71 eV which was attributed to

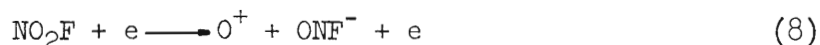


The ionization potential of NO_2F was directly measured to be 13.15 ± 0.12 eV. The lower limits of the ionization potentials of ONF , NO_3F ,

ONNF_2 , and O_2NNF_2 were estimated to be 11.78, 12.62, 10.08, and 11.71 eV, respectively. The appearance potential of ONF_2^+ for the process



was measured to be 14.15 eV. Combining this with Dibeler and Walker's photoionization value of 13.59 eV⁷⁰ led to $I_{\text{vert.}} - I_{\text{adaib.}}(\text{ONF}_2) = 0.56$ eV. This relatively high value is not surprising since ONF_2^+ is planar whereas ONF_3 is nearly tetrahedral. The electron affinity of ONF was estimated to be 2.69 eV from $A(\text{O}^+)_{\text{exptl.}}$ from NO_2F of 14.06 ± 0.28 eV which was attributed to the process



An extensive list of the bond dissociation energies at 298°K in N-O-F species was tabulated. These values were calculated from the quantities derived in this thesis and other thermodynamic values from the literature.

On the basis of evidence found in this thesis pure O_2F_2 is a yellow solid at low temperatures rather than an orange or yellow-orange solid as previously thought.

The Linnett Double Quartet Model was used to construct stable electronic configurations for the known species ONF, NO_2F , NO_3F , ONNF_2 , ONF_3 , O_2NNF_2 , the ONF_2 radical, and the ONF^- and ONF_2^+ ions. The Double Quartet Model was also used to propose the most likely structures of a wide variety of postulated N-O-F species and to draw approximate conclusions regarding their likely existence. The compounds F_2NONNF_2 , FO_2NO , FONO , ONNFNFNO , and $\text{F}_{3-n}\text{N}(\text{OF})_n$ ($n = 1, 2, 3$) were shown to have marginal stabilities, which suggests the possible isolation of these species

in the future. The compounds $(\text{ONNF}_2)_2$, FOO_2NO , O_2NF_2 , F_2NONF_2 , $\text{F}_2\text{NO}_2\text{NF}_2$, and $\text{F}_{3-n}\text{N}(\text{O}_2\text{F})_n$ ($n = 1, 2, 3$) were shown to be unlikely. It was impossible to construct any plausible covalent structures for NF_5 and F_3NNF_3 .

CHAPTER I

INTRODUCTION

Brief History and Objectives

In the last ten to fifteen years a tremendous effort has been put forth by government agencies, private companies, and universities for the development of high performance rocket propellants. Today, even though research funds are more difficult to acquire, interest is still at a very high level. Any break-throughs in the area of propellants would give a vigorous boost to the present Apollo program, the Mars landing experiments of the 1970's and especially to future interplanetary travel.

Extensive treatments of the theory of propellant energetics and types of propulsion systems can be found elsewhere¹⁻⁵. In general, the performance of a propellant is rated by its specific impulse, I_{sp} , which is defined as follows:

$$I_{sp} = \frac{\text{thrust produced}}{\text{mass ejected per second}} \quad (1)$$

If several approximations are made, it can be shown that

$$I_{sp} = c \left(\frac{T}{M} \right)^{\frac{1}{2}} \quad (2)$$

where T is the flame temperature in the combustion chamber, M is the mean molecular weight of the exhaust gases, and c is a constant. Thus, it can be seen from Eq. 2 that an ideal propellant, either fuel plus

oxidizer or monopropellant alone, would undergo a highly exothermic reaction to give low molecular weight products.

There are many different propulsion systems in use today and postulated for the future⁵. Among these are conventional chemical systems, nuclear and thermonuclear rockets, ion rockets, free radical devices, plasmajets, electromagnetic plasma accelerators, and even "solar sailboats." Of these, the conventional chemical propellants have the lowest specific impulse (300-400 sec), but they are of great importance since they are the only system which produces thrusts high enough to propel a space vehicle out of the Earth's gravitational pull.

Several nitrogen-oxygen-fluorine compounds have been known for almost half a century. This knowledge, however, was rather limited and only of academic interest until the potential of such compounds as propellants was recognized in the 1950's^{6,7}. Since then very thorough studies have been made in this field since thermodynamics predicts^{4,8} that the search for new and improved oxidizers should be directed toward the development of new compounds consisting of nitrogen, oxygen, and fluorine atoms. Oxygen and fluorine would form very strong bonds with low molecular weight fuels, while nitrogen would serve as a carrier atom.

This thesis is mainly concerned with the synthesis and mass spectrometric study of nitrogen-oxygen-fluorine compounds. The ultimate goal is the synthesis of new N-O-F compounds, some of which may be used as high energy oxidizers. Dioxygen difluoride (O_2F_2) and tetrafluorohydrazine (N_2F_4) will be used as reagents in searching for new N-O-F compounds in a majority of the experiments.

The search for and identification of new N-O-F compounds in the

mass spectrometer assumes that the known compounds can be readily identified. There are five N-O-F compounds reported in the literature: nitrosyl fluoride (ONF), nitryl fluoride (NO_2F), fluorine nitrate (NO_3F), nitrosodifluoramine (ONNF_2), and trifluoramine oxide (ONF_3). Mass spectrometric data on these compounds are virtually nonexistent, except for ONF_3 , as will be seen in the next section. Thus, a secondary, but essential, goal of this thesis is the preparation of the five known N-O-F compounds and their characterization in the mass spectrometer.

Heats of formation of the N-O-F compounds will be determined from appearance potential data. These will be compared to literature values whenever possible. Also, the electronic structures of the known and postulated N-O-F species will be discussed using Linnett's Double Quartet Model.

Known N-O-F Compounds

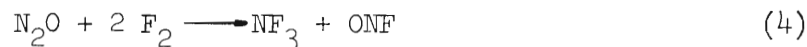
Nitrosyl Fluoride (ONF)

Extensive reviews on nitrosyl fluoride have appeared elsewhere⁸⁻¹¹. This compound was discovered in 1905 by Ruff and Stauber¹² who passed nitrosyl chloride through a platinum tube containing silver fluoride at 200-225°C. Ruff later discovered¹³ that ONF can be conveniently formed by the highly exothermic gas phase reaction of nitric oxide and fluorine according to

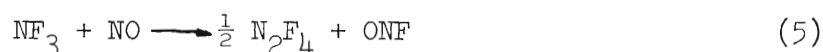


A detailed description of the numerous preparations of ONF can be found in the above reviews. However, a few of the more important methods are:

1) the reaction of nitrous oxide and fluorine at 700°C



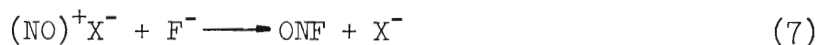
2) the reaction of nitrogen trifluoride and nitric oxide at 600°C and atmospheric pressure



3) the reaction of tetrafluorohydrazine with nitrates, such as



and 4) the reaction of some readily accessible nitrosyl salts with alkali fluorides at 200-300°C according to



where X^- is $(\text{BF}_4)^-$, $(\text{SbF}_6)^-$, or $(\text{S}_2\text{O}_7)^{2-}$.

Nitrosyl fluoride is colorless in the solid, liquid, and gaseous states. It is a strong oxidizing agent, but it is distinctly less reactive than elemental fluorine. It readily attacks quartz and glass, even at -196°C, to form dinitronium hexafluorosilicate, $(\text{NO}_2)_2\text{SiF}_6$, a white flaky material which dissociates at room temperature. It attacks metals in varying degrees, but can be easily handled in passivated copper or nickel systems. It is thermally stable up to at least 300°C in pre-fluorinated metal vessels¹⁴.

The structure of ONF has been determined from its ir¹⁵⁻¹⁹ and microwave^{16,20,21} spectra. Accordingly, it is a bent unsymmetric molecule

with N the central atom. The structural parameters were initially calculated as an O-N-F bond angle of 110° and F-N and O-N bond distances of 1.52 and 1.13 Å, respectively²⁰. These values were recently refined to be $110^\circ 5' \pm 10'$, 1.512 ± 0.005 Å, and 1.136 ± 0.003 Å, respectively²¹.

The only determination of the heat of formation of nitrosyl fluoride²² employed a steady flow calorimeter to measure the heat of reaction for



From the measured value of -74.8 kcal./mole for the heat of reaction of Eq. 8, ΔH_f° of ONF was calculated to be -15.8 kcal./mole. Thermodynamic functions of the ideal gas have been calculated between 273.16°K and 1500°K using the rigid rotator, harmonic oscillator approximation²³.

Nielsen and coworkers²⁴ claimed to have observed ONF in a time-of-flight mass spectrometer, however, they did not present its identifying fragmentation pattern.

Some properties of nitrosyl fluoride are listed in Table 3.

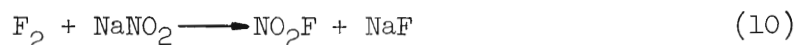
Nitryl Fluoride (NO_2F)

Nitryl fluoride has been well reviewed⁸⁻¹¹. It was first prepared and characterized in 1929 by Ruff²⁵ by the highly exothermic gas phase reaction of fluorine and nitrogen dioxide according to

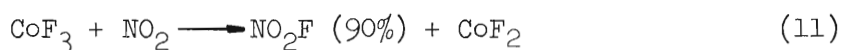


A particularly convenient method of preparation produces almost quantitative yields of nitryl fluoride from the reaction of sodium nitrite and

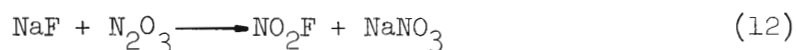
fluorine at room temperature,²⁶



Other important methods include: 1) the oxidation of nitrogen dioxide with cobalt trifluoride,²⁷



and 2) the reaction of N_2O_3 with sodium fluoride,²⁸



Nitryl fluoride, a colorless compound, is extremely reactive and can function as a fluorinating, oxidizing, or nitrating agent. On contact with most substances it is even more reactive than nitrosyl fluoride⁹. However, it attacks glass only at elevated temperatures to form $(\text{NO}_2)_2\text{SiF}_6$ ²⁶. Numerous reactions involving nitryl fluoride can be found in the above reviews. It is known to be stable up to at least 300°C ²⁶.

The structure of NO_2F has been well determined by its ^{19}F -nmr,²⁸ microwave,²⁹⁻³¹ and vibrational (both ir and Raman)^{32,33} spectra. It is a planar molecule of C_{2v} symmetry with N as the central atom. The structural parameters were first obtained by Smith and Magnuson²⁹ based upon their microwave data. They assumed an O-N-O angle of 125° and calculated F-N and O-N bond distances of 1.35 and $1.23 \overset{\circ}{\text{A}}$, respectively. Using the same data Clayton and coworkers³⁴ revised the calculations by making the more reasonable assumption that the O-N-O angles in both NO_2F and NO_2Cl were equal (129.5°). They calculated F-N and O-N distances

of 1.40 and 1.21 Å, respectively. However, recently Legon and Millen's investigation³⁰ of the microwave spectrum of the isotopic species of nitryl fluoride showed that the nitro-group parameters are significantly different from those of nitryl chloride and nitric acid. They calculated an O-N-O angle of $136^\circ \pm 1.5^\circ$ and F-N and O-N bond distances of 1.467 ± 0.015 and 1.1798 ± 0.0035 Å, respectively. Thermodynamic functions of the ideal gas from 100 to 1500°K and force constants have been recalculated³³ which considerably change earlier tabulations³⁵⁻³⁷.

The heat of formation of NO_2F was reported to be 26 kcal./mole based on a heat of hydrolysis of 31 kcal./mole³⁸. The heat of reaction of Eq. 9 at 298°K was measured to be -27.1 ± 2 kcal./mole using a flow calorimeter from which the heat of formation of NO_2F was calculated to be -19 ± 2 kcal./mole³⁹. However, these values were later corrected due to the presence of N_2O_4 , and -33.9 and -25.8 ± 2 kcal./mole were obtained for the above heat of reaction and heat of formation, respectively⁴⁰. Evidently, Hetherington and Robinson³⁸ omitted the negative sign in reporting their value of 26 kcal./mole.

It has been reported that nitryl fluoride had been observed in a mass spectrometer, but no data were given^{24,41}.

Some properties of nitryl fluoride appear in Table 3.

Fluorine Nitrate (NO_3F)

Fluorine nitrate (also known as nitroxy fluoride, nitryl oxyfluoride, or nitryl hypofluorite) was discovered in 1934 by Cady⁴² who bubbled fluorine gas, heavily diluted with air, through concentrated nitric acid. His work was beset with explosions of the fluorine nitrate during its

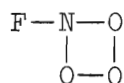
preparation. Ruff and Kwasnick⁴³ noted that the risk of the explosions was somewhat reduced if pure fluorine gas and 100 percent nitric acid was used. A more convenient method was developed by Yost and Beerbower⁴⁴ who readily obtained NO_3F by passing fluorine gas over solid potassium nitrate, according to



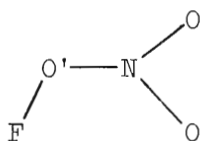
Their yields were essentially quantitative. The reaction of fluorine gas with sodium nitrate (similar to Eq. 13) also gives quantitative yields of NO_3F ³⁹. Varying amounts of NO_3F can also be produced by reacting OF_2 with NO_2 ⁴⁵.

Fluorine nitrate is a colorless compound which is dangerously explosive in the gas, liquid, and solid states, even at liquid air temperatures⁴²⁻⁴⁴. Reviews listing a variety of reactions of NO_3F can be found elsewhere^{10,11}. In general, NO_3F is a powerful oxidizing agent which explodes on contact with many organic compounds, such as ethyl alcohol, ether, and aniline. However, it does not attack Pyrex, quartz, copper, brass, steel, or iron⁴³.

Based upon parachor studies,⁴⁶ NO_3F was proposed to have the following cyclic structure:

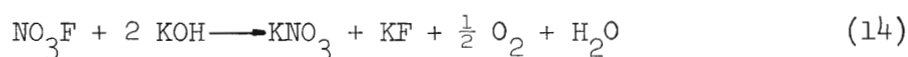


Shortly thereafter, an electron diffraction study⁴⁷ yielded the following structure,



with F-O', O'-N and O-N bond lengths of 1.42, 1.39 and 1.29 Å, respectively, and F-O'-N and O-N-O angles of 105 and 125°, respectively. It was assumed that the FO'-N plane was perpendicular to the -NO₃ plane. Recently it has been determined that the C atom in methyl nitrate is coplanar with the nitro group,⁴⁸ and that nitric acid is also planar⁴⁹. Consequently, Miller and coworkers⁵⁰ concluded that the similarly structured NO₃F should also be planar. The ir spectrum of NO₃F has been reported⁵⁰⁻⁵² and it suggests the planar structure of C_s symmetry as above. Thermodynamic functions of NO₃F in the ideal gas state have been calculated from 100-1500° K.⁵⁰

The heat of formation of NO₃F at 21°C was determined by measuring the heat of reaction of



in an adiabatic calorimeter⁵³ and yielded $\Delta H_f = -4.2 \pm 0.9$ kcal./mole. Breazeale and MacLaren⁴⁰ determined the heat of formation to be $+2.5 \pm 0.6$ kcal./mole based upon results from an adiabatic calorimetric investigation of the synthesis reaction of NO₃F from F₂ and NaNO₂. This latter value has been accepted by the JANAF Tables⁵⁴ as the best value.

The decomposition of fluorine nitrate has been studied⁵¹. Spark induced explosive decompositions resulted in the production of ONF and O₂, but the slow thermal decomposition proceeded according to



The half life of this reaction at 107° was about thirty minutes. The activation energy for the rate determining step



was determined to be 29.7 kcal./mole⁵¹. This value is actually a measure of the upper limit of the O-F bond dissociation energy in NO_3F .

No mass spectrometric data for NO_3F are available in the literature. Lawless and Smith⁸ incorrectly state that the mass spectrum of NO_3F was reported by Anderson and MacLaren⁴¹.

Several properties of fluorine nitrate are listed in Table 3.

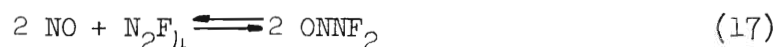
Nitrosodifluoramine (ONNF_2)

In 1962 Colburn and Johnson⁵⁵ obtained evidence for the substance nitrosodifluoramine. They passed a 10/1 mixture of $\text{NO}/\text{N}_2\text{F}_4$ through a hot capillary at 300°C and allowed the products to impinge on a glass finger at -196°C . A dark purple deposit formed, which was purified by pumping away excess NO at -183°C . The substance decomposed to essentially all N_2F_4 and NO when warmed to room temperature. They reported the ^{19}F -nmr spectrum and absorption spectrum of the new compound, which they observed to decompose even at -70°C . The dark purple color of ONNF_2 is present in the solid, liquid, and gaseous states.

The dissociation of tetrafluorohydrazine (N_2F_4) to difluoramine radicals (NF_2) has been well studied⁵⁶. At 25°C and one atmosphere pressure the equilibrium NF_2 concentration is 0.05 percent. The radical concentration increases to 90 percent at 300°C and 1 atm., at 150°C and

1 torr, or at 25°C and 10^{-10} atm. Thus, under the above experimental conditions of Colburn and Johnson, ONNF_2 was formed by the direct combination of NO and NF_2 radicals.

In a later article Johnson and Colburn⁵⁷ studied the gas phase equilibrium



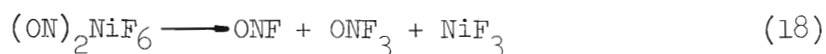
by measuring the absorption spectra of mixtures of NO and N_2F_4 at room temperature. In none of their experiments did the concentration of ONNF_2 exceed 0.1 percent. From their data they calculated the heat of reaction of Eq. 17 to be -0.4 ± 0.2 kcal./mole of N_2F_4 and the heat of formation of ONNF_2 to be 20.4 ± 1.4 kcal./mole. Using the more recent value of -5 kcal./mole for $\Delta H_f^\circ(298)(\text{N}_2\text{F}_4)$ (see Table 19), one recalculates Johnson and Colburn's value of $\Delta H_f^\circ(298)(\text{ONNF}_2)$ to be 18.9 ± 1.4 kcal./mole.

It is interesting to note that Johnson and Colburn are the only investigators who have reported the isolation of ONNF_2 , although some ambiguous evidence for its existence has appeared elsewhere⁵⁸.

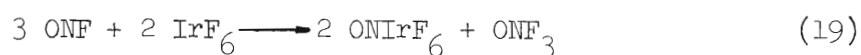
Trifluoramine Oxide (ONF_3)

Trifluoramine oxide is the most recent member of the known N-O-F compounds to be reported in the literature. The discovery of ONF_3 was reported independently in 1966 and 1967 by Bartlett and coworkers and by scientists at Rocketdyne and Allied Chemical. The Rocketdyne scientists⁵⁹ reported that ONF_3 could be prepared by an electric discharge at -196°C of a 1/1 air-fluorine mixture. The Allied Chemical group prepared ONF_3 by an electric discharge of NF_3 and O_2 or OF_2 to give 10-15 percent

yields^{60,61} and by the reaction of ONF and F₂ at 350°C and almost 5000 psig⁶². Bartlett and coworkers^{63,64} first observed ONF₃ as a trace product in the reaction of ONF with PtF₆ and OsF₆. They later found⁶⁵ that it could be obtained in good yield by: 1) the pyrolysis of nitrosyl hexafluoronickelate(IV) in fluorine, according to



or by 2) the interaction of nitrosyl fluoride with iridium hexafluoride,



ONF₃ is thermally stable up to 300°C in a nickel or Monel vessel. It is relatively inert, not attacking glass, many metals, and even water at room temperature. It is a strong oxidizing agent, but it requires a rather high activation energy to undergo thermodynamically favorable reactions. The mode of oxidation by ONF₃ usually involves fluorination rather than oxygenation⁶⁰.

The structure of ONF₃ has been determined to be very nearly tetrahedral with C_{3v} symmetry based upon its ir,^{59,60,65,66} ¹⁹F-nmr,^{60,65,66} ¹⁴N-nmr,⁶⁷ Raman,⁶⁸ and microwave⁶⁹ spectra. The only determination of the structural parameters of ONF₃ was made by Curtis and coworkers⁵⁹. Based upon their ir data, they assumed tetrahedral angles (109.5°) and an O-N bond distance of 1.15 Å and calculated a F-N bond distance of 1.48 Å.

The mass spectrum of ONF₃ has been reported by two groups of authors. Fox and coworkers⁶⁶ obtained the positive ion mass spectrum of ONF₃ in a Consolidated Electrodynamics Model 21-202 spectrometer

operating at 70 eV (see Table 1). Dibeler and coworkers⁷⁰ studied ONF_3 using the monoenergetic photon impact method (see Table 2). From their data and known heats of formation, they were able to derive $\Delta H_f^\circ(\text{ONF}_3) = -3.02 \text{ eV} (-69.6 \text{ kcal./mole})$, $D(\text{O}-\text{NF}_3) = 4.3 \text{ eV}$, and $D(\text{ONF}_2-\text{F}) = 1.9 \text{ eV}$. The spectra of Tables 1 and 2 differ significantly because the ionizing energy of the latter was not sufficiently high to produce additional fragment ions.

An independent determination of the heat of formation of ONF_3 was reported from studies of the equilibrium⁷¹



as a function of temperature ($260 - 370^\circ\text{C}$) and pressure ($100 - 350 \text{ atm.}$). The result was $\Delta H_f^\circ(\text{ONF}_3) = -34.1 \pm 0.5 \text{ kcal./mole}$.

In recent patents obtained by Allied Chemical,^{72,73} ONF_3 is claimed to be useful as an oxidizer ingredient in missile fuels.

Several properties of ONF_3 are listed in Table 3.

Unconfirmed and Postulated N-O-F Compounds

Very few predictions are reported in the literature concerning new types of compounds comprised of nitrogen, oxygen and fluorine atoms. In 1966 Spratley and Pimentel⁷⁴ developed a bonding model which explained the weak F-N bond in ONF and weak O-F bond in O_2F_2 and also furnished predictions for a host of new compounds. They explained the unusual bonding in ONF and O_2F_2 as resulting from the electron sharing in the antibonding π^* orbitals of the parent molecules, NO and O_2 . In each case, a weak bond is formed with an atom of high electronegativity, such

Table 1. Mass Spectrum of ONF_3 By Electron Impact at 70 eV^a

m/e	Ion	Rel. Abund. (%)	m/e	Ion	Rel. Abund. (%)
14	N^+	12.5	33	FN^+	4.1
16	O^+	3.7	49	FNO^+	1.6
19	F^+	9.8	52	F_2N^+	1.3
24.5	FNO^{2+}	0.8	68	F_2NO^+	78.1
30	NO^+	100.0	87	F_3NO^+	0.2

^aData from Fox, et al.,⁶⁶Table 2. Mass Spectrum of ONF_3 By Photon Impact^a

Ion Process	Ion	m/e	Rel. Abund. @ 21.22 eV	Appearance Potential (eV)
$\text{ONF}_3 + h\nu \rightarrow \text{NO}^+ + 3\text{F} + e$	30	NO^+	55.0	15.21 ± 0.02
$\rightarrow \text{ONF}_2^+ + \text{F} + e$	68	ONF_2^+	100.0	13.59 ± 0.01
$\rightarrow \text{ONF}_3^+ + e$	87	ONF_3^+	0.3	13.26 ± 0.01

^aData from Dibeler and Walker⁷⁰

Table 3. Properties of N-O-F Compounds

Property	ONF		NO ₂ F		NO ₃ F		ONNF ₂		ONF ₃	
	Value	Ref.	Value	Ref.	Value	Ref.	Value	Ref.	Value	Ref.
Melting pt. (°C)	-132.5	13	-166.0	13,38	-181	46	>-183 <-140	55	-160	60
Boiling pt. (°C)	-59.9	13	-72.4	13,38	-45.9	43	--	--	-85	60
Temp. @vap. pres. of 1 torr (°C)	-132	13	-144	13,38	-133	43	--	--	-157	66
Heat of formation (kcal./mole)	-15.8	22	(-)26 -25.8	38 40	-4.2	53	+18.9 ^a	57	-69.6 -34.1	70 71
Heat of vaporiza- tion (kcal./mole)	4.6	13	4.32	13	4.726	43	--	--	3.85	66
Trouton constant (cal./deg.mole)	21.6	13	21.5	13	20.8	43	--	--	20.7	66
Critical temp. (°C)	--		--		67.2	43	--	--	29.5	66
Critical pres. (atm)	--		--		--		--	--	63.5	66
Bond lengths (Å)	F-N 1.512	21	F-N 1.467	30	O-N 1.29				F-N 1.48 ^b	59
	O-N 1.136		O-N 1.1798		O'-N 1.39	47	--	--	O-N 1.15 ^b	
			F-O 1.42							

Table 3. Properties of N-O-F Compounds (Continued)

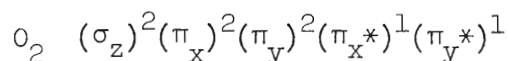
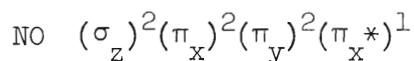
Property	ONF		NO ₂ F		NO ₃ F		ONNF ₂		ONF ₃	
	Value	Ref.	Value	Ref.	Value	Ref.	Value	Ref.	Value	Ref.
Bond angles (deg.)	O-N-F 110° 5'	21	O-N-O 136° O-N-F 105°	30	O-N-O 125° N-O'-F 105°	47	--		O-N-F 109.5° ^{ob} F-N-F 109.5° ^{ob}	59
Dipole moment (Debyes)	1.81	20	0.466	30	--		--		0.0390	69

^aRevised from 20.4 kcal./mole using the most recent value of $H_f^O(N_2F_4)$

^bAssumed

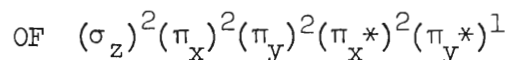
as F, and the parent molecule is little affected.

They represented the simplified molecular orbital description of the orbital occupancies of NO and O₂ as



Thus, NO has one singly occupied antibonding π^* orbital available, which consists of a planar four-lobe distribution, and O₂ has two such singly occupied π^* orbitals, oriented in two perpendicular planes. Consequently, in ONF a fluorine atom can overlap with one of the lobes of the π_x^* orbital of NO, and in O₂F₂ one F atom can overlap with a π_x^* lobe and another F atom with a π_y^* lobe of O₂ at the opposite ends of the molecule to reduce repulsion effects. The highly electronegative F atom releases very little electron density and therefore forms weak F-N or O-F bonds in these molecules. Spratley and Pimentel denote these types of bonds as (p- π^*) σ and (s- π^*) σ bonds.

Spratley and Pimentel concluded that NO and O₂ might take the role of the fluorine atom in similar compounds since the effect on either NO or O₂ is slight as fluorine bonds to it and thus the three species must have comparable electron-attracting power. Also, they surmised that OF might substitute for NO and O₂ since the simple MO description predicts a 1.5 bond order and an orbital occupancy as follows



Thus, OF has a singly occupied π^* orbital which can accept electrons to form weak bonds, as do NO and O_2 .

From these conclusions, Spratley and Pimental postulated the existence of several families of compounds which include $F(O_2)_nF$, $F(O_2)_nOF$, $FO(O_2)_nOF$, $F(O_2)_n$, $FO(O_2)_n$, $ON(O_2)_nNO$, $F(O_2)_nNO$, $FO(O_2)_nNO$, and $ON(O_2)_n$. This research is particularly concerned with the second and third to last families since they are N-O-F compounds. The first several members of these families are listed in Table 4. It is interesting to note that nitrosyl fluoride (ONF) exists in the form given in Table 4, but nitryl fluoride (NO_2F) and fluorine nitrate (NO_3F) exist in different isomeric forms.

In a study of "superoxidizers" in 1961 Martinez and coworkers⁵⁸ obtained evidence for blue and red colored low temperature complexes from their reactions of N_2F_4 with O, O_2 , O_3 , NO, and NO_2 . They suggested compounds of the type NF_2O_2 , NF_2OONF_2 , $NO \cdot N_2F_4$ (or $NONF_2$) and $NO_2 \cdot N_2F_4$ (or NO_2NF_2). They also postulated an intermediate species $ONNFNFNO$ which decomposes to F, N_2 , and NO in the ratio 2:1:2. However, they were unable to identify any of the unstable colored materials. Since then the dark purple, unstable $ONNF_2$ has been discovered⁵⁵. Also, this thesis research has confirmed the existence of $ONNF_2$ and identified the new compound O_2NNF_2 .

In 1967 Miller and coworkers⁷⁵ obtained questionable evidence for a new, unstable nitrogen-fluorine compound from the fission-fragment radiolysis (produced by neutron irradiation of fully enriched UF_4) of a mixture of NF_3 and F_2 . Their gas chromatograph evidence indicated a boiling point near $-50^\circ C$. Results from mass spectrometry showed a peak

Table 4. Families of Predicted N-O-F Compounds^a

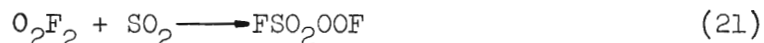
	$F(O_2)_n NO$	$FO(O_2)_n NO$
$n = 0$	$\begin{array}{c} N \equiv O \\ \\ F \\ FNO \end{array}$	$\begin{array}{c} N \equiv O \\ \\ F - O \\ FNO_2 \end{array}$
$n = 2$	$\begin{array}{c} O = O \\ \quad \\ F \quad N \equiv O \\ FNO_3 \end{array}$	$\begin{array}{c} O = O \\ \quad \\ F - O \quad N \equiv O \\ FNO_4 \end{array}$
$n = 3$	$\begin{array}{c} O = O \quad O \equiv O \\ \quad \quad \\ F \quad O \quad N \equiv O \\ FNO_5 \end{array}$	$\begin{array}{c} O = O \quad O \equiv O \quad O \equiv O \\ \quad \quad \quad \\ F \quad O \quad O \quad N \equiv O \\ FNO_6 \end{array}$

^aTaken from Spratley and Pimentel⁷⁴

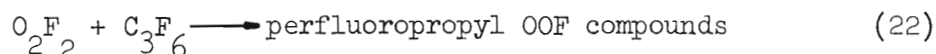
at $m/e = 90$, which would correspond to NF_4^+ . They suggested the new compound might be NF_5 or F_3NNF_3 , of which they claimed to have made 1-10 micromoles. This compound is not a member of the N-O-F family, but it is included here because of its close relation as a high energy oxidizer.

In their review of high energy oxidizers, Lawless and Smith⁸ stated that attempts by several laboratories to produce compounds of the type $\text{N}(\text{OF})_3$ and NF_2OF had failed. Although this comprehensive review was not "classified", the authors had access to many results which came from classified sources and unpublished reports from many private companies. It seems safe to assume, as others have done,¹¹ that much of the relevant information in this area still remains classified.

This research employed N_2F_4 and O_2F_2 as reagents in a majority of experiments attempting to produce N-O-F compounds. The importance of N_2F_4 , which easily forms NF_2 radicals, in the search for new N-O-F compounds is evident from the preceding discussion in this chapter. O_2F_2 will be used as a potential source of O_2F radicals. Even though O_2F_2 is a very reactive fluorinating agent, Solomon and coworkers⁷⁶⁻⁷⁸ have demonstrated that under controlled conditions it is also a source of O_2F radicals. They showed 1) that the O_2F radical can be transferred to SO_2 in the reaction



2) that O_2F_2 reacts with C_3F_6 as follows



and 3) that the reaction of O_2F_2 and BF_3 can be explained in terms of the O_2F radical.

CHAPTER II

APPARATUS AND EXPERIMENTAL TECHNIQUE

Mass Spectrometer

The major piece of apparatus used in this thesis was a Bendix Model 14-107 time-of-flight (TOF) mass spectrometer. Analysis by mass spectrometry has several advantages over other conventional methods such as nuclear magnetic resonance (nmr), infrared (ir), electron paramagnetic resonance (epr), and Raman spectroscopy. One important feature of the mass spectrometer is that the output data (mass spectra) are obtained quickly and are usually readily interpreted. Other types of spectroscopic methods have become fairly routine, but they still require an expert in that particular field for interpretation. Also, the mass spectrometer can analyze for very small quantities of a material, as long as it exerts a vapor pressure of 10^{-4} to 10^{-5} torr⁷⁹ and can be separated from other substances present by means of their different volatilities. Most important, though, is that the mass spectrometer is readily adaptable for low temperature analysis of unstable species. This adaptation, denoted cryochemical reactor and analytical facility, is described below.

A disadvantage of the mass spectrometer is that quite often the molecular positive ion of a substance containing F atoms is not observable and other fragment ions frequently have low intensities. This is due to the high electronegativity of F and its reluctance to give up an

an electron. Also, the structure of a molecule cannot be determined on the basis of mass spectrometric data.

Cryogenic Reactor and Analytical Facility

A generalized cryochemical reaction system would involve four steps: 1) activation of a parent substance or mixture to produce free radicals, excited species, or other highly reactive intermediates; 2) fast quenching of products in a cryogenic reactor; 3) purification; and 4) analysis. It is essential that the purification and analysis in the mass spectrometer be performed without previous warm-up to avoid the decomposition of any unstable species which may be present.

The apparatus used in this thesis to perform the above operations is denoted as "cryogenic reactor and analytical facility," designed, built, and described in detail by Holzhauer and McGee⁸⁰.

The refrigerant used in this work consisted of a 65/35 weight percent mixture of isopentane/2-methyl pentane which freezes at -168°C and boils at 35°C . In a typical experiment, reaction products were quenched in a reactor immersed in a one liter dewar of either liquid N_2 (-196°C) or liquid O_2 (-183°C). Upon completion of the reaction, the one liter Dewar was quickly replaced by a 21 cm I.D. Dewar filled with liquid N_2 to allow for precooling of the suspended components of the facility. After several minutes the liquid N_2 Dewar was removed and quickly replaced by another large Dewar containing the refrigerant mixture near its freezing point. Even though this Dewar exchange took about five seconds, no rapid decompositions or explosions ever occurred, even in the case of condensed ozone. The temperature gap from liquid O_2 to

to the freezing point of the refrigerant (-183 to -168°C) did not prove to be troublesome since none of the compounds of interest were pumped away at these temperatures. However, some difficulty was encountered in maintaining the refrigerant temperature between -168 and -165°C during the analysis of ONF_3 due to the increased viscosity of the refrigerant mixture near its freezing point.

During the controlled warm-up and analysis, the pressure within the reactor, which was continuously pumped, was monitored by a Vacuum-Electronics Corp. model #DG2-2T thermocouple gage located in the pump-out line immediately downstream from the reactor. The optimum reactor pressure for observation and appearance potential determination of a particular species was determined to be approximately 0.1-0.2 torr. At lower pressures the sensitivity was too low; at higher pressures the products were pumped away too quickly.

Another important feature of the cryochemical reactor and analytical facility is that it is readily adaptable to many synthesis techniques. The arrangement of the facility permits interchange of reactors in a minimum of time since only one soldered connection is required between the inlet valve and the reactor. The various reactors, whether Pyrex glass or metal, were connected to the all copper tubing vacuum manifold system by means of Cajon Ultra Torr O-ring couplings and Whitey brass valves with Teflon packings and Swagelock fittings. The pump-out line of the vacuum system contained a soda lime trap, with optional bypass, to protect the pump oil from fluorine gas. System pressures were monitored by a thermocouple gage (1-1000 μ), a Hg manometer protected by a layer of Kel-F oil (1-50 torr), and by standard dial pressure gages (30 in. vac. to 15 psig).

Synthesis Techniques

Several general synthesis techniques were used in this thesis to investigate the N-O-F compounds. These included: 1) electric discharge, as in the preparations of O_2F_2 and ONF_3 ; 2) radio frequency discharge, which proved to be rather unsuccessful; 3) pyrolysis, as in the preparations of $ONNF_2$ and O_2NNF_2 ; and 4) chemical activation, as in ONF , NO_2F , and NO_3F .

In the electric discharge experiments, power was supplied by a variable high voltage 60-cycle transformer (neon sign type) with a 15,000 ohm power resistor in series. In the Pyrex glass reactor of Figure 1, the glow discharge occurs between the two copper wire electrodes. In the metal reactor of Figure 2, the discharge is established between the center electrode and the grounded cold walls of the reactor. The enlarged cross section in the metal reactor prevents the discharge from occurring near the Teflon insulator.

The radio frequency (rf) discharge experiments were conducted in the apparatus of Figure 3. Power was supplied to a 67-turn, 1-1/8 in. O.D. copper antenna wire coil by means of a Hallicrafters model HT-4B radio transmitter which operated at about 3.5 MHz and had a maximum power output of 320 watts. An impedance matching network⁸¹ was used to match the impedance of the transmitter to that of the plasma and thus attain maximum power transfer.

The glass pyrolysis apparatus is shown in Figure 4. The reactor is the same as in Figure 1, only the electrodes have been removed and replaced by the furnace attachment. The 1-mm I.D. capillary furnace is 15 in. long and is heated over a 4.5 in. length by a 15 ohm wire heater

made of 28-gage bare nickel chromium wire which is secured to the outside of the capillary by Sauereisen Electrotemp Cement No. 8. The exit of the capillary is just below the top of the wide portion of the reactor. The furnace was calibrated at atmospheric pressure by inserting a copper-constantan thermocouple into the heated segment of the capillary and recording the input voltage to the heater versus temperature. These results are plotted in Figure 5.

The experiments involving only chemical activation were characterized by a high negative heat of reaction. In the gas-gas reaction of F_2 and NO to form ONF, the reactants were bled from separate storage vessels ($P = 2-20$ psia) into a room temperature $\frac{1}{4}$ in. copper tube at low pressure (0.2-2.0 torr) where they reacted to form ONF. The products were then pumped through a trap immersed in liquid nitrogen. In the gas-solid reactions to form NO_2F and NO_3F , the F_2 gas was pumped over a bed of powdered $NaNO_2$ and KNO_3 , respectively. The solid $NaNO_2$ and KNO_3 were contained in a $\frac{3}{4}$ in. O.D. Pyrex tube which was connected to the vacuum system with O-ring couplings. The products were then pumped through a liquid N_2 trap connected to the cryogenic analytical facility. Two types of traps were used in these experiments. One was an all glass trap, as in Figure 1, but with the electrodes removed. The other was an all metal U-tube constructed of $\frac{1}{2}$ in. O.D. Monel tubing silver soldered to copper couplings. These particular gas-gas and gas-solid reaction techniques are not useful for preparing unstable species since only the room temperature reaction products are condensed.

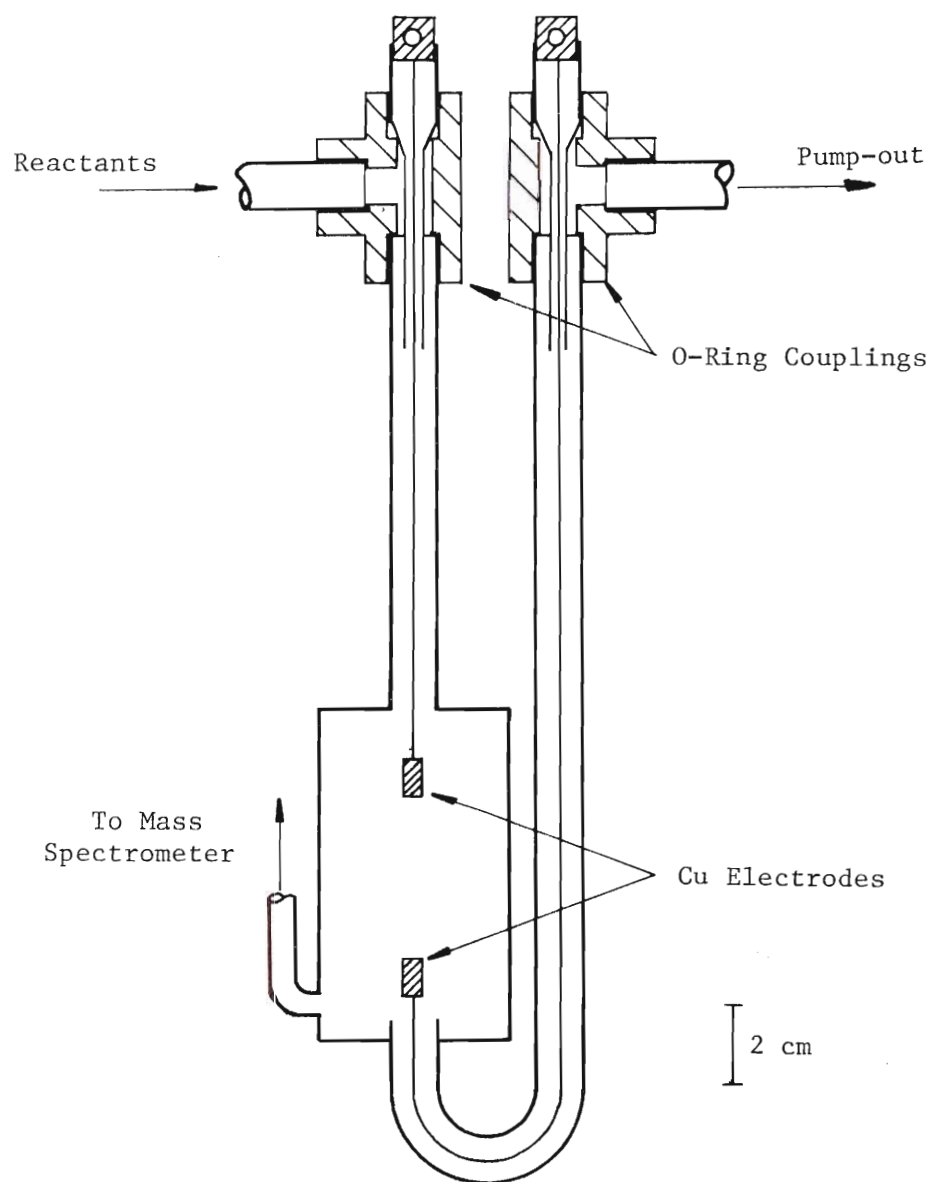


Figure 1. Glass Electric Discharge Reactor

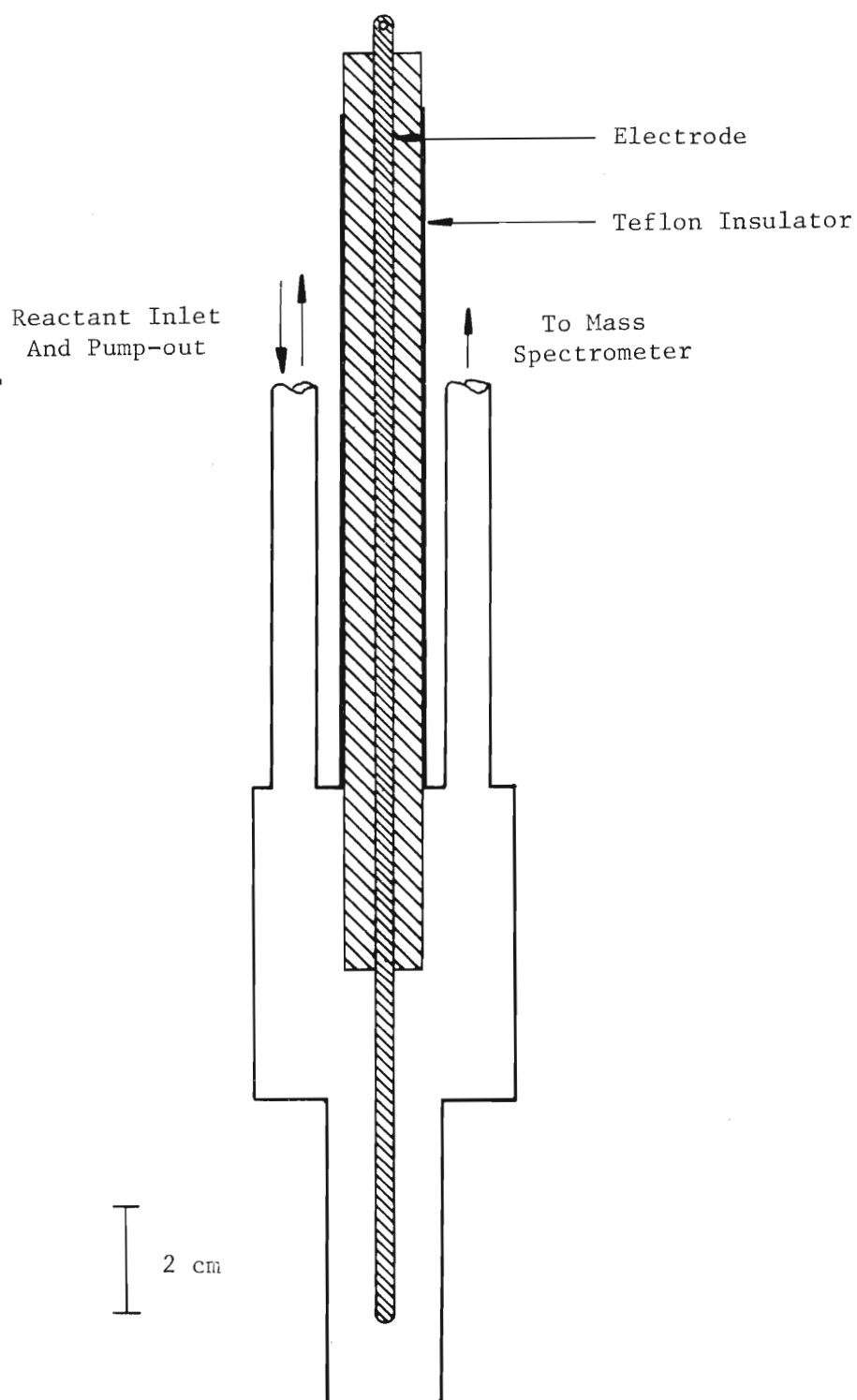


Figure 2. Metal Discharge Reactor

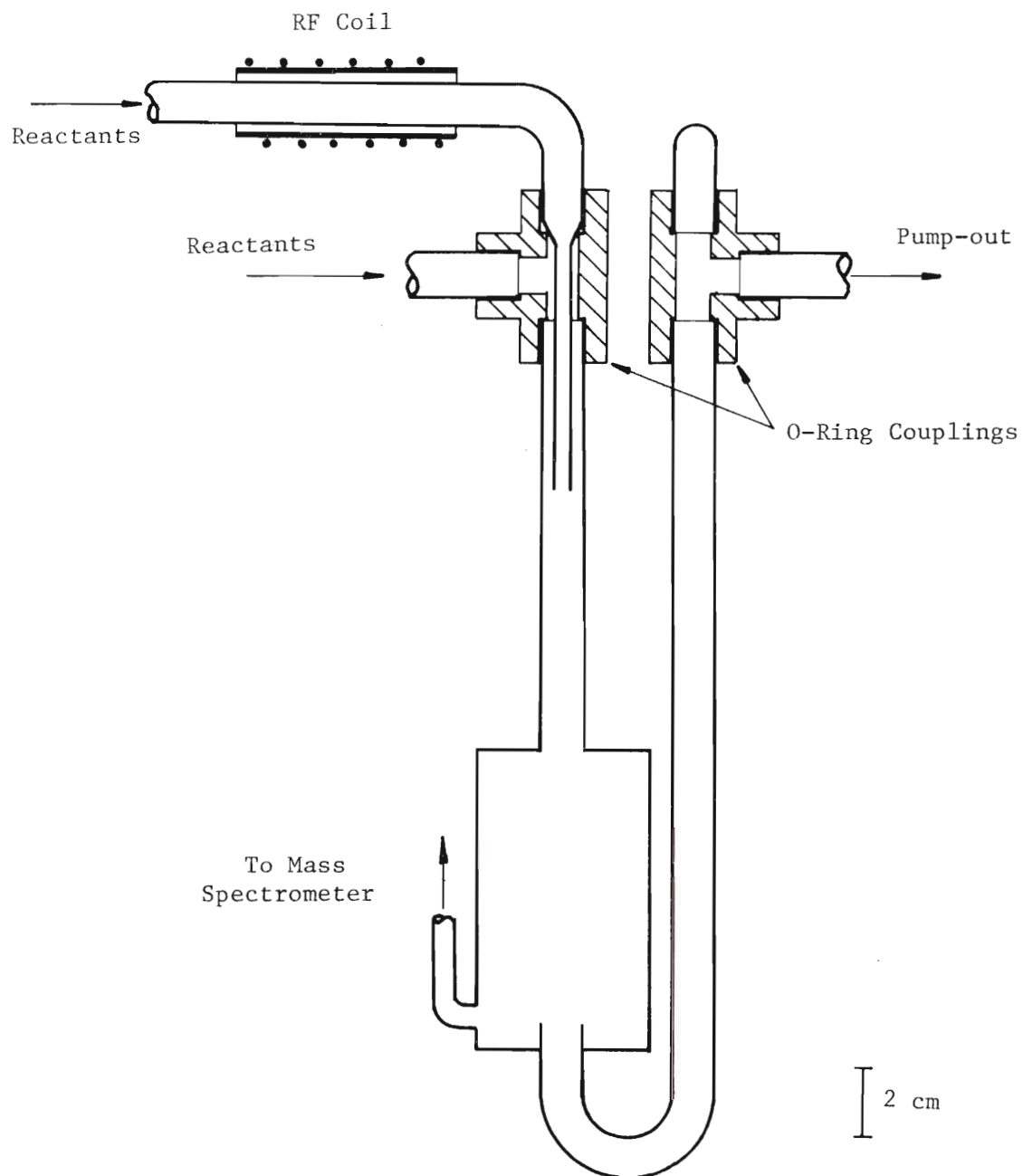


Figure 3. Radio Frequency Discharge Reactor

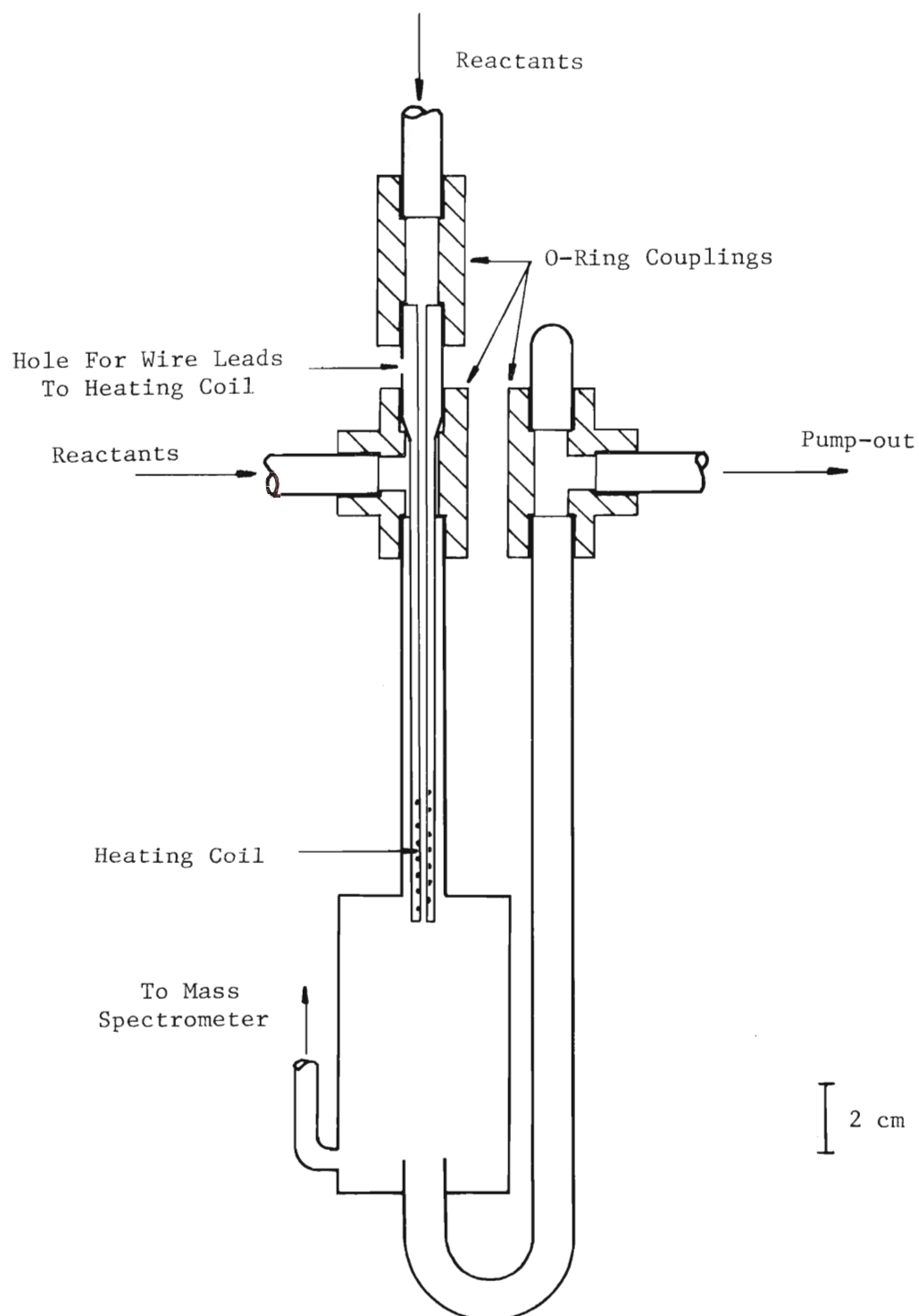


Figure 4. Glass Capillary Pyrolysis Reactor

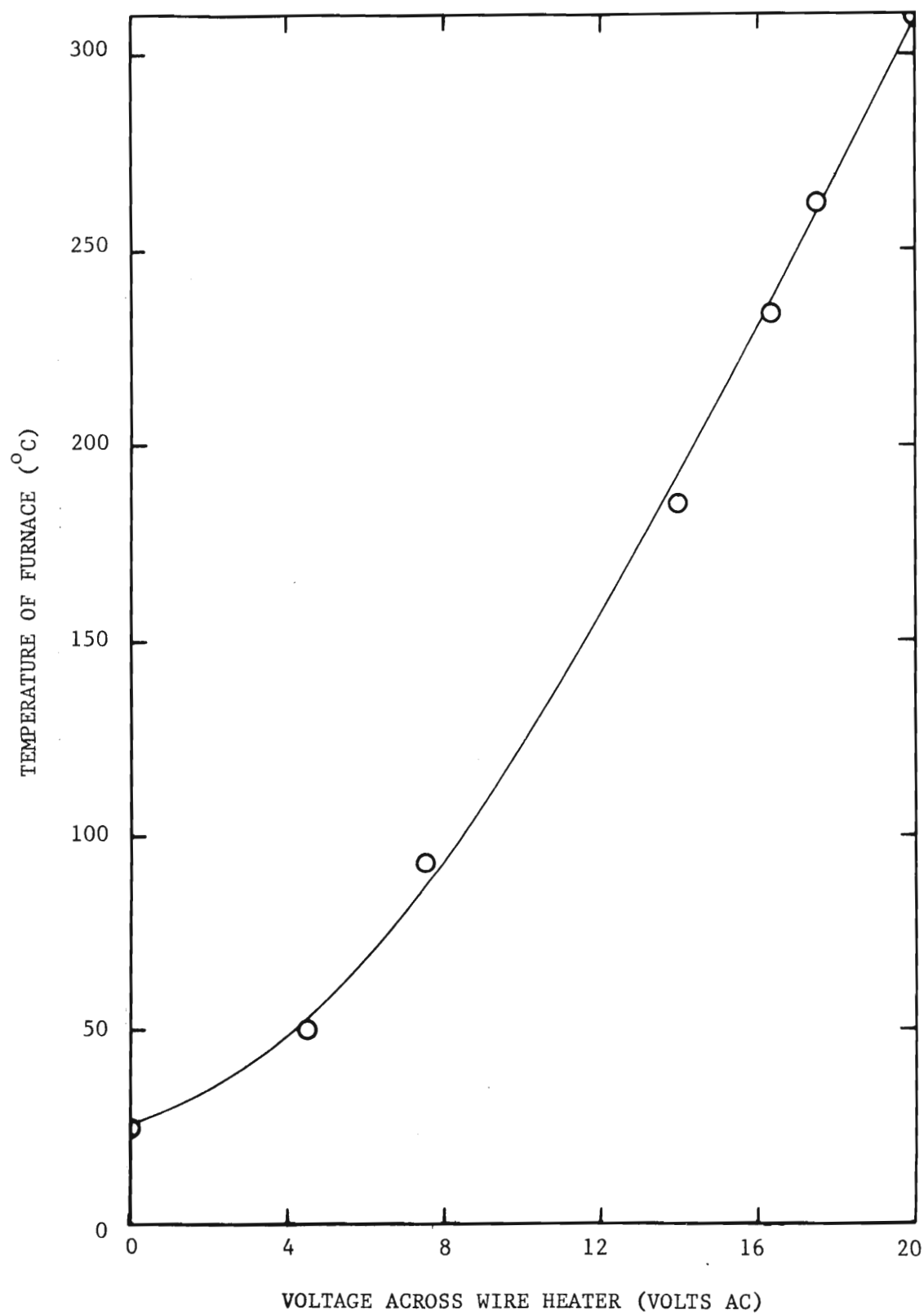


Figure 5. Calibration of Furnace Attachment For Pyrolysis Reactor

Positive and Negative Ion Mass Spectra

Positive ion mass spectra were recorded on a Hewlett-Packard Moseley 7002B X-Y recorder in conjunction with a Hewlett-Packard Moseley 17108A External Time Base, and visually observed on a Tektronix Type 547 oscilloscope. Unambiguous mass assignments were easily made up to $m/e = 100$ using as reference peaks from the ever present N_2 , O_2 , and H_2O . The ionizing voltage of the spectrometer was maintained at 70 eV during the recording of all positive ion spectra. Mass spectra of several miscellaneous compounds encountered in this work are reported in Appendix D.

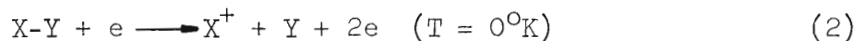
Unfortunately, the Bendix 14-107 mass spectrometer is not adapted to record negative ion spectra. However, negative ions could be displayed on the oscilloscope, but with the distinct disadvantage that the maximum ion current intensities sometimes produced only barely discernible mass peaks even at very high ion source pressures (10^{-6} torr). The intensity of each negative ion mass peak was estimated at the ionizing voltage yielding the maximum intensity. Consequently, the negative ion spectra of the N-O-F compounds reported in the text are of a very approximate nature. Mass assignments were easily made since F^- was usually the most abundant negative ion present due to its high electronegativity.

Appearance Potential Measurements

The appearance potential (AP) of an ion is defined as the least amount of energy required to produce that ion in a given ion process where the reactants and products are ideal gases in their ground states at $0^\circ K$. Since $\Delta(PV)$ is negligible for an ion-source reaction, then

$$AP = \Delta E = \Delta H - \Delta(PV) \approx \Delta H_r \quad (1)$$

Thus, $A(X^+)$ from X-Y is the heat of reaction for



The differences in heats of reaction at 298° and $0^\circ K$ are sufficiently small in comparison to experimental errors in appearance potentials so that the AP is usually taken as the heat of reaction at $298^\circ K$. Thus, AP's can be combined with known standard heats of formation to calculate unknown heats of formation and bond dissociation energies (D).

It is not the purpose of this work to give a critical analysis of all the methods of determining appearance potentials. In their comprehensive listing of appearance potential data of positive ions up to June 1966, Franklin and coworkers⁸² listed the various methods available and their estimated precisions. Table 5 shows their results along with references describing each method. A detailed discussion of factors affecting the reliability of AP data can be found elsewhere⁸³⁻⁸⁵.

In general, electron impact methods suffer from lack of an absolute energy scale and from a wide energy spread in the electron beam. Thus, a calibrating gas, usually argon, must be used to fix the energy scale with the assumption that the ionization cross-sections of argon and of the ion under study are similar.

The extrapolated voltage difference (EVD) method developed by Warren⁸⁶ was chosen to be used in this thesis because of its fairly good accuracy, speed in plotting of data on the X-Y recorder, and ease in interpretation. The RPD method is the only electron impact method of higher precision, but the data taken by others in this laboratory^{79,87} and several preliminary trials by this author showed this method to be

Table 5. Experimental Appearance Potential Techniques^a

Abbre- viation	Method	Ref.	Estimated Precision in Measurement of AP of	
			Parent Ion (eV)	Fragment Ion (eV)
S	Optical spectroscopy	88	0.01	--
PI	Photoionization	89,90	0.01	0.05
EM	Electron monochromator	91,92	0.05	0.05
RPD ^b	Retarding potential difference	93,94	0.05	0.1
PE	Photoelectron spectroscopy	95	0.1	--
SI	Surface ionization	96	0.1	--
EVD ^{b,c}	Extrapolated voltage difference	83,86,97	0.2	0.3
CS ^b	Critical slope	98	0.2	0.3
SL ^b	Semi-log plot	97,99	0.2	0.3
FDP ^b	First differential plot	100	0.2	0.3
MSD ^b	Morrison 2nd differential plot	100	0.2	0.3
VC ^b	Vanishing current or initial break	83,97	0.2	0.3
VDF ^b	Voltage difference at fixed % of standard ion current	99,101	0.3	0.4
EC ^b	Energy compensation	97,101	0.3	0.5
LE ^{b,c}	Linear extrapolation	83,97	0.4	0.5

^aFrom Franklin et al⁸².^bApplicable to electron impact^cMethods used in this work

rather unreliable for the RPD arrangement used therein.

The procedure used for the EVD method is as follows. The ionization efficiency (IE) curve of the ion under study is plotted directly on the X-Y recorder for the first several electron volts above the onset of ionization. The IE curve for argon, which is introduced into the ion source simultaneously with the sample gas, is then plotted with the intensity of the curve adjusted electronically so that the two curves are nearly parallel. The trap and filament currents in the ion source are automatically held constant, usually at 0.02 microamps and 3.5 amps, respectively. The voltage difference between the two curves is then plotted versus ion intensity and extrapolated to zero intensity. This difference is used to calculate the appearance potential of the ion based upon the ionization potential of argon of 15.76 eV.

The above method works fine when applied to an ion whose IE curve results from only one ion-source process. This is usually the case for parent molecular ions and some major fragment ions. However, for many fragment ions, especially those of low intensity, the IE curves are usually "long-tailed" and arise from two or more ion-source processes of differing but close threshold energies. The method used by this author to measure the AP's due to these competing processes is as follows. The AP of lowest energy is measured by increasing the instrumental sensitivity and applying the usual EVD technique. If the intensity of the IE curve at maximum sensitivity is still too low or if the signal-to-noise ratio is so low that the EVD method becomes meaningless, then the linear intercept (LI) method is used to approximate the lowest energy AP. The AP of next higher threshold energy is then determined by subtracting from

the IE curve the linearly increasing contribution from the ion-source process of lower energy and then applying the EVD technique to the resulting curve.

In the following chapter the individual AP's of the N-O-F compounds are given and rated as excellent, good, fair, or poor, depending upon the nature of the IE curves and quality of the EVD fit with argon. In Appendix C several typical IE curves are presented which demonstrate the above techniques and the wide variation in the quality of the raw data.

Electron impact measurements of appearance potentials may be slightly high due to the Frank-Condon Principle, which qualitatively states that there is no change in the internuclear coordinates for a molecule or fragment during its ionization by electron impact due to the small mass of the electron. Thus, if the equilibrium configuration of the ion differs considerably from that of the neutral molecule, the amount of energy required for ionization will be greater than the adiabatic, or minimum, value. Transitions which follow the Frank-Condon Principle are called vertical transitions. Spectroscopic and photoionization measurements can usually yield adiabatic values. Figure 6 shows the qualitative difference between the vertical and adiabatic ionization potentials of a general diatomic molecule. For most appearance potentials this difference is quite small (0-0.2 eV), but for large changes in internuclear coordinates, such as in NO_2 and ONF_2 (to be discussed in a later section), the difference may be 0.5-1.0 eV.

Stevenson¹⁰² has formulated an empirical rule that where a molecule can dissociate by two processes:

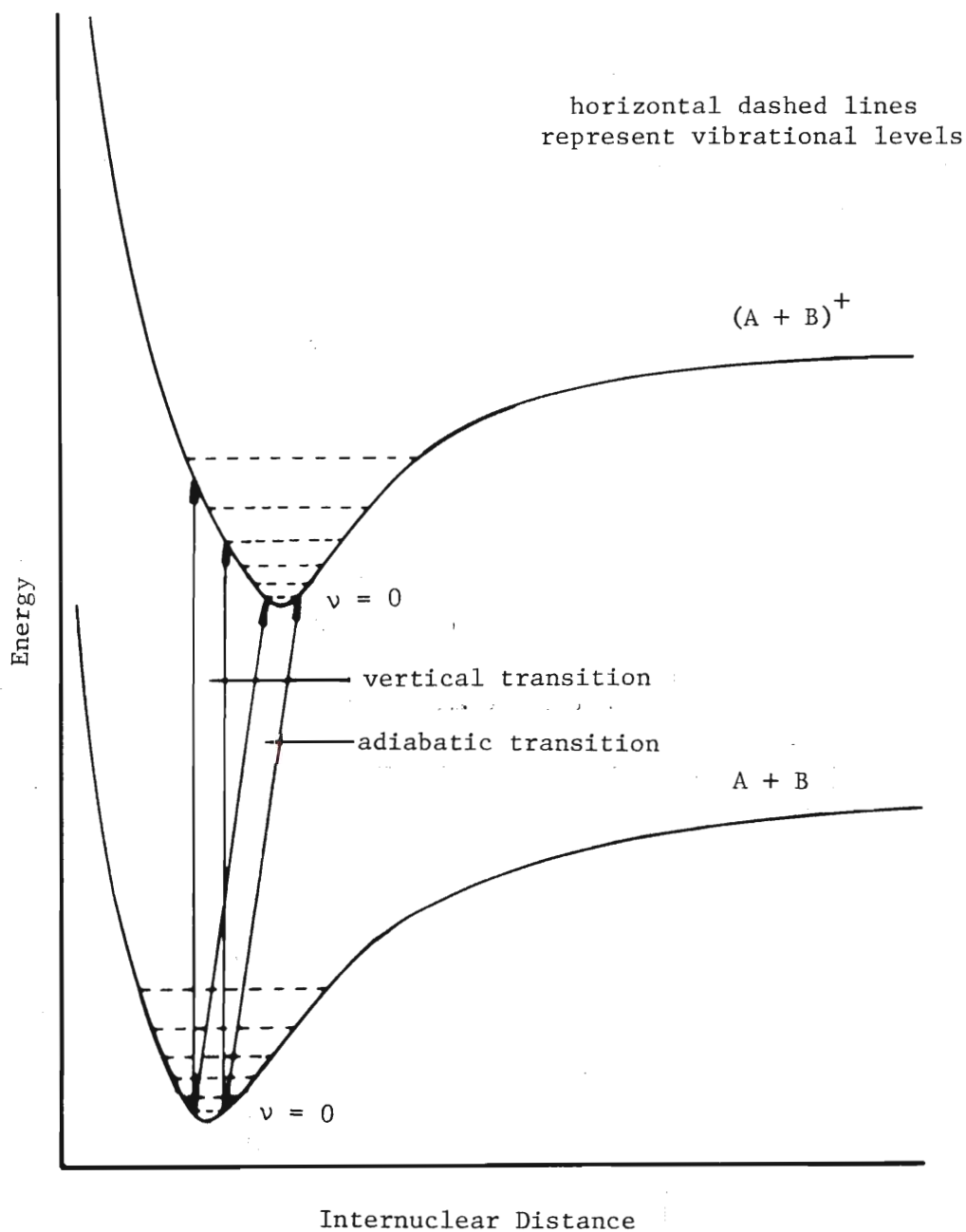


Figure 6. Diagram Of The Potential Energy Curves For The General Diatomic Species AB And AB^+ Comparing The Vertical And Adiabatic Ionization Potentials



the radicals R_1^+ and R_2 will be produced (Eq. 3) in their lowest states or without excess kinetic energy only when the ionization potential of R_1 is less than that of R_2 . Although there is no theoretical explanation for this, it has been found to hold in almost all cases. Thus, it allows the bond dissociation energy to be calculated from the appearance potential of the ion with the lower ionization potential.

Franklin¹⁰³ has developed a technique to detect and measure kinetic energies of fragment ions. Also, he has correlated the total excess energy E^* with the experimentally measured excess translational energy of the fragments \bar{e}_t , according to

$$\bar{e}_t = \frac{E^*}{\alpha N} \quad (5)$$

where α is an arbitrary parameter shown to be constant for a large number of molecules, and N is the number of classical oscillators in the molecule. Holt¹⁰⁵ has applied this technique to the three membered ring compounds cyclopropane, cyclopropanone, cyclopropene, and cyclobutanone. The major drawback of this technique is that it requires a very rough extrapolation of the excess translational energy near the appearance potential of the ion where the data tend to scatter over a wide range. The probability of excess energy increases with the number of bonds broken. Therefore, appearance potentials reported in this work, upon which the energetics of the N-O-F compounds are derived, are not expected to contain much

excess energy because they involve the cleavage of only one bond. The Franklin method of calculating excess energies was not used in this study.

CHAPTER III

RESULTS AND DISCUSSION

Preparation of Known N-O-F CompoundsNitrosyl Fluoride (ONF)

Initial experiments on the direct addition of NO to F₂ indicated that a spontaneous reaction was occurring. However, absence of a parent peak of ONF⁺ and poor analytical technique (mass spectra were not obtained over a continuous warm-up) delayed the identification of ONF.

An attempt was made to produce ONF from KF and NO₂. Ten grams of KF·2H₂O were baked in an oven at 350°C for two hours and then pumped under vacuum overnight. A glass trap was then charged with the KF and gaseous NO₂ to 1 atm. The trap was allowed to stand for three days at ambient temperature. After this time the dark red-brown color of NO₂ vapor had not diminished noticeably. This indicated a low conversion of NO₂ at best. An accurate analysis of the products was not obtained.

The successful preparation and identification of ONF was obtained by combining NO and F₂ at low pressures (1-2 torr) in 1/4 in. copper tubing and pumping the products continuously through either an all metal or a glass trap at -196°C. In a typical experiment 40 mmoles of both NO and F₂ were combined at a rate of about 5 mmoles/min. If a glass trap was used, the products consisted of mostly ONF plus some NO₂F, N₂O₃, a trace of ONF₃, and a flaky white solid, probably (NO₂)₂SiF₆. This flaky white substance evidently serves as a protective coating on the

glass walls which are readily attacked by ONF. Conversion of NO to products was complete. If a metal trap was used, the results were similar except that no N_2O_3 and $(NO_2)_2SiF_6$ were formed.

The mass spectra and appearance potentials of ONF were obtained between -145 and $-140^\circ C$. At this temperature NO_2F and ONF_3 were completely pumped away, and N_2O_3 and $(NO_2)_2SiF_6$ exerted negligible vapor pressures.

Nitryl Fluoride (NO_2F)

NO_2F was prepared in high yields by pumping F_2 over a bed of solid $NaNO_2$. The products were trapped in either a glass or metal trap at $-196^\circ C$. In a typical experiment ten grams of $NaNO_2$ were dried at $200^\circ C$ under vacuum and pumped overnight. About 50 mmoles of F_2 were pumped through the glass tube containing the $NaNO_2$ at flow rates from 0.5 to 1.0 mmoles/min. A large portion of the F_2 passed unreacted through the trap. Mass spectrometric analysis of the reaction products showed mostly NO_2F with possibly a small amount of NO_3F . If a glass rather than metal trap was used, N_2O_3 , NO_2 , and $(NO_2)_2SiF_6$ were formed as additional products in small quantities.

The mass spectra and appearance potentials of NO_2F were obtained between -155 and $-150^\circ C$. The presence of NO_3F , as indicated by the mass peak $m/e = 35$ (OF^+), was not observed until the temperature rose above $-150^\circ C$.

Fluorine Nitrate (NO_3F)

NO_3F was prepared in high yields from KNO_3 and F_2 . In a typical run 10 grams of KNO_3 were dried at $200^\circ C$ for two hours and pumped

overnight. About 50 mmoles of F_2 were then pumped over the bed of KNO_3 at a rate of 0.3-0.5 mmoles/min. Products were condensed at $-183^\circ C$.

Mass spectrometric analysis indicated the condensed material to be almost entirely NO_3F . The mass spectra and appearance potentials of NO_3F were obtained from -145° to $-140^\circ C$.

Nitrosodifluoramine ($ONNF_2$)

Several methods were used in attempting to prepare and identify $ONNF_2$. In one method a 10/1 mixture of NO/N_2F_4 was pumped at 1 mmole/min. through an 11 foot long, 1/4 in. O.D. copper coil heated to $130^\circ C$. Purple, red-brown, and white solids were condensed in a glass trap at $-196^\circ C$. Mass spectrometric analysis with a room temperature inlet showed only NO and N_2F_4 as products.

In another experiment a 10/1 mixture of NO/N_2F_4 was passed at 0.5 mmoles/min. through an 11 foot long, 1/4 in. O.D. copper coil at $200^\circ C$ and condensed at $-196^\circ C$. The trap, in which a dark purple solid collected, was not pumped during the reaction. As soon as the pump-out valve was opened, the dark purple substance "popped," or exploded mildly. As a result, the purple color disappeared leaving only a red-brown substance on the reactor walls. No warm-up and analysis were made since it was erroneously thought that the red-brown color was due to N_2F_4 .

In a third experiment, 30 mmoles of a 5/1 mixture of NO/N_2F_4 were passed at 0.5 mmoles/min. through an rf discharge (plate current 90-100 mamps dc). The reaction products were pumped through a glass trap at $-196^\circ C$, whereby white, blue, and red-brown solids were collected. Unreacted NO was pumped away at $-183^\circ C$. The controlled warm-up and mass

spectrometric analysis was begun at -155°C . At this temperature the small amount of red-brown substance quickly disappeared. The remaining products were mostly unreacted NO and N_2F_4 and small amounts of N_2O , NO_2F , N_2O_3 , NO_2 , and possibly some ONF.

ONNF₂ was successfully prepared and identified in the glass capillary furnace of Figure 4. In a typical run 90 mmoles of a 10/1 mixture of NO/ N_2F_4 were pumped at 1-3 mmoles/min. through the capillary heated to 310°C followed by a fast quench at -196°C , whereby dark purple and white solids were condensed. Excess NO was pumped away at -183°C , leaving the dark purple substance on the walls. Warm-up and analysis using the cold inlet system was begun at -161°C . Mass spectra of ONNF₂ were obtained from -153 to -148°C . The spectra were occasionally corrected for trace amounts of N_2F_4 , assuming that all of $m/e = 85$ (N_2F_3^+) was from N_2F_4 . Conversion of the N_2F_4 to ONNF₂ was roughly estimated at 90-95 percent.

The above procedure for the preparation of ONNF₂ was repeated for the purpose of checking the necessity of the cold inlet system of the mass spectrometer. The usual dark purple substance was condensed at -196°C . However, upon admitting the reaction products at about -150°C into the mass spectrometer using the room temperature inlet system, only the decomposition products (NO and N_2F_4) were observed.

Trifluoramine Oxide (ONF₃)

It was mentioned earlier that ONF₃ was prepared in trace amounts in the reaction of NO and F_2 to form ONF. Several attempts were made to increase the yield of ONF₃ from this reaction. Increasing the F_2/NO ratio up to 3/1 and varying the flow rate from 1 to 26 mmoles/min. had

very little affect. Passing the NO and F_2 under similar conditions through an 11 foot long, 1/4 in. O.D. copper coil heated to $160^\circ C$ gave only a slightly higher yield of ONF_3 . In a slightly modified approach ONF was prepared in the usual manner and then evaporated into an 800 cc stainless steel storage vessel. Ar and F_2 were added to a pressure of 1 atm and in a ratio of $ONF/F_2/Ar$ of 1/1/1. The mixture was heated to $200^\circ C$ for 45 minutes and then condensed at $-196^\circ C$. No appreciable increase in the ONF_3 yield was observed.

An rf discharge of O_2 pumped over solid NF_3 at $-196^\circ C$ produced no reaction. The plate current was varied up to 200 mamps dc. An rf discharge of a 1/1/2 mixture of $OF_2/NF_3/He$ was carried out at 0.1 mmoles/min. and 60-100 mamps dc plate current. Products were trapped at $-196^\circ C$. Very little reaction occurred. The products consisted of mostly SiF_4 , N_2O , N_2 , and O_2 .

Several electric discharge experiments of O_2 and NF_3 were performed. In the glass reactor of Figure 1, a 2/1 mixture of NF_3/O_2 was discharged at 1-15 torr, 20-80 mamps ac, and 750-1000 volts. The products obtained were mostly O_2F_2 with smaller amounts of ONF_3 , NO_2F , ONF , and $(NO_2)_2SiF_6$. The use of higher currents (60-80 mamps) caused slight vaporization of the Cu electrodes without any noticeable change in the product yield. An electric discharge of a 1/1 mixture of O_2/NF_3 was also performed in the metal reactor of Figure 2 at $-183^\circ C$. Reaction conditions were 2-10 torr, 20-30 mamps, and 500-1000 volts. Once again the major product was O_2F_2 with small amounts of NO_2F , ONF , and ONF_3 . The estimated yield of ONF_3 in these discharge experiments was less than 5 percent.

The highest yields of ONF_3 (about 20-40 percent) were obtained by

the electric discharge of a 1/1/2 mixture of $\text{OF}_2/\text{NF}_3/\text{Ar}$ at -183°C in the glass reactor of Figure 1. In a typical experiment 60 mmoles of reactants were slowly pumped through the discharge region at 1-4 mmoles/min. The reactor pressure was estimated at slightly greater than 1 torr. The discharge occurred at 30-40 mamps and 900-1100 volts ac. Both ONF_3 and O_2F_2 were obtained in high yields along with a much smaller amount of NO_2F , ONF , and $(\text{NO}_2)_2\text{SiF}_6$. In a similar experiment using a lower discharge current of 5-10 mamps, no ONF_3 and only O_2F_2 , NO_2F , ONF , and $(\text{NO}_2)_2\text{SiF}_6$ were produced.

The mass spectra and appearance potentials of ONF_3 were obtained at about -165°C . A great amount of difficulty was encountered in trying to maintain this temperature in the cryostat due to the high viscosity of the refrigerant mixture near its freezing point (-168°C).

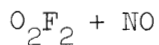
Reactions With Dioxygen Difluoride (O_2F_2)

The preparation and characterization of the oxygen fluorides O_2F_2 , O_3F_2 , and O_4F_2 have been discussed extensively^{106,79}. Doubt still remains whether O_3F_2 , a dark red liquid at -196°C , exists as a molecular entity, or whether it is a mixture of O_4F_2 , a reddish brown solid at -196°C , and O_2F_2 , a yellow-orange solid at -196°C .

No difficulties were encountered in preparing the orange solid, O_2F_2 , by the usual electric discharge of F_2 (or OF_2) and O_2 at -183°C . This orange substance liberated O_2 between -165 and -150°C before turning to a pure yellow substance which exhibited the mass spectrum of O_2F_2 at -140 to -135°C . The yellow color did not change when the reactor was

cooled back down to -196°C . The spectrum obtained for O_2F_2 at -140°C using the cold inlet system is shown in Appendix D.

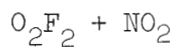
These experiments suggest that O_2F_2 is actually pure yellow (not orange), and that the degree of redness is due to the amount of O_4F_2 dissolved in it. No mass spectrometric evidence for O_4F_2 was obtained in this work other than the large O_2 liberation from -165 to -150°C mentioned above. (The literature also contains no mass spectrometric data on O_4F_2). All the following reactions of O_2F_2 , however, involve this yellow-orange substance, unless otherwise stated. For matters of simplicity, this will be referred to as O_2F_2 and not a mixture of O_2F_2 and O_4F_2 (or O_2F_2 and " O_3F_2 ").



The reaction of O_2F_2 with NO was studied with the hope of preparing the unknown compounds FO_2NO or FONO .

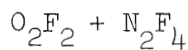
Several experiments were performed in combining O_2F_2 and NO. In a typical run 36 mmoles of a 1/1 mixture of O_2/F_2 were discharged at -183°C in the reactor of Figure 1. Reaction conditions were 5-20 torr, 20 mamps and 500-1500 volts ac. NO was then slowly condensed onto the O_2F_2 at -183°C . A bright blue solid (N_2O_3) appeared on the reactor walls. Warm-up and analysis with the cold inlet system showed unreacted O_2F_2 along with NO_2F , ONF , N_2O_3 , and $(\text{NO}_2)_2\text{SiF}_6$.

In a separate experiment the above procedure was repeated. Furthermore, the discharge was run at 10 mamps for several minutes at both -183 and -155°C after the NO had been added. Besides the production of N_2 and O_2 from the excited NO, no additional products were observed other than those listed above.



The reaction of O_2F_2 with NO_2 was studied with the hope of preparing FO_2NO_2 .

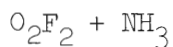
O_2F_2 was prepared by the electric discharge (Figure 1) of 62 mmoles of a 1/1 O_2/F_2 mixture at -183°C , 10-20 torr, 15-20 mamps, and 750 volts ac. Forty mmoles of NO_2 were pumped into the reactor at -183°C at 1.3 mmoles/min. The resulting condensed substance appeared to be mostly white solid with red-orange streaks and a small ring of blue-green material ($\text{N}_2\text{O}_3\text{-NO}_2$). Analysis using the cold inlet showed the products to be unreacted O_2F_2 and NO_2 plus NO_2F , ONF , N_2O_3 , and $(\text{NO}_2)_2\text{SiF}_6$ in fairly high yields.



The reaction of O_2F_2 with N_2F_4 was studied with the hope of preparing the unknown species FO_2NF_2 or FONF_2 .

O_2F_2 was prepared by discharging (Figure 1) 70 mmoles of a 1/1 mixture of O_2/F_2 at -183°C , 10-30 torr, and 20-40 mamps. N_2F_4 was added up to several torr to the reactor containing the O_2F_2 at -155°C . No indication of a spontaneous reaction was evident, i.e., no change in pressure or in color of condensed material. The discharge was turned on (20-30 mamps) and the reactor pressure immediately increased to 30-50 torr. The volatile products at this temperature were NF_3 , F_2 , N_2 , and O_2 . These were pumped away and the discharge process repeated several times. All of the O_2F_2 eventually reacted or decomposed. Analysis of the products condensed at -155°C showed only large quantities of SiF_4 and NO_2 .

In another experiment the O_2F_2 was prepared as usual and then transferred to a second trap so that the discharge electrodes could be removed and the glass capillary furnace (Figure 4) installed. After the O_2F_2 was transferred back to the reactor, only a small amount of yellow O_2F_2 remained. An 8/1 mixture of Ar/ N_2F_4 was then pumped at 1.5-2.0 mmoles/min. through the furnace at $310^\circ C$ and then condensed onto the O_2F_2 at $-196^\circ C$. Analysis of the products showed almost entirely unreacted O_2F_2 and N_2F_4 .



The reaction of O_2F_2 with NH_3 was studied with the hope of preparing compounds of the type $N(O_2F)_aF_b$ or $N(OF)_aF_b$ where $a + b = 3$.

O_2F_2 was reacted with NH_3 in two separate experiments. In the first O_2F_2 was prepared as usual at $-183^\circ C$. A 5/1 Ar/ NH_3 mixture was then slowly added to the reactor until the pressure increased to 20-50 torr. The volatile Ar was pumped away and more Ar/ NH_3 mixture added. An occasional dim "flash" accompanied the addition of the NH_3 . Warm-up and analysis showed unreacted O_2F_2 along with SiF_4 , HF, and NO_2 .

In the second experiment a 5/1 mixture of He/ NH_3 was pumped continuously through the reactor containing the condensed O_2F_2 , first at -196° and then at $-183^\circ C$. No "flashes" were observed during the addition of the NH_3 . However, the reaction products were the same as above.

An investigation was made into the possible use of CF_3Cl as a solvent for NH_3 in controlling the reaction of NH_3 and O_2F_2 . CF_3Cl and NH_3 were mixed and allowed to stand at $25^\circ C$. A spectrum of the mixture showed that no reaction had taken place. CF_3Cl was then condensed

above NH_3 in a glass trap at -196°C . At -145°C the CF_3Cl was allowed to melt to the bottom of the trap, but a large amount of solid (NH_3) still remained on the walls. In another experiment a mixture of NH_3 and CF_3Cl was frozen into a trap at -196°C . The CF_3Cl was allowed to melt to the bottom at -140°C leaving the white solid NH_3 on the walls once again. It was thus concluded that NH_3 is only slightly soluble at best in CF_3Cl .

Reactions With Tetrafluorohydrazine (N_2F_4)

$\text{N}_2\text{F}_4 + \text{NO}_2$

The reaction of nitrogen dioxide with tetrafluorohydrazine was studied with the hope of preparing nitrodifluoramine (O_2NNF_2).

A mixture of NO_2 and N_2F_4 was found to be chemically unstable as follows. A 2.5/1 mixture of $\text{NO}_2/\text{N}_2\text{F}_4$ was added to an 800 cc stainless steel vessel to a pressure of 10 psia. A mass spectrum of this mixture at 25°C showed that all the N_2F_4 had been converted to NF_3 . Further analysis of the mixture was not made. Other products were probably ONF and NO_2F , as reported in the literature⁸.

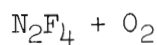
Direct evidence for the existence of the new compound O_2NNF_2 was obtained by reacting NO_2 with NF_2 radicals from the capillary furnace of Figure 4. The instability of the $\text{NO}_2/\text{N}_2\text{F}_4$ mixture eliminated the possibility of preparing O_2NNF_2 by exactly the same method as for ONNF_2 , i.e., by passing the entire mixture through the capillary furnace. However, in this procedure the NO_2 was passed around the outside of the furnace. In a typical experiment 23 mmoles of a 3/1 mixture of $\text{Ar}/\text{N}_2\text{F}_4$ were passed at 0.15-0.25 mmoles/min. through the hot capillary at 310°C .

while 10 mmoles of NO_2 were passed at 0.08-0.12 mmoles/min. around the outside of the furnace. Reaction products were quenched immediately at -196°C . The condensed products contained a small ring of dark purple solid (ONNF_2) and a large amount of white solid with a light blue tint.

Mass spectrometric analysis of the reaction products using the cold inlet system was begun at -160°C . A small amount of ONNF_2 was observed and completely pumped away at -140°C . The mass spectra and appearance potentials attributed to the new compound O_2NNF_2 were obtained over the range -135 to 130°C . Corrections in the spectra were made for small amounts of N_2F_4 assuming that all of $m/e = 85$ (N_2F_3^+) was from N_2F_4 . Other products observed were N_2O_3 (light blue solid) and unreacted N_2F_4 and NO_2 . The yield of O_2NNF_2 is roughly estimated at 50-75 percent. Analysis of the condensed O_2NNF_2 at -140 to 125°C using the room temperature inlet system showed only the decomposition products NO_2 and N_2F_4 .

Experiments were conducted to check if the mass peak at $m/e = 46$ (NO_2^+) in the spectrum of O_2NNF_2 could be coming from molecular NO_2 or N_2O_3 . In one experiment NO_2 was condensed into a glass trap at -157°C . Mostly white solid with a slight blue-green tint (due to N_2O_3) was obtained. NO_2^+ first appeared in the mass spectra at -105°C as a small fraction of the NO^+ peak due to N_2O_3 . At -75°C the small amount of N_2O_3 was pumped away and the spectrum of NO_2 became increasingly stronger. In another experiment a 1/1 mixture of NO/NO_2 was condensed in a glass trap at -196°C , leaving an intensely blue solid (N_2O_3) near the top of the trap and a white solid with a blue-green tint near the bottom. Excess NO was pumped away at -183°C and the spectra of the condensed products observed from -163 to -30°C . NO_2^+ from N_2O_3 was first observed

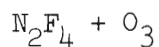
at -104°C . All the N_2O_3 was pumped away at -86°C . The spectra of the remaining NO_2 was observed and recorded from -76 to -30°C . These two experiments on NO_2 and N_2O_3 prove that NO_2^+ can not be coming from either molecular NO_2 or N_2O_3 at -135°C . The vapor pressure data for N_2O_3 and NO_2 ¹⁰⁷ suggest this same result (see Table 43).



The reaction of N_2F_4 and O_2 was studied with the hope of preparing O_2NF_2 or $\text{F}_2\text{NO}_2\text{NF}_2$.

N_2F_4 and O_2 were reacted in the glass capillary furnace of Figure 4. In a typical experiment 85 mmoles of a 9/1 mixture of $\text{O}_2/\text{N}_2\text{F}_4$ were passed at 1.0-1.5 mmoles/min. through the furnace at 310°C . Products were immediately trapped at -196°C . At the end of the experiment a small amount of white solid with a light purple ring had collected in the trap. Analysis of the products showed mostly N_2F_4 (with the usual impurities NF_3 and N_2F_2 contained in N_2F_4) and very small amounts of ONNF_2 and O_2NNF_2 .

The purity of the O_2 reactant gas was checked by pumping 35 mmoles of O_2 through the trap at -196°C . After the trap was warmed to 25°C , a small amount of NO_2 was observed in the spectrum. It is probable that the trace amounts of ONNF_2 and O_2NNF_2 were formed from the presence of NO_2 in the O_2 feed gas. If this is so, then O_2 does not react with NF_2 radicals at 310°C .



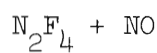
The reaction of N_2F_4 and O_3 was studied with the hope of preparing O_2NF_2 , $\text{F}_2\text{NO}_2\text{NF}_2$, or F_2NONF_2 .

Ozone was prepared by passing O_2 through a Welsbach Model #T-23 ozonator at 4-5 psig, 100 volts ac and flow rates of 0.010-0.020 S.C.F.M. The resulting O_2 - O_3 mixture was then passed through a cold trap at $-90^\circ C$ to remove any NO_2 and then throttled into a glass reactor (Figure 4) at $-196^\circ C$ where the O_3 condensed and the O_2 was pumped away.

About 1-2 ml of the dark blue liquid ozone was prepared in the above manner and allowed to flow to the bottom of the glass reactor at $-196^\circ C$. About 60 mmoles of a 6/1 mixture of Ar/N_2F_4 mixture was passed at 2 mmoles/min. through the glass furnace at $310^\circ C$ and into the reactor containing the O_3 at $-196^\circ C$. At completion of the reaction a small amount of O_3 was still visible along with a light purple colored substance. Mass spectrometric analysis indicated the condensed products to be mostly unreacted N_2F_4 and O_3 with small amounts of ONF_3 , $ONNF_2$, O_2NNF_2 , ONF , NO_3F , and possibly some NO_2F . An attempted repeat of the above experiment to obtain a more positive identification of the reaction products resulted in a violent explosion when the N_2F_4/Ar mixture was initially added to the condensed ozone at $-196^\circ C$. Therefore, further investigation of the gas-liquid reaction of N_2F_4 and O_3 was abandoned due to the inherent danger of the reaction system.

In another experiment, the reaction of N_2F_4 with O_3 in the gas phase was studied. A 7/1 Ar/N_2F_4 mixture was passed through the capillary furnace at $310^\circ C$ at about 4 mmoles/min. The O_2 - O_3 mixture from the ozonator was simultaneously passed around the outside of the furnace and contacted with the N_2F_4/Ar mixture at the exit of the capillary. Products were immediately quenched at $-196^\circ C$. The N_2F_4/O_3 ratio was roughly estimated at 1/1. The condensed products contained a slight

purple color, but the dark blue color of ozone was not observed. The mass spectrometric analysis of condensed products showed almost all N_2F_4 with trace amounts of ONNF_2 , O_2NNF_2 , and NO_2 . Evidently, the O_3 decomposed to O_2 and was pumped away at -196°C . A blank experiment showed that O_3 did survive the pyrolysis incurred along the outside of the furnace in the absence of the $\text{N}_2\text{F}_4/\text{Ar}$ mixture.



In an earlier section on the preparation of ONNF_2 it was mentioned that an unidentified red-brown substance was observed either by passing a mixture of $\text{NO}/\text{N}_2\text{F}_4$ through a copper coil at $150\text{--}200^\circ\text{C}$ or by an rf discharge of NO and N_2F_4 . This reaction of NO and N_2F_4 was studied further with the hope of identifying this red-brown substance.

In a typical experiment, 30 mmoles of a 5/1 mixture of NO and N_2F_4 were condensed directly into a glass reactor at -196°C . The condensed material appeared to be mostly white with small amounts of red-brown and purple solids. Excess NO was pumped away at -183°C , the red-brown material still remaining. After the liquid O_2 dewar (-183°C) was replaced with refrigerant at -168°C , the red brown material quickly disappeared. However, the mass spectrometer with the cold inlet indicated only a small liberation of NO and N_2F_4 with trace amounts of NF_3 and N_2F_2 (the usual impurities of N_2F_4). Further warm-up showed mostly N_2F_4 and a small amount of ONNF_2 . No mass spectrometric evidence was obtained which could possibly be attributed to the unknown red-brown substance in question.

Reaction of NF_3 With F_2

An attempt was made to prepare the compounds NF_5 or F_3NNF_3 by an electric discharge of NF_3 and F_2 at -183°C .

Sixty mmoles of a 2/1/1 mixture of $\text{Ar}/\text{NF}_3/\text{F}_2$ were passed continuously at 1.0-2.5 mmoles/min., 20-30 mamps, and 900-1000 volts ac through the reactor in Figure 1. Only a small amount of yellow solid was condensed at -183°C . Analysis indicated only a very small amount of O_2F_2 and N_2O had been prepared, probably from the contamination of the feed gas with trace amounts of O_2 .

Summary and Discussion of Reactions Studied

The five previously known N-O-F compounds were prepared by methods similar to those published in the literature. These preparations are summarized in Table 6. Nitrosyl fluoride (ONF), nitryl fluoride (NO_2F), and fluorine nitrate (NO_3F) were prepared by the exothermic reactions of fluorine gas with nitric oxide, sodium nitrite, and potassium nitrate, respectively. Nitrosodifluoramine (ONNF_2) was prepared by the pyrolysis of nitric oxide and tetrafluorohydrazine at 310°C followed by a fast quench at -196°C . Trifluoramine oxide (ONF_3) was most easily prepared by an electric discharge of NF_3 and OF_2 at -183 or -196°C .

The results of the reactions of O_2F_2 with NO , NO_2 , N_2F_4 , and NH_3 are summarized in Table 7. These results were rather disappointing since no new compounds containing O_2F or OF radicals were observed. In fact, in the four reactions studied, O_2F_2 always acted as a simple fluorinating agent. All of these reactions, except O_2F_2 with N_2F_4 , proceeded spontaneously, indicating highly exothermic reactions. It is probable

Table 6. Summary of Preparations of Previously Known N-O-F Compounds

Nitrosyl Fluoride:	$\text{NO (g)} + \text{F}_2\text{(g)}$	\longrightarrow	ONF
Nitryl Fluoride:	$\text{NaNO}_2\text{(s)} + \text{F}_2\text{(g)}$	\longrightarrow	NO_2F
Fluorine Nitrate:	$\text{KNO}_3\text{(s)} + \text{F}_2\text{(g)}$	\longrightarrow	NO_3F
Nitrosodifluoramine:	$\text{NO(g)} + \text{NF}_4\text{(g)}$	$\xrightarrow[\text{fast quench @ } -196^\circ\text{C}]{310^\circ\text{C}}$	ONNF_2
Trifluoramine Oxide:	$\text{NF}_3\text{(g)} + \text{OF}_2\text{(g)}$	$\xrightarrow[\text{@ } -183 \text{ or } -196^\circ\text{C}]{\text{elec. dis.}}$	$\text{ONF}_3 (+ \text{O}_2\text{F}_2)$

Table 7. Summary of Reactions With Dioxxygen Difluoride (O_2F_2)

$\text{O}_2\text{F}_2 + \text{NO}$	$\xrightarrow{-183^\circ\text{C}}$	$\text{O}_2\text{F}_2 + \text{ONF} + \text{NO}_2\text{F} + \text{N}_2\text{O}_3 + (\text{NO}_2)_2\text{SiF}_6$
$\text{O}_2\text{F}_2 + \text{NO}_2$	$\xrightarrow{-183^\circ\text{C}}$	$\text{O}_2\text{F}_2 + \text{NO}_2 + \text{ONF} + \text{NO}_2\text{F} + \text{N}_2\text{O}_3 + (\text{NO}_2)_2\text{SiF}_6$
$\text{O}_2\text{F}_2 + \text{N}_2\text{F}_4$	$\xrightarrow[-196^\circ\text{C}]{-155 \text{ to}}$	no reaction
$\text{O}_2\text{F}_2 + \text{N}_2\text{F}_4$	$\xrightarrow[\text{@ } -155^\circ\text{C}]{\text{elec. dis.}}$	$\text{NF}_3 + \text{F}_2 + \text{N}_2 + \text{O}_2$
$\text{O}_2\text{F}_2 + \text{NH}_3$	$\xrightarrow{-196^\circ\text{C}}$	$\text{O}_2\text{F}_2 + \text{NO}_2 + \text{HF} + \text{SiF}_4$ (occasional flashes)

that transfer of the O_2F or OF radical is just not feasible under these conditions due to the high heat release during reaction. As mentioned in the Introduction, Solomon and coworkers⁷⁶⁻⁷⁸ used O_2F_2 as a source of O_2F radicals, but their reactions were carried out in inert solvents which could readily absorb any heat released during reaction.

The results of the reactions of N_2F_4 with NO_2 , O_2 , O_3 , and NO are summarized in Table 8. The room temperature addition of NO_2 to N_2F_4 caused decomposition to NF_3 and other stable products. However, the pyrolysis of N_2F_4 at 310°C to form NF_2 radicals and the subsequent addition of NO_2 with a fast quench at -196°C resulted in the formation of the new compound nitrodifluoramine (O_2NNF_2). The pyrolysis of N_2F_4 and O_2 at 310°C produced no reaction. The pyrolysis of N_2F_4 with subsequent quenching on a thin film of O_3 at -196°C produced a vigorous reaction (once a violent explosion) to form all the known N-O-F compounds. No evidence was found for a compound of the type O_2NF_2 , F_2NONF_2 , or $\text{F}_2\text{NO}_2\text{NF}_2$ in this reaction. The trapping at -196°C of a room temperature mixture of N_2F_4 and NO produced small amounts of red-brown and purple solids. The purple substance was identified as ONNF_2 . However, the red-brown substance decomposed between -183 and -168°C before it could exert a sufficiently high vapor pressure to be detected in the mass spectrometer. Since this unidentified red-brown substance probably results from the reversible reaction of NO with either N_2F_4 or NF_2 radicals, then the only likely possibilities are F_2NONNF_2 and $(\text{ONNF}_2)_2$. On the basis of the Double Quartet discussion in Appendix B, the unidentified red-brown substance is attributed to F_2NONNF_2 .

The electric discharge at -183°C of NF_3 with excess F_2 produced no

Table 8. Summary of Reactions With Tetrafluorohydrazine (N_2F_4)

$\text{N}_2\text{F}_4 + \text{NO}_2$	$\xrightarrow{25^\circ\text{C}}$	$\text{NF}_3 + \text{others}$
$\text{N}_2\text{F}_4(310^\circ\text{C}) + \text{NO}_2(25^\circ\text{C})$	$\xrightarrow[\text{@ } -196^\circ\text{C}]{\text{fast quench}}$	O_2NNF_2
$\text{N}_2\text{F}_4 + \text{O}_2$	$\xrightarrow[\text{quench @ } -196^\circ\text{C}]{310^\circ\text{C with fast}}$	no reaction (trace of $\text{ONNF}_2 + \text{O}_2\text{NNF}_2$) ^a
$\text{N}_2\text{F}_4 + \text{O}_3$	$\xrightarrow{-196^\circ\text{C}}$	$\text{ONF}_3 + \text{ONNF}_2 + \text{O}_2\text{NNF}_2 + \text{ONF} + \text{NO}_3\text{F}^{\text{b}} + \text{NO}_2\text{F}$
$\text{N}_2\text{F}_4 + \text{NO}$	$\xrightarrow[\text{quench @ } -196^\circ\text{C}]{25^\circ\text{C with}}$	red-brown + purple solids ($\text{F}_2\text{NONNF}_2?$) (ONNF_2)

^aProbably due to NO_2 impurity in O_2 feed gas^bReactant mixture exploded violently on one occasion

reaction. No evidence was obtained which would suggest the existence of the doubtful compounds NF_5 and F_3NNF_3 .

Mass Spectra

Positive Ions

The positive ion mass spectra of the six N-O-F compounds are presented in Table 9. The temperature intervals over which the data were taken, which correspond to the observed vapor pressures of 0.1-0.2 torr, are also give.

It is evident from Table 9 that fragments containing the fluorine atom are reluctant to release an electron to form a positive ion. In all cases the major ion mass peak is either NO^+ or NO_2^+ . Only in ONF_3 , where the ONF_2^+ intensity is 75 percent, does the intensity of a positive ion fragment containing F exceed 30 percent. However, even in this molecule the major peak is NO^+ which results from the rupture of three bonds, which is very unusual for a major ion fragment. Also, the parent molecular ions do not exist except for the two compounds NO_2F and ONF_3 , which have very low intensities of 1.5 and 0.1 percent respectively.

Although all the N-O-F compounds possess large NO^+ peaks and all but NO_3F have somewhat smaller NF^+ peaks, the mass spectrum of each N-O-F compound is unique, and identification of each is straightforward. ONF is readily identified in the absence of other N-O-F compounds since its ion of highest mass/charge is NF^+ ($m/e = 33$). Nitryl fluoride and fluorine nitrate have somewhat similar spectra, but NO_2F has peaks at NF^+ and NO_2F^+ which NO_3F lacks, and NO_3F has a peak at OF^+ which all the other N-O-F compounds lack. Trifluoramine oxide is easily distinguished by its large

Table 9. Positive Ion Mass Spectra of N-O-F Compounds

m/e	Ion	Relative Intensity @ 70 eV (%)					
		ONF	NO ₂ F	NO ₃ F	ONNF ₂	ONF ₃	O ₂ NNF ₂
14	N ⁺	6.0	4.5	2.0	8.0	3.0	6.0
16	O ⁺	4.0	11.0	10.0	2.5	2.5	8.0
19	F ⁺	5.0	3.5	2.0	3.0	7.0	2.0
28	N ₂ ⁺				3.0		4.0
30	NO ⁺	100.0	75.0	43.0	100.0	100.0	80.0
33	NF ⁺	3.5	1.5		28.0	5.5	20.0
35	OF ⁺			4.0			
44	N ₂ O ⁺				0.2 ^a		0.5
46	NO ₂ ⁺		100.0	100.0			100.0
47	N ₂ F ⁺				0.1 ^a		0.3 ^a
52	NF ₂ ⁺				18.0	1.5	15.0
65	NO ₂ F ⁺		1.5				
68	ONF ₂ ⁺					75.0	
87	ONF ₃ ⁺					0.1	
Temperature ^b		-140	-150	-140	-148	-165	-130
(°C)		to -145	to -155	to -145	to -153		to -135

^aPossibly due to impurities^bCorresponds to observed vapor pressure of 0.1-0.2 torr

peak at ONF_2^+ . The similar spectra of nitroso- and nitro-difluoramine differ from the others due to their relatively high peaks at NF^+ and NF_2^+ . They differ from each other in that O_2NNF_2 has its largest peak at NO_2^+ which is completely absent in ONNF_2 .

One may ask why is the last spectrum listed in Table 9 attributed to a new compound, namely O_2NNF_2 . There are two obvious possibilities: the spectrum is due either to a new compound or to a combination of known compounds. The latter possibility is ruled out in the following manner. The compound ONNF_2 cannot be contributing to the spectrum since ONNF_2 is a purple solid which is pumped away below -140°C , whereas the substance in question is a white solid at -130 to -135°C . The peak at NO_2^+ cannot be arising from NO_2F or NO_3F since there are no additional peaks at NO_2F^+ or OF^+ . Furthermore, the NO_2^+ peak cannot be arising from an oxide of nitrogen, namely NO_2 (N_2O_4) or N_2O_3 , since the vapor pressures of these compounds are exceedingly low at -130°C . The fact that the spectrum in question cannot be attributed to known compounds and the fact that it uniformly increased with increasing temperature and uniformly decreased when the substance was pumped away very strongly suggest that the spectrum is due to a new compound. Since the preparation of this compound involved the combination of NO_2 and NF_2 radicals, since the mass spectrum suggests that the structure contains NO_2 and NF_2 groups, and since a stable configuration for O_2NNF_2 can be drawn using the Double Quartet Model (see Appendix B), it was concluded that this new compound is very likely nitrodifluoramine, O_2NNF_2 . The volatility of O_2NNF_2 is slightly less than that of ONNF_2 (see Table 11). This is reasonable since they are similarly structured but O_2NNF_2 has a slightly

higher molecular weight due to an additional oxygen atom.

Negative Ions

The approximate negative ion mass spectra of the six N-O-F compounds are shown in Table 10. The F^- ion was the predominate peak in each spectra except for NO_3^- from NO_3F and NO_2^- from O_2NNF_2 . The ONF^- ion was not observed in the spectra of ONF or NO_2F , but it did appear in the spectrum of ONF_3 . No parent molecular negative ions were observed. The only rearrangement ion observed was F_2^- from ONF_3 .

Estimation of Vapor Pressures

Vapor pressure data are available for only four of the six N-O-F compounds (see Table 3). Mass spectrometric data obtained in this work provide an estimate of the vapor pressures for the remaining two compounds. As explained earlier, the mass spectra and appearance potential data were obtained over a $6^\circ C$ range for each compound where the observed pressure in the reactor containing the particular compound was 0.1-0.2 torr. These temperature ranges are listed in Table 11. For the four compounds ONF_3 , NO_2F , NO_3F , and ONF the quantity Δ is calculated where Δ ($^\circ C$) is defined as the temperature at which the vapor pressure is known to be one torr minus the median of the temperature range of the observed vapor pressure of 0.1-0.2 torr. Table 11 shows that Δ_{ave} is $9.1^\circ C$, with the individual Δ 's ranging from 8 to $10.5^\circ C$. This is an excellent agreement considering the technique used. For $ONNF_2$ and O_2NNF_2 , estimates were made of the temperature at which the vapor pressure should be 1.0 torr by adding Δ_{ave} to the appropriate temperature range of the observed vapor pressure of 0.1-0.2 torr. The results indicate that $ONNF_2$ and

Table 10. Negative Ion Mass Spectra of N-O-F Compounds

m/e	Ion	Relative Intensity (%)					
		ONF	NO ₂ F	NO ₃ F	ONNF ₂	ONF ₃	O ₂ NNF ₂
16	O ⁻	20	9	40	15	-	5
19	F ⁻	100	100	95	100	100	50
35	OF ⁻	-	-	65	-	-	-
38	F ₂ ⁻	-	-	-	-	30	-
46	NO ₂ ⁻	-	7	95	-	-	100
49	ONF ⁻	-	-	-	-	20	-
52	NF ₂ ⁻	-	-	-	30	-	50
62	NO ₃ ⁻	-	-	100	-	-	-
68	ONF ₂ ⁻	-	-	-	-	30	-

Table 11. Vapor Pressures of N-O-F Compounds

Compound	X Temp. Range of Observed Vap. Press. of 0.1-0.2 torr (°C)	Y Known Temp. at Vap. Press. of 1.0 torr (°C)	Δ^a (°C)	Z ^b Estimated Temp. at Vap. Press. of 1.0 torr (°C)
ONF ₃	-165	-157	8	-
NO ₂ F	-150 to -155	-144	8.5	-
ONNF ₂	-148 to -153	-	-	-141 ± 2
NO ₃ F	-140 to -145	-133	9.5	-
ONF	-140 to -145	-132	10.5	-
O ₂ NNF ₂	-130 to -135	-	-	-123 ± 2
<hr/>				
^a $\Delta = Y - X$				
^b $Z = X + \Delta_{ave}$				

O_2NNF_2 have vapor pressures of 1.0 torr at -141 ± 2 °C and -123 ± 2 °C, respectively.

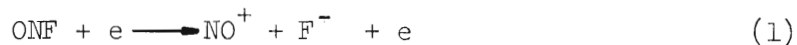
Appearance Potentials and Molecular Energetics

The best literature values of heats of formation, ionization potentials, and electron affinities of N-O-F species are given in Tables 19, 20 and 21 in Appendix A. These best values are used in the following presentation of the molecular energetics of N-O-F compounds.

Nitrosyl Fluoride (ONF)

The appearance potential data for ONF are shown in Table 12. The ionization efficiency curve of NO^+ from ONF was of high intensity and gave a very good match with the IE curve of argon. The NF^+ IE curve was of much lower intensity and provided only a fair match with the Ar curve. The IE curve for F^+ was of low intensity and very long-tailed, which resulted in a poor match with Ar.

The ion-source processes attributed to the measured appearance potentials are also shown in Table 12 along with the AP's calculated from the best literature values listed in Tables 19-21. The attributed ion-source process for NO^+ is



where

$$A(\text{NO}^+) = \Delta H_f(\text{NO}) + \Delta H_f(\text{F}) - \Delta H_f(\text{ONF}) + I(\text{NO}) - EA(\text{F}) \quad (2)$$

Thus, $A(\text{NO}^+)_{\text{calc.}} = 0.94 + 0.69 - (-0.68) + 9.25 - 3.45 = 8.11$ eV. This is 0.22 eV lower than the measured value of 8.33 eV.

Table 12. Appearance Potentials of Nitrosyl Fluoride (ONF)

Ion	AP exptl (ev)	No. of Trails	Ave. Dev. (ev)	Method	Quality of Data	Process	calc. (ev)	AP exptl.-calc. (ev)
NO^+	8.33	5	0.10	EVD	good	$\text{ONF} + e \rightarrow \text{NO}^+ + \text{F}^- + e$	8.11	+0.22
NF^+	18.39	2	0.01	EVD	fair	$\rightarrow \text{NF}^+ + 0 + 2e$	18.14	+0.25
F^+	21.41	2	0.09	EVD	poor	$\rightarrow \text{F}^+ + \text{NO} + 2e$	19.73	+1.68

For the NF^+ ion the attributed process is



where

$$A(\text{NF}^+) = \Delta H_f(\text{NF}^+) + \Delta H_f(\text{O}) - \Delta H_f(\text{ONF}) \quad (4)$$

Thus, $A(\text{NF}^+)_{\text{calc.}} = 14.88 + 2.58 - (-0.68) = 18.14$ eV, which is 0.25 eV lower than the measured value of 18.39 eV.

For the F^+ ion the attributed process is



where

$$A(\text{F}^+) = \Delta H_f(\text{F}) + \Delta H_f(\text{NO}) = \Delta H_f(\text{ONF}) + I(\text{F}) \quad (6)$$

Thus, $A(\text{F}^+)_{\text{calc.}} = 0.69 + 0.94 - (-0.68) + 17.42 = 19.73$ eV, which is 1.68 eV lower than the measured value of 21.41 eV.

For NO^+ and NF^+ the experimental and calculated AP's are in fairly good agreement (within 0.25 eV). For F^+ , however, the deviation is 1.68 eV. This large discrepancy is attributed partially to the poor quality of the EVD fit for the F^+ IE curve with argon and partially to the production of a large amount of excess energy in Eq. 5, which is expected from Stevenson's rule. Since the data for $A(\text{NO}^+)$ are the most reliable, the derived $\Delta H_f(\text{ONF})$ can be obtained as follows:

$$\Delta H_f(\text{ONF})_{\text{derived}} = \Delta H_f(\text{NO}) + \Delta H_f(\text{F}) + I(\text{NO}) - EA(\text{F}) - A(\text{NO}^+)_{\text{exptl.}} \quad (7)$$

Thus, $\Delta H_f(\text{ONF})_{\text{derived}} = 0.94 + 0.69 + 9.25 - 3.45 - 8.33 = -0.90 \pm 0.10$ eV.

The above measured AP's also provide an estimate of the lower limit of the ionization potential of ONF. Since the parent ion ONF^+ is not observed in the mass spectrometer, then the bond dissociation energy $D(\text{ON}^+ - \text{F})$ must be less than zero. Now, $D(\text{ON}^+ - \text{F}) = \Delta H_f(\text{NO}) + I(\text{NO}) + \Delta H_f(\text{F}) - \Delta H_f(\text{ONF}^+) < 0$. Therefore, $\Delta H_f(\text{ONF}^+) > 0.94 + 9.25 + 0.69 = 10.88$ eV. Using the derived $\Delta H_f(\text{ONF})$ and the fact that $I(\text{ONF}) = \Delta H_f(\text{ONF}^+) - \Delta H_f(\text{ONF})$ gives $I(\text{ONF}) > 10.88 - (-0.90) = 11.78$ eV. This may be compared with the ionization potential of the isoelectronic O_3 molecule, which is 12.80 eV^{108} .

Nitryl Fluoride (NO_2F)

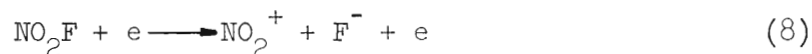
The appearance potential data from the NO_2F molecule are shown in Table 13. The IE curve of the molecular ion NO_2F^+ was of moderately low intensity, but the EVD fit with argon was quite good. The IE curve for NO_2^+ exhibited a sharp break several volts above the threshold energy. The EVD fit for the lower AP of NO_2^+ , $A_1(\text{NO}_2^+)$, was not good due to the low intensity of the IE curve of NO_2 . However, a very good EVD fit was obtained for the higher AP, $A_2(\text{NO}_2^+)$, by subtracting the contribution from the lower energy process. Similarly, the IE curves for F^+ and O^+ exhibited breaks several volts above onset, but these curves were of much lower intensity. Consequently, the poor quality of the first and second AP's of F^+ and O^+ is reflected in the high average deviations obtained. The AP of NO^+ was not measured due to the constantly changing slope of the IE curve of NO^+ near the threshold of ionization, which suggested that several competing ion source processes were occurring.

The ionization potential $I(\text{NO}_2\text{F}) = 13.15 \pm 0.12$ eV measured here has not been previously reported.

Table 13. Appearance Potentials of Nitryl Fluoride (NO_2F)

Ion	AP exptl (eV)	No. of Trails	Ave. Dev. (eV)	Method	Quality of Data	Process	calc. exptl.-calc. (eV)	AP exptl.-calc. (eV)
NO_2F^+	13.15	10	0.12	EVD	excellent	$\text{NO}_2\text{F} + \text{e} \rightarrow \text{NO}_2\text{F}^+ + 2\text{e}$	-	-
NO_2^+	10.27	4	0.12	EVD	fair	$\rightarrow \text{NO}_2^+ + \text{F}^- + \text{e}$	9.70	+0.57
NO_2^+	13.49	8	0.12	EVD	good	$\rightarrow \text{NO}_2^+ + \text{F} + 2\text{e}$	13.15	+0.34
F^+	15.70	4	0.48	LI	poor	$\rightarrow \text{F}^+ + \text{NO}_2^- + \text{e}$	15.58	+0.12
F^+	20.00	6	0.39	EVD	poor	$\rightarrow \text{F}^+ + \text{NO}_2 + 2\text{e}$	19.57	+0.43
O^+	14.06	5	0.28	EVD	poor	$\rightarrow \text{O}^+ + \text{ONF}^- + \text{e}$	-	-
O^+	19.58	3	0.19	EVD	fair	$\rightarrow \text{O}^+ + \text{NO} + \text{F} + 2\text{e}$	18.94	+0.64

For NO_2^+ the lower energy appearance potential is attributed to the process



where

$$A_1(\text{NO}_2^+) = \Delta H_f(\text{NO}_2) + \Delta H_f(\text{F}) + I(\text{NO}_2) - EA(\text{F}) - \Delta H_f(\text{NO}_2\text{F}) \quad (9)$$

Thus, $A_1(\text{NO}_2^+)_{\text{calc.}} = 0.34 + 0.69 + 11.0 - 3.45 - (-1.12) = 9.70$ eV, which is 0.57 eV lower than the measured value of 10.27 eV. The higher energy AP of NO_2^+ is attributed to the process

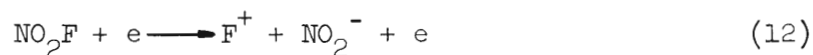


where

$$A_2(\text{NO}_2^+) = \Delta H_f(\text{NO}_2) + \Delta H_f(\text{F}) + I(\text{NO}_2) - \Delta H_f(\text{NO}_2\text{F}) \quad (11)$$

Thus, $A_2(\text{NO}_2^+)_{\text{calc.}} = 0.34 + 0.69 + 11.0 - (-1.12) = 13.15$ eV, which is 0.34 eV lower than the measured value of 13.49 eV.

For F^+ the lower AP is attributed to



where

$$A_1(\text{F}^+) = \Delta H_f(\text{F}) + \Delta H_f(\text{NO}_2) + I(\text{F}) - EA(\text{NO}_2) - \Delta H_f(\text{NO}_2\text{F}) \quad (13)$$

Thus, $A_1(\text{F}^+)_{\text{calc.}} = 0.69 + 0.34 + 17.42 - 3.99 - (-1.12) = 15.58$ eV, which is 0.12 eV lower than the measured value of 15.70 eV. The process attributed to the higher AP of F^+ is

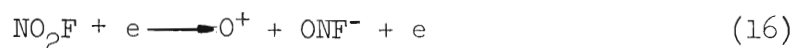


where

$$A_2(\text{F}^+) = \Delta H_f(\text{F}) + \Delta H_f(\text{NO}_2) + I(\text{F}) - \Delta H_f(\text{NO}_2\text{F}) \quad (15)$$

Thus, $A_2(\text{F}^+)_{\text{calc.}} = 0.69 + 0.34 + 17.42 - (-1.12) = 19.57$ eV, which is 0.43 eV lower than the measured value of 20.00 eV.

For the O^+ ion the lower energy process might possibly involve the production of an ONF negative ion as follows:



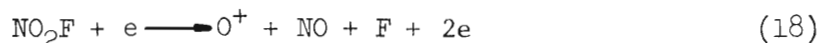
where

$$A_1(\text{O}^+) = \Delta H_f(\text{O}) + \Delta H_f(\text{ONF}) + I(\text{O}) - \text{EA}(\text{ONF}) - \Delta H_f(\text{NO}_2\text{F}) \quad (17)$$

Since $\text{EA}(\text{ONF})$ is unknown, it is impossible to obtain $A_1(\text{O}^+)_{\text{calc.}}$. However, substitution of $A_1(\text{O}^+)_{\text{exptl.}}$ and the appropriate literature values into Eq. 17 gives $\text{EA}(\text{ONF}) = 2.58 + (-0.68) + 13.61 - (-1.12) - 14.06 = 2.57$ eV. This value of $\text{EA}(\text{ONF})$ may seem quite large since most large positive electron affinities involve molecules or atoms containing an odd number of electrons, such as the monatomic halides, NO, NO_2 , NO_3 , and NF_2 . However, O_3 , which is isoelectronic with ONF, has a similarly large positive electron affinity of 2.88 eV¹⁰⁹. Other molecules having an even number of electrons and a positive electron affinity include SO_2 (2.8 eV),¹⁰⁹ SeO_2 (2.3 eV),¹⁰⁹ and O_2 (0.43 eV)¹¹⁰. In Appendix B Linnett's Double Quartet Model is used to derive a stable electronic structure for the ONF^- ion, thus lending support to the existence of the

ion-source process described by Eq. 16. However, some doubt is cast on this process since the ONF^- ion was not observed in the negative ion spectra of ONF or NO_2F , but only in that of ONF_3 (see Table 10).

The higher AP of O^+ is attributed to



where

$$A_2(\text{O}^+) = \Delta H_f(\text{O}) + \Delta H_f(\text{NO}) + \Delta H_f(\text{F}) + I(\text{O}) - \Delta H_f(\text{NO}_2\text{F}) \quad (19)$$

Thus, $A_2(\text{O}^+)_{\text{calc.}} = 2.58 + 0.94 + 0.69 + 13.61 = (-1.12) = 18.94 \text{ eV}$,

which is 0.64 eV lower than the measured value of 19.58 eV.

Table 13 shows that the experimental exceed the calculated AP's by 0.1-0.6 eV. However, the most reliable data are $A(\text{NO}_2\text{F}^+)$ and $A_2(\text{NO}_2^+)$, which exhibited good EVD fits with argon and low average deviations. According to Stevenson's rule a minimal amount of excess energy is expected in the ion-source processes corresponding to these two measurements. Thus, $\Delta H_f(\text{NO}_2\text{F})$ can be calculated from Eq. 11 and $A_2(\text{NO}_2^+)_{\text{exptl.}}$ accordingly: $13.49 = 0.34 + 0.69 + 11.0 - \Delta H_f(\text{NO}_2\text{F})_{\text{derived}}$; and thus $\Delta H_f(\text{NO}_2\text{F})_{\text{derived}} = -1.46 \pm 0.12 \text{ eV}$. Substitution into Eq. 17 of this value and the $\Delta H_f(\text{ONF})_{\text{derived}}$ of -0.90 eV from the previous section recalculates the electron affinity of ONF as follows: $14.06 = 2.58 + (-0.90) + 13.61 - \text{EA}(\text{ONF}) - (-1.46)$; and $\text{EA}(\text{ONF}) = 2.69 \text{ eV}$ with a deviation of $\{(.28)^2 + (.10)^2 + (.12)^2\}^{\frac{1}{2}} \text{ eV}$, or $2.69 \pm 0.32 \text{ eV}$.

The bond dissociation energy $D(\text{NO}_2^+-\text{F})$ corresponds to the heat of reaction of



Therefore, $D(\text{NO}_2^+-\text{F}) = A_2(\text{NO}_2^+) - I(\text{NO}_2\text{F}) = 13.49 - 13.15 = 0.34$ eV with a deviation of $\{(.12)^2 + (.12)^2\}^{\frac{1}{2}}$ eV; or $D(\text{NO}_2^+-\text{F})_{\text{derived}} = 0.34 \pm 0.17$ eV. The value of $D(\text{NO}_2^+-\text{F})$ should, in fact, be positive since the NO_2F^+ parent ion is observable in the mass spectrometer.

Since $EA(\text{ONF})$ is now known, $D(\text{ON}-\text{F}^-)$ can be estimated from



where

$$D(\text{ON}-\text{F}^-) = \Delta H_{\text{F}}(\text{NO}) + \Delta H_{\text{F}}(\text{F}) - EA(\text{F}) - \Delta H_{\text{F}}(\text{ONF}) + EA(\text{ONF}) \quad (22)$$

Thus, $D(\text{ON}-\text{F}^-) = 0.94 + 0.69 - 3.45 + 0.90 + 2.69 = 1.77$ eV with a deviation of $\{(.10)^2 + (.32)^2\}^{\frac{1}{2}}$; or $D(\text{ON}-\text{F}^-) = 1.77 \pm 0.34$ eV. This positive value for $D(\text{ON}-\text{F}^-)$ is another fact supporting the stability of the ONF^- ion.

Fluorine Nitrate (NO_3F)

The appearance potential data obtained on the NO_3F molecule are given in Table 14. The high intensity IE curve of NO_2^+ , which indicated that only a single ion-source process was occurring, gave an excellent EVD fit with argon. For the low intensity IE curve of OF^+ , the lower AP was estimated by the linear intercept method and the higher was determined by EVD. The two lowest AP's of F^+ determined by linear intercepts were quite poor due to the very low intensity of the F^+ ion and to the fact that at least one more higher energy process was also occurring. The O^+ IE curve indicated several ion-source processes occurring, but

Table 14. Appearance Potentials of Fluorine Nitrate (NO_3F)

Ion	AP exptl (eV)	No. of Trails	Ave. Dev. (eV)	Method	Quality of Data	Process	calc. (eV)	AP exptl.-calcd. (eV)
NO_2^+	12.62	7	0.10	EVD	excellent	$\text{NO}_3\text{F} + e \rightarrow \text{NO}_2^+ + \text{OF} + 2e$	12.48	+0.14
OF^+	15.60	4	0.25	LI	poor	$\rightarrow \text{OF}^+ + \text{NO}_2 + 2e$	15.15	+0.45
OF^+	18.59	4	0.31	EVD	fair	$\rightarrow \text{OF}^+ + \text{NO} + 0 + 2e$	18.33	+0.26
F^+	13.50	3	0.47	LI	poor	$\rightarrow \text{F}^+ + \text{NO}_3^- + e$	14.34	-0.84
F^+	18.45	3	0.48	LI	poor	$\rightarrow \text{F}^+ + \text{NO}_3 + 2e$	18.85	+0.40
						$\rightarrow \text{F}^+ + \text{NO}_2^- + 0$	16.92	+1.54
						+ e		
O^+	13.62	4	0.10	LI & EVD	fair	$\rightarrow \text{O}^+ + \text{NO}_2 + \text{F}^-$	13.65	-0.03
						$\rightarrow \text{O}^+ + \text{NO}_2^- + \text{F}$	13.11	+0.51
						+ e		

only the lowest energy process was measured using both the LI and EVD methods. The AP of NO^+ was not measured due to the constantly changing slope of the IE curve of NO^+ near the threshold of ionization.

For the NO_2^+ ion, the AP is attributed to the process

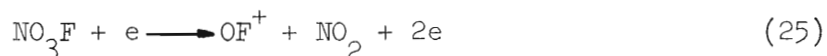


where

$$A(\text{NO}_2^+) = \Delta H_f(\text{NO}_2) + \Delta H_f(\text{OF}) + I(\text{NO}_2) - \Delta H_f(\text{NO}_3\text{F}) \quad (24)$$

Therefore, $A(\text{NO}_2^+)_{\text{calc.}} = 0.34 + 1.26 + 11.0 - (0.12) = 12.48$ eV, which is 0.14 eV lower than the measured value of 12.62 eV.

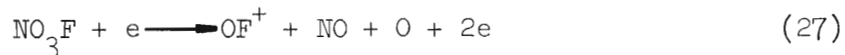
The first AP of OF^+ is attributed to



where

$$A_1(\text{OF}^+) = \Delta H_f(\text{OF}^+) + \Delta H_f(\text{NO}_2) - \Delta H_f(\text{NO}_3\text{F}) \quad (26)$$

Therefore, $A_1(\text{OF}^+)_{\text{calc.}} = 14.93 + 0.34 - 0.12 = 15.15$ eV, which is 0.45 eV lower than the measured value of 15.60 eV. The second AP of OF^+ is attributed to the process



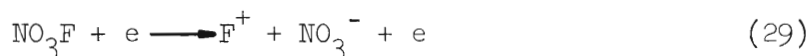
where

$$A_2(\text{OF}^+) = \Delta H_f(\text{OF}^+) + \Delta H_f(\text{NO}) + \Delta H_f(\text{O}) - \Delta H_f(\text{NO}_3\text{F}) \quad (28)$$

Thus, $A_2(\text{OF}^+)_{\text{calc.}} = 14.93 + 0.94 + 2.58 - 0.12 = 18.33$ eV, which is

0.26 eV lower than the measured value of 18.59 eV.

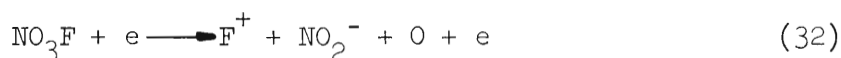
The first AP of F^+ is attributed to



where

$$A_1(F^+) = \Delta H_f(F) + \Delta H_f(NO_3^-) + I(F) - \Delta H_f(NO_3F) \quad (30)$$

Thus, $A_1(F^+)_{\text{calc.}} = 0.69 - 3.65 + 17.42 - 0.12 = 14.34$ eV, which is 0.84 eV higher than the measured value of 13.50 eV. The second AP of F^+ could be due to one or both of the following two competing ion-source processes:



in which the respective appearance potentials are

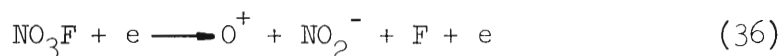
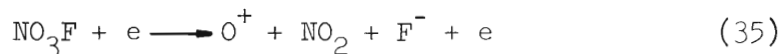
$$A_2(F^+) = \Delta H_f(F) + \Delta H_f(NO_3) + I(F) - \Delta H_f(NO_3F) \quad (33)$$

$$A_2'(F^+) = \Delta H_f(F) + \Delta H_f(NO_2) + \Delta H_f(O) + I(F) - EA(NO_2) - \Delta H_f(NO_3F) \quad (34)$$

Therefore, the respective calculated AP's are: $A_2(F^+)_{\text{calc.}} = 0.69 + 0.74 + 17.42 - 0.12 = 18.85$ eV; and $A_2'(F^+)_{\text{calc.}} = 0.69 + 0.34 + 2.58 + 17.42 - 3.99 - 0.12 = 16.92$ eV. These are 0.40 eV higher and 1.54 lower, respectively, than the measured value of 18.45 eV. Even though $A_2(F^+)_{\text{calc.}}$ and $A_2'(F^+)_{\text{calc.}}$ differ by almost 2.0 eV, it is impossible to choose between Eqs. 33 and 34 due to the very high average deviation in $A_2(F^+)_{\text{exptl.}}$

(0.48 eV) and to the possibility of the production of excess energy in the ion-source process.

Similarly, the AP of O^+ can be attributed to one or both of the following two processes:



in which the respective AP's are

$$A(O^+) = \Delta H_f(O) + \Delta H_f(NO_2) + \Delta H_f(F) + I(O) - EA(F) - \Delta H_f(NO_3F) \quad (37)$$

$$A'(O^+) = \Delta H_f(O) + \Delta H_f(NO_2) + \Delta H_f(F) + I(O) - EA(NO_2) - \Delta H_f(NO_3F) \quad (38)$$

Thus, the respective calculated AP's are: $A(O^+)_{\text{calc.}} = 2.58 + 0.34 + 0.69 + 13.61 - 3.45 - 0.12 = 13.65$ eV; and $A'(O^+)_{\text{calc.}} = 2.58 + 0.34 + 0.69 + 13.61 - 3.99 - 0.12 = 13.11$ eV. These are 0.03 eV higher and 0.51 eV lower than the measured value of 13.62.

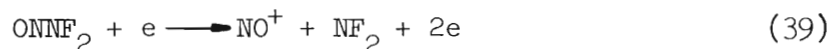
The only AP data on the positive ions of NO_3F of high enough quality to have quantitative significance is $A(NO_2^+)_{\text{exptl.}}$. Table 14 shows that $A(NO_2^+)_{\text{exptl.}}$ is greater than $A(NO_2^+)_{\text{calc.}}$ by 0.14 eV. However, much uncertainty remains regarding the "accepted" value of $\Delta H_f(OF)$. This problem, which is directly related to $D(FO-F)$ and $D(O-F)$, is discussed in Appendix A. It is most likely that $\Delta H_f(OF)$ is the least accurate of the quantities involved in Eq. 24. By substituting $A(NO_2^+)_{\text{exptl.}}$ and the literature values of $\Delta H_f(NO_2)$, $I(NO_2)$ and $\Delta H_f(NO_3F)$ into Eq. 24, the heat of formation of OF is derived accordingly: $12.62 = 0.34 + \Delta H_f(OF) + 11.0 - 0.12$; or $\Delta H_f(OF)_{\text{derived}} = 1.40 \pm 0.10$ eV.

The value of $A(\text{NO}_2^+)_{\text{exptl.}}$ can also be used to calculate the lower limit of the ionization potential of NO_3F . Since the molecular ion, NO_3F^+ , is not observable in the mass spectrometer, then $D(\text{NO}_2^+-\text{OF}) < 0$. Since $D(\text{NO}_2^+-\text{OF}) = A(\text{NO}_2^+) - I(\text{NO}_3\text{F})$, then $I(\text{NO}_3\text{F}) > A(\text{NO}_2^+)$, or $I(\text{NO}_3\text{F}) > 12.62$ eV.

Nitrosodifluoramine (ONNF_2)

The AP data for the ONNF_2 molecule are shown in Table 15. The high intensity IE curves for NO^+ and NF_2^+ both indicated only one ion-source process occurring and both gave good or excellent matches with the IE curve of argon in applying the EVD method. The IE curve for NF^+ showed a break several volts above the threshold, thus indicating two ion-source processes of differing threshold energies. The lower AP of NF^+ was determined using both linear intercepts and EVD. The second AP of NF^+ was obtained by EVD by subtracting the contribution to the IE curve of NF^+ from the lower energy process.

For the NO^+ ion the attributed ion-source process is



where

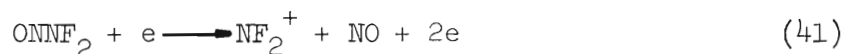
$$A(\text{NO}^+) = \Delta H_f(\text{NO}) + \Delta H_f(\text{NF}_2) + I(\text{NO}) - \Delta H_f(\text{ONNF}_2) \quad (40)$$

By substituting the literature values into Eq. 40, $A(\text{NO}^+)_{\text{calc.}} = 0.94 + 0.37 + 9.25 - 0.82 = 9.74$ eV., which is 0.34 eV lower than the measured value of 10.08 eV.

For the NF_2^+ ion the attributed process is

Table 15. Appearance Potentials of Nitrosodifluoramine (ONNF_2)

Ion	AP	No. of Trails	Ave. Dev. (eV)	Method	Quality of Data	Process	calc.	AP
	exptl (eV)						(eV)	exptl.-calc. (eV)
NO^+	10.08	8	0.13	EVD	good	$\text{ONNF}_2 \rightarrow \text{NO}^+ + \text{NF}_2 + 2\text{e}$	9.74	+0.34
NF_2^+	12.81	7	0.03	EVD	excellent	$+e \rightarrow \text{NF}_2^+ + \text{NO} + 2\text{e}$	12.49	+0.32
NF^+	11.61	6	0.08	LI & EVD	fair	$\rightarrow \text{NF}^+ + \text{NO} + \text{F}^- + \text{e}$	12.24	-0.63
NF^+	15.76	4	0.08	EVD	good	$\rightarrow \text{NF}^+ + \text{NO} + \text{F} + 2\text{e}$	15.69	+0.07

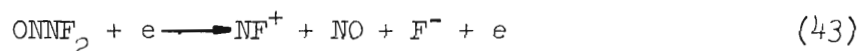


where

$$A(\text{NF}_2^+) = \Delta H_f(\text{NF}_2) + \Delta H_f(\text{NO}) + I(\text{NF}_2) - \Delta H_f(\text{ONNF}_2) \quad (42)$$

Thus, $A(\text{NF}_2^+)_{\text{calc.}} = 0.37 + 0.94 + 12.0 - 0.82 = 12.49$ eV, which is 0.32 eV lower than the measured value of 12.81 eV.

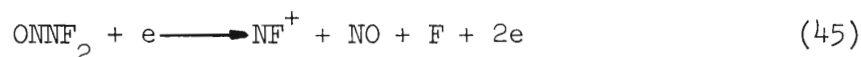
For NF^+ the attributed lower energy process is



where

$$A_1(\text{NF}^+) = \Delta H_f(\text{NF}^+) + \Delta H_f(\text{NO}) + \Delta H_f(\text{F}) - \text{EA}(\text{F}) - \Delta H_f(\text{ONNF}_2) \quad (44)$$

Thus, $A_1(\text{NF}^+)_{\text{calc.}} = 14.88 + 0.94 + 0.69 - 3.45 - 0.82 = 12.24$ eV, which is 0.63 eV higher than the measured value of 11.61 eV. The higher energy process for NF^+ is attributed to



where

$$A_2(\text{NF}^+) = \Delta H_f(\text{NF}^+) + \Delta H_f(\text{NO}) + \Delta H_f(\text{F}) - \Delta H_f(\text{ONNF}_2) \quad (46)$$

Therefore, $A_2(\text{NF}^+)_{\text{calc.}} = 14.88 + 0.94 + 0.69 - 0.82 = 15.69$ eV, which is 0.07 eV lower than the measured value of 15.76 eV.

For the above measured data on ONNF_2 , only the AP's of NO^+ and NF_2^+ are of high enough quality to have quantitative significance. The experimental minus the calculated AP's for NO^+ and NF_2^+ are +0.34 and

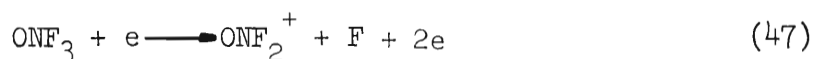
+0.32 eV, respectively. Therefore, the AP data for both NO^+ and NF_2^+ both indicate that the heat of formation of ONNF_2 should be 0.33 eV less than the literature value of 0.82 eV obtained by an equilibrium constant method⁵⁷. Therefore, $\Delta H_f(\text{ONNF}_2)_{\text{derived}} = 0.49 \pm 0.13$ eV. The low value for $A_1(\text{NF}^+)_{\text{exptl.}}$ is unexplained, but it is probably attributable to inaccuracy in the method.

The lower limit to the ionization potential of ONNF_2 can be calculated as follows. Since ONNF_2^+ is not observable in the mass spectrometer, then it is assumed that $D(\text{ON}^+-\text{NF}_2) < 0$. Since $D(\text{ON}^+-\text{NF}_2) = A(\text{NO}^+) - I(\text{ONNF}_2)$, and $A(\text{NO}^+)_{\text{exptl.}} = 10.08$ eV, the $I(\text{ONNF}_2) > 10.08$ eV.

Trifluoramine Oxide (ONF_3)

The only appearance potential determinations on positive ions from ONF_3 were made on ONF_2^+ . The high intensity IE curve for ONF_2^+ indicated only one ion-source process occurring, and the EVD fit with argon was excellent. The value of $A(\text{ONF}_2^+)_{\text{exptl.}}$ was determined to be 14.15 ± 0.03 eV from nine measurements. The intensity of the parent molecular ion, ONF_3^+ , was much too low to obtain a direct measurement of the ionization potential of ONF_3 . The IE curves for the other fragment ions, especially NO^+ and F^+ , were of constantly changing slope near the threshold of ionization, thus indicating several competing ion-source processes for each fragment. It was not possible to determine the AP's of these fragments.

The ion-source process attributed to the formation of ONF_2^+ is



where

$$A(\text{ONF}_2^+) = \Delta H_f(\text{ONF}_2^+) + \Delta H_f(\text{F}) - \Delta H_f(\text{ONF}_3) \quad (48)$$

and

$$\Delta H_f(\text{ONF}_2^+) = \Delta H_f(\text{ONF}_2) + I(\text{ONF}_2) \quad (49)$$

Dibeler and Walker⁷⁰ measured $A(\text{ONF}_2^+)$ for Eq. 47 to be 13.59 eV by photon impact. Thus, by combining Eqs. 48 and 49, it is reasonable to conclude that

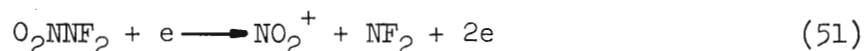
$$\begin{aligned} I_{\text{vert.}}(\text{ONF}_2) - I_{\text{adiab.}}(\text{ONF}_2) &= A(\text{ONF}_2^+)_{\text{this work}} - A(\text{ONF}_2^+)_{\text{Dibeler}} \quad (50) \\ &\approx 14.15 - 13.59 \\ &= 0.56 \pm 0.03 \text{ eV} \end{aligned}$$

This large difference between the vertical and adiabatic ionization potentials of ONF_2 is not surprising since ONF_3 is nearly tetrahedral whereas the ONF_2^+ ion is planar^{111,112}.

Nitrodifluoramine (O_2NNF_2)

The AP data for the new compound O_2NNF_2 is given in Table 16. The IE curves for NO_2^+ and NF_2^+ both indicated only one ion-source process and both gave good or excellent EVD fits with argon. For the NO^+ and NF^+ ions, the IE curves indicated at least two ion-source processes in each. These curves gave fair to poor results for the first and second AP's of NO^+ and NF^+ .

The process attributed to the formation of NO_2^+ is



where

Table 16. Appearance Potentials of Nitrodifluoramine (O_2NNF_2)

Ion	AP exptl (eV)	No. of Trails	Ave. Dev. (eV)	Method	Quality of Data	Process	calc. (eV)	AP exptl.-calc. (eV)
NO_2^+	11.71	9	0.11	EVD	excellent	$O_2NNF_2 + e \rightarrow NO_2^+ + NF_2 + 2e$	-	-
NO^+	9.70	3	0.17	LI	poor	$\rightarrow NO^+ + O + NF_2^- + e$	9.89	-0.19
NO^+	13.20	2	0.01	EVD	fair	$\rightarrow NO^+ + O + NF_2 + 2e$	13.14	+0.06
NF_2^+	12.28	5	0.17	EVD	good	$\rightarrow NF_2^+ + NO_2 + 2e$	12.71	-0.43
NF^+	11.75	2	0.25	LI	poor	$\rightarrow NF^+ + F^- + NO_2 + e$	12.46	-0.71
						$\rightarrow NF^+ + F + NO_2^- + e$	11.92	-0.17
NF^+	15.52	3	0.02	EVD	fair	$\rightarrow NF^+ + F + NO_2 + 2e$	15.91	-0.39

$$A(\text{NO}_2^+) = \Delta H_f(\text{NO}_2) + \Delta H_f(\text{NF}_2) + I(\text{NO}_2) - \Delta H_f(\text{O}_2\text{NNF}_2) \quad (52)$$

Substitution of $A(\text{NO}_2^+)_{\text{exptl.}}$ and the appropriate literature values into Eq. 52 gives: $11.71 = 0.34 + 0.37 + 11.0 - \Delta H_f(\text{O}_2\text{NNF}_2)_{\text{derived}}$; or $\Delta H_f(\text{O}_2\text{NNF}_2)_{\text{derived}} = 0.00 \pm 0.11$ eV.

The attributed process for the lower AP of NO^+ is

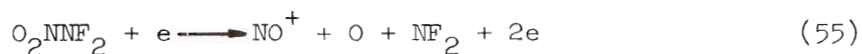


where

$$A_1(\text{NO}^+) = \Delta H_f(\text{NO}) + \Delta H_f(\text{O}) + \Delta H_f(\text{NF}_2) + I(\text{NO}) - EA(\text{NF}_2) - \Delta H_f(\text{O}_2\text{NNF}_2) \quad (54)$$

If $\Delta H_f(\text{O}_2\text{NNF}_2)_{\text{derived}}$ is used along with the appropriate literature values, then $A_1(\text{NO}^+)_{\text{calc.}} = 0.94 + 2.58 + 0.37 + 9.25 - 3.25 - 0.00 = 9.89$ eV, which is 0.19 eV higher than the measured value of 9.70 eV.

The second AP of NO^+ is attributed to

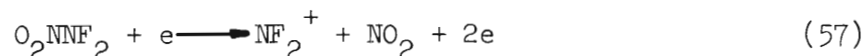


where

$$A_2(\text{NO}^+) = A_1(\text{NO}^+)_{\text{calc.}} + EA(\text{NF}_2) \quad (56)$$

Therefore, $A_2(\text{NO}^+)_{\text{calc.}} = 9.89 + 3.25 = 13.14$ eV, which is 0.06 eV lower than the measured value of 13.20 eV.

For the NF_2^+ ion the attributed process is

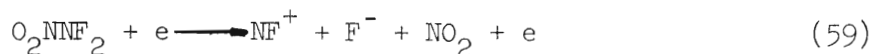


where

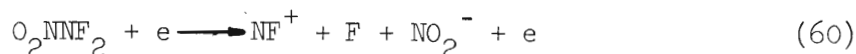
$$A(\text{NF}_2^+) = \Delta H_f(\text{NF}_2) + \Delta H_f(\text{NO}_2) + I(\text{NF}_2) - \Delta H_f(\text{O}_2\text{NNF}_2) \quad (58)$$

Therefore, $A(\text{NF}_2^+)_{\text{calc.}} = 0.37 + 0.34 + 12.0 - 0.00 = 12.71$ eV, which is 0.43 eV higher than the measured value of 12.28 eV.

The lower energy process for NF^+ can be attributed to one or both of the following:



or



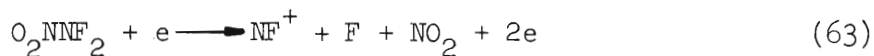
where

$$A_1(\text{NF}^+) = \Delta H_f(\text{NF}^+) + \Delta H_f(\text{F}) + \Delta H_f(\text{NO}_2) - \text{EA}(\text{F}) - \Delta H_f(\text{O}_2\text{NNF}_2) \quad (61)$$

and

$$A_1'(\text{NF}^+) = \Delta H_f(\text{NF}^+) + \Delta H_f(\text{F}) + \Delta H_f(\text{NO}_2) - \text{EA}(\text{NO}_2) - \Delta H_f(\text{O}_2\text{NNF}_2) \quad (62)$$

Substitution into Eqs. 61 and 62 gives $A_1(\text{NF}^+)_{\text{calc.}} = 12.46$ eV and $A_1'(\text{NF}^+)_{\text{calc.}} = 11.92$ eV which are 0.71 eV higher and 0.17 eV lower, respectively, than the measured value of 11.75 eV. The higher energy process for NF^+ is attributed to



where

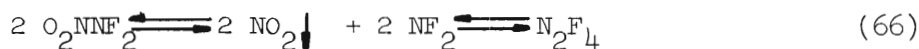
$$A_2(\text{NF}^+) = \Delta H_f(\text{NF}^+) + \Delta H_f(\text{F}) + \Delta H_f(\text{NO}_2) - \Delta H_f(\text{O}_2\text{NNF}_2) \quad (64)$$

This yields $A_2(\text{NF}^+)_{\text{calc.}} = 15.91 \text{ eV}$, which is 0.39 eV higher than the measured value of 15.52 eV.

It is evident from Table 16 that the data on $A(\text{NO}_2^+)$ are consistent with $A_1(\text{NO}^+)$ and $A_2(\text{NO}^+)$ within experimental error. However, for $A(\text{NF}_2^+)$, $A_1(\text{NF}^+)$, and $A_2(\text{NF}^+)$ the experimental minus the calculated values are consistently negative. These values should be positive, if anything, due to the production of excess energy as predicted from Stevenson's Rule. As mentioned in an earlier section, the spectrum of $\text{O}_2\text{N NF}_2$ was never completely void of N_2F_4 . This suggests that $\text{O}_2\text{N NF}_2$ is decomposing slightly, even at -130 to -135°C . Decomposition should occur in the gas phase according to:



But since NO_2 has a negligible vapor pressure at -130°C , the decomposition process (Eq. 65) is modified to be:



This suggests that the gaseous components would consist entirely of molecular $\text{O}_2\text{N NF}_2$ and N_2F_4 and NF_2 radicals. Therefore, in relation to the appearance potentials, NO_2^+ must be coming from $\text{O}_2\text{N NF}_2$, whereas NF_2^+ and NF^+ could arise from $\text{O}_2\text{N NF}_2$, NF_2 , or N_2F_4 . Since $I(\text{NF}_2) = 12.0 \text{ eV}$ and $A(\text{NF}^+, \text{NF}_2) = 11.8$ and 15.5 eV ,⁸² then the low values obtained for $A(\text{NF}_2^+)_{\text{exptl.}}$, $A_1(\text{NF}^+)_{\text{exptl.}}$, and $A_2(\text{NF}^+)_{\text{exptl.}}$ are most probably due to the presence of NF_2 radicals in the gas phase.

The lower limit of the ionization potentials of $\text{O}_2\text{N NF}_2$ can be calculated in the following manner since $\text{O}_2\text{N NF}_2^+$ is not observable in

the mass spectrometer:



where

$$D(\text{O}_2\text{N}^+ - \text{NF}_2) = A(\text{NO}_2^+) - I(\text{O}_2\text{NNF}_2) < 0 \quad (68)$$

Thus, $I(\text{O}_2\text{NNF}_2) > 11.71 \text{ eV}$.

Summary of Results from Appearance Potential Data

The results derived from the appearance potential data on the six N-O-F compounds are tabulated in Table 17. The heats of formation of ONF, NO_2F , OF, ONNF_2 , and O_2NNF_2 were derived to be -0.90 ± 0.10 , -1.46 ± 0.12 , $+1.40 \pm 0.10$, $+0.49 \pm 0.13$, and $0.00 \pm 0.11 \text{ eV}$, respectively. The ionization potential of NO_2F was measured to be $13.15 \pm 0.12 \text{ eV}$. The difference between the vertical and adiabatic ionization potentials of ONF_2 was derived to be 0.56 eV . The lower limits to the ionization potentials of ONF, NO_3F , ONNF_2 , and O_2NNF_2 were derived to be 11.78, 12.62, 10.08, and 11.71 eV, respectively. Other derived results were: $EA(\text{ONF}) = 2.69 \text{ eV}$; $D(\text{NO}_2^+ - \text{F}) = 0.34 \text{ eV}$; and $D(\text{ON-F}^-) = 1.77 \text{ eV}$. The derived results in Table 17 are compared to literature values of Table 19 whenever possible.

Bond Dissociation Energies in N-O-F Species

The bond dissociation energies at 298°K for many N-O-F species are tabulated in Table 18. These values were derived from the heats of formation obtained in this work (Table 17) along with other necessary heats of formation from the literature (Table 19). The bond orders

Table 17. Summary of Thermodynamic Quantities
Derived from Appearance Potential Data

Quantity	X This Work (eV)	Y Literature ^a (eV)	X - Y Difference (eV)
ΔH_f (ONF)	-0.90 ± 0.10	-0.68	-0.22
ΔH_f (NO ₂ F)	-1.46 ± 0.12	-1.12	-0.34
ΔH_f (OF)	$+1.40 \pm 0.10$	+1.26	+0.14
ΔH_f (ONNF ₂)	$+0.49 \pm 0.13$	+0.82	-0.33
ΔH_f (O ₂ NNF ₂)	0.00 ± 0.11	--	--
I (ONF)	>11.78	--	--
I (NO ₂ F)	13.15 ± 0.12	--	--
I (NO ₃ F)	>12.62	--	--
I (ONNF ₂)	>10.08	--	--
$I_{\text{vert.}} - I_{\text{adiab.}}$ (ONF ₂)	0.56 ± 0.03	--	--
I (O ₂ NNF ₂)	>11.71	--	--
EA (ONF)	2.69 ± 0.32	--	--
D (NO ₂ ⁺ -F)	0.34 ± 0.17	--	--
D (ON-F ⁻)	1.77 ± 0.34	--	--

^a See Table 19

(equal to one-half the number of electrons in a particular bond) were determined from the Double Quartet structures given by this author in Appendix B and by Linnett^{113,114}. From Table 18 it can be seen that increasing bond order generally results in increasing bond dissociation energy.

Table 18. Bond Dissociation Energies at 298°K in N-O-F Species

Type Bond	Species	D (eV)	Bond Order
N-F	NF-F	3.15	1
	ON-F	2.53	0.5-1
	O ₂ N-F	2.49	0.5-1
	NF ₂ -F	2.44	1
	N-F	2.39	1
	ONF ₂ -F	1.9 ^a	0.5-1
N-O	FN-O	6.68	2-2.5
	N-O	6.54	2.5
	F ₃ N-O	4.22 ^b	1-2
	O ₂ NNO-O	3.35	1.5
	ON-O	3.18	1.5-2
	FNO-O	3.14	1.5-2
	F ₂ NNO-O	3.07	1.5
	F ₃ N-O	2.68 ^c	1-2
	NN-O	1.73	1-2
	O ₂ N-OF	1.62	1-1.5
	O-F	1.87	1.5
	FO-F	1.84	1
O-F	O ₂ NO-F	1.31	1
	FO ₂ -F	0.75	0.5-1
	O ₂ -F	0.42	0-0.5

Table 18. Bond Dissociation Energies at 298°K in N-O-F Species (Continued)

Type Bond	Species	D (eV)	Bond Order
N-N	N-N	9.80	3
	ON-N	4.99	2-3
	F ₂ N-NF ₂	0.96	1
	ON-NF ₂	0.82	1
	O ₂ N-NF ₂	0.71	1
	O ₂ N-NO ₂	0.59	1
	O ₂ N-NO	0.42	1
O-O	O-O	5.16	2
	FO-O	3.71	1.5-2
	FO-OF	2.59	1.5-2
	O ₂ -O	1.10	1.5
F-F	F-F	1.38	1

^aEstimated by Dibeler and Walker⁷⁰ assuming $I(\text{ONF}_2) = I(\text{NF}_2)$

^bUsing Dibeler et al.'s⁷⁰ value of $\Delta H_f(\text{ONF}_3) = -3.02$ eV

^cUsing Bougen et al.'s⁷¹ value of $\Delta H_f(\text{ONF}_3) = -1.48$ eV

CHAPTER IV

CONCLUSIONS AND RECOMMENDATIONS

Conclusions

The work described in the preceding chapters has led to the following conclusions:

1) The five previously known N-O-F compounds (ONF , NO_2F , NO_3F , ONNF_2 and ONF_3) were readily prepared using low temperature, vacuum methods published in the literature.

2) The previously unidentified compound, nitrodifluoramine (O_2NNF_2), was prepared by pyrolyzing N_2F_4 at 310°C to form NF_2 radicals and then adding NO_2 with a subsequent fast quench at -196°C . This compound, a white solid at -196°C , is unstable at room temperature, decomposing to N_2F_4 and NO_2 .

3) The reactions of O_2F_2 with NO , NO_2 , N_2F_4 and NH_3 , of N_2F_4 with O_2 and O_3 , and of NF_3 with F_2 produced no evidence for new N-O-F compounds.

4) Pure O_2F_2 is a yellow solid at low temperatures rather than an orange or yellow-orange solid as previously thought.

5) An unidentified red-brown substance was observed by condensing a mixture of N_2F_4 and NO at -196°C . This substance decomposed between -183 and -168°C before exerting a sufficiently high vapor pressure to be detected in the mass spectrometer. On the basis of Linnett's Double Quartet Model, this substance is postulated to be F_2NONNF_2 .

6) The six N-O-F compounds were identified by their unique positive and negative ion spectra in a Bendix TOF mass spectrometer. The mass spectra of the known N-O-F compounds were previously unreported except for the positive ion spectra of ONF_3 .

7) The temperatures at which the vapor pressures of ONNF_2 and O_2NNF_2 are one torr were estimated to be $-141 \pm 2^\circ\text{C}$ and $-123 \pm 2^\circ\text{C}$ by comparing the observed vapor pressures of 0.1-0.2 torr for ONF_3 , NO_2F , ONNF_2 , NO_3F , ONF and O_2NNF_2 .

8) The appearance potentials were measured for most of the positive ions of the six N-O-F compounds. These were compared to the appearance potentials of the attributed ion-source processes calculated from the best literature values of heats of formation, ionization potentials and electron affinities. The heats of formation of ONF , NO_2F , OF , and O_2NNF_2 were derived to be -0.90 ± 0.10 , -1.46 ± 0.12 , $+1.40 \pm 0.10$ and $+0.49 \pm 0.13$ eV, respectively. These were compared to the literature values of -0.68 , -1.12 , $+1.26$ and $+0.82$ eV, respectively. The heat of formation of the previously unreported O_2NNF_2 was derived to be 0.00 ± 0.11 eV. The previously unreported $I(\text{NO}_2\text{F})$ was directly measured to be 13.15 ± 0.12 eV. The lower limits of the ionization potentials of ONF , NO_3F , ONNF_2 and O_2NNF_2 were estimated to be 11.78, 12.62, 10.08, and 11.71 eV, respectively. The vertical minus the adiabatic ionization potentials of ONF_2 was derived to be 0.56 ± 0.03 eV. The electron affinity of ONF was estimated to be 2.69 ± 0.32 eV. An extensive list of bond dissociation energies at 298°K in N-O-F species was tabulated. These values were calculated from the quantities derived in this thesis and other thermodynamic quantities from the literature.

9) The Linnett Double Quartet Model was used to construct stable electronic configurations for the known species ONF , NO_2F , NO_3F , ONNF_2 , ONF_3 , O_2NNF_2 , the ONF_2 radical, and the ONF^- and ONF_2^+ ions. The Double Quartet Model was also used to propose the most likely structures of a wide variety of postulated N-O-F species and to draw approximate conclusions regarding their likely existence. The compounds F_2NONNF_2 , FO_2NO , FONO , ONNFNFNO , and $\text{F}_{3-n}\text{N}(\text{OF})_n$ ($n = 1, 2, 3$) were shown to have marginal stabilities, which suggests the possible isolation of these species in the future. The compounds $(\text{ONNF}_2)_2$, FOO_2NO , O_2NF_2 , F_2NONF_2 , $\text{F}_2\text{NO}_2\text{NF}_2$, and $\text{F}_{3-n}\text{N}(\text{O}_2\text{F})_n$ ($n = 1, 2, 3$) were shown to be unlikely. It was impossible to construct any plausible covalent structures for NF_5 and F_3NNF_3 .

Recommendations

The results of this work have led to the following recommendations and proposals.

1) Further work should be directed toward the synthesis of FO_2NO , FONO , ONNFNFNO , and $\text{F}_{3-n}\text{N}(\text{OF})_n$ ($n = 1, 2, 3$), which were predicted to have marginal stabilities. Some new experimental procedures might involve a reactor which accommodates two types of activation simultaneously, such as rf discharge and pyrolysis or electric discharge and pyrolysis, followed by a fast quench at low temperatures. The reactions of NO and NO_2 with O_2F_2 in an appropriate solvent, such as CF_3Cl , should be studied with hopes of preparing one of the above compounds.

2) The physical and chemical properties of the new compound nitrodifluoramine, O_2NNF_2 , should be studied thoroughly. Several important areas would be low temperature nmr and ir spectra, vapor pressure data,

heat of formation from equilibrium data, and reactions with various hydrocarbons.

3) The identity of the unstable red-brown substance observed in the condensation of N_2F_4 and NO should be determined. Low temperature ir may prove useful in this task.

4) Work is presently underway in this laboratory to parameterize the MINDO molecular orbital computer program for calculating heats of formation and ionization potentials of compounds containing N-N, N-O and N-F bonds. This work should be extended to include the six known N-O-F compounds and the several compounds predicted by the Double Quartet Model.

APPENDICES

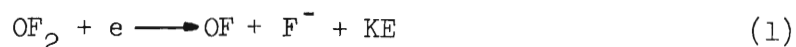
APPENDIX A

SUMMARY OF BEST LITERATURE VALUES
FOR THERMODYNAMIC QUANTITIES OF N-O-F SPECIES

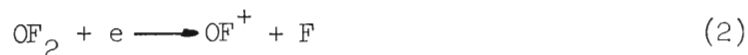
In order to calculate bond dissociation energies and heats of formation from appearance potential data, it is necessary to accumulate an accurate list of the particular thermodynamic quantities required for these calculations. Tables 19, 20, and 21 summarize the latest and best values from the literature for standard heats of formation, ionization potentials, and electron affinities of N-O-F species. Table 19 also shows the relatively small enthalpy difference between 0 and 298°K for many species. In this thesis all calculations are referred to 298°K. Wherever applicable, the listed values have been revised to allow for internal consistency. For example, $\Delta H_f^0_{298}(\text{ONNF}_2)$ was reported as 20.4 kcal./mole in 1963 based upon the heat of reaction between NO and N_2F_4 ⁵⁴. However, this value is revised to 18.9 kcal./mole using the more recent value of $\Delta H_f^0_{298}(\text{N}_2\text{F}_4)$ listed in Table 19.

The following values from Tables 19, 20 and 21 require qualification: the heats of formation and ionization potentials of OF and NF; the ionization potentials of NO₂ and NF₂; and the electron affinities of NO₂, NO₃, and NF₂.

Dibeler et al.¹¹⁵ derived $D(\text{O-F}) = 1.1 \text{ eV}$, $D(\text{FO-F}) = 2.8 \text{ eV}$, and $I(\text{OF}) = 13.00 \text{ eV}$ based upon their data for



and



However, their results were based upon the then "accepted" values of $\text{EA}(\text{F}) = 3.6 \text{ eV}$, $\Delta H_f(\text{OF}_2) = 7.6 \text{ kcal./mole}$, $\Delta H_f(\text{F}) = 18.9 \text{ kcal./mole}$, and $\Delta H_f(\text{O}) = 59.2 \text{ kcal./mole}$.

The more recent values from Tables 19, 20, and 21 recalculate Dibeler's results (referred to 298°K) to be $\text{D}(\text{O-F}) = 1.49 \text{ eV}$, $\text{D}(\text{FO-F}) = 2.65 \text{ eV}$, and $\text{I}(\text{OF}) = 13.15 \text{ eV}$. Dibeler's data also lead to $\Delta H_f(\text{OF}) = 2.21 \text{ eV}$ and $\Delta H_f(\text{OF}^+) = 14.93 \text{ eV}$. Dibeler's revised values for $\text{D}(\text{O-F})$, $\text{D}(\text{FO-F})$, $\text{I}(\text{OF})$, and $\Delta H_f(\text{OF})$ are somewhat suspect because they are based upon the negative ion mass spectrometric determination of $\text{A}(\text{F}^-)$ and K.E. for Eq. 1. However, $\Delta H_f(\text{OF}^+)$ determined from $\text{A}(\text{OF}^+)$ in Eq. 2 should be accurate to about 0.2 eV .

Troe et al.¹¹⁶ derived $\text{D}(\text{FO-F}) = 37 \text{ kcal./mole}$ (1.60 eV) from their data on the unimolecular decomposition of OF_2 . They further derived $\text{D}(\text{O-F}) = 53 \text{ kcal./mole}$ (2.30 eV) using outdated values for the heats of formation of OF_2 , O , and F . The latest values from Table 19 for the ΔH_f 's of OF_2 , O and F and Troe's result for $\text{D}(\text{FO-F})$ leads to $\text{D}(\text{O-F}) = 2.11 \text{ eV}$ and $\Delta H_f(\text{OF}) = 1.16 \text{ eV}$.

Recently O'Hare and Wahl¹¹⁷ have discussed in detail the problem of the bond dissociation energies $\text{D}(\text{FO-F})$ and $\text{D}(\text{O-F})$. They concluded that the most likely value for $\text{D}(\text{FO-F})$ was $1.7 \pm 0.2 \text{ eV}$, from which they derived $\text{D}(\text{OF}) = 2.2 \pm 0.2 \text{ eV}$. Their calculations were referred to 0°K and they used the questionable heat of formation of F of 18.4 kcal./mole (0.8 eV). If one accepts the heats of formation of O , F and OF_2 from Table 19, $\text{D}(\text{FO-F}) = 1.7 \pm 0.2 \text{ eV}$ leads to $\Delta H_f(\text{OF}) = \text{D}(\text{FO-F}) +$

$\Delta H_f(\text{OF}_2) - \Delta H_f(\text{F}) = 1.26 \pm 0.2$ eV, which is taken as the best value for purposes of calculation in this work.

The values of $\Delta H_f(\text{NF})$ and $I(\text{NF})$ were reported by Dibeler and Walker⁷⁰ in a mass spectrometric photoionization study of NF_3 . They derived $\Delta H_f(\text{NF}^+)$ to be 14.88 eV. They combined this with the assumption that $I(\text{NF}) = I(\text{NF}_2)$ (11.7 eV) and calculated $\Delta H_f(\text{NF})$ to be 3.2 eV. They considered their assumption of $I(\text{NF}) = I(\text{NF}_2)$ to be reasonable since O_2 , which is isoelectronic with NF , has an approximately equal ionization potential of 12.07 eV.

Two values for $I(\text{NF}_2)$ are listed in Table 20. The value of 11.73 eV derived by Dibeler et al. in a photoionization study of NF_3 should correspond to the adiabatic ionization potential. The value of 12.00 eV reported by Franklin et al.⁸² was determined by an electron impact measurement on NF_2 radicals and should correspond to the vertical IP of NF_2 . This latter value is therefore taken as the best value for purposes of calculation in this thesis.

The ionization potential of NO_2 has been the subject of much controversy. Franklin et al.⁸² reported the nine most reliable determinations of $I(\text{NO}_2)$ to be 9.78, 9.80, 10.2, 11.1, 10.97, 11.0, 11.3, 11.27, and 11.3 eV. These values generally fall into two groups: those centered around 10.0 eV ($I_{\text{adiab.}}$) and those centered around 11.0 eV ($I_{\text{vert.}}$). The large difference between $I_{\text{adiab.}}$ and $I_{\text{vert.}}$ is due to the fact that the NO_2 molecule is bent while the NO_2^+ ion is linear. As part of this thesis research, the ionization potential of NO_2 was re-measured using the extrapolated voltage difference method with Ar as

reference. The result was $I(\text{NO}_2) = 10.99 \pm 0.15$ eV from nine measurements. Therefore, the value of $I(\text{NO}_2) = 11.0$ eV was taken as the best value for purposes of calculation in this thesis.

Reports of the electron affinity of NO_2 vary from 1.62 to 3.99 eV (see Table 21). The high value of 3.99 eV was selected as the best value as was also recommended by the JANAF Tables (1966)¹¹⁰.

Two values reported for $\text{EA}(\text{NO}_3)$ are 3.88 and 3.99 eV (see Table 21). The value of $\text{EA}(\text{NO}_3) = 4.39$ eV calculated according to

$$\text{EA}(\text{NO}_3) = \Delta H_f(\text{NO}_3) + \Delta H_f(\text{NO}_3^-) \quad (3)$$

where $\Delta H_f(\text{NO}_3)$ and $\Delta H_f(\text{NO}_3^-)$ are taken from Table 19 was selected for use herein.

The only report of $\text{EA}(\text{NF}_2)$ was given as 3.25 eV in the Chemistry and Physics Handbook¹¹⁸. It was not possible to locate the original reference to this value.

Table 19. Best Literature Values of Standard Heats of Formation

Species	ΔH_f° 0		ΔH_f° 298		Reference
	(kcal./mole)	(eV)	(kcal./mole)	(eV)	
N	112.5	4.90	113.0	4.90	54
O	58.99	2.56	59.59	2.58	54
F	15.45	0.67	15.91 ^a	0.69	119
O ₃	34.8	1.51	34.1	1.48	54
NO	21.46	0.93	21.58	0.94	54
NO ₂	8.59	0.37	7.91	0.34	54
NO ₃	18.5	0.78	17.0	0.74	54
N ₂ O	20.43	0.89	19.61	0.85	54
N ₂ O ₃	--	--	19.80	0.86	54
N ₂ O ₄	4.47	0.19	2.17	0.09	54
N ₂ O ₅	--	--	2.7	0.12	54
NF	--	--	74.5	3.2	70
NF ₂	9.1 ^a	0.39	8.5	0.37	120
NF ₃	-30.35 ^a	-1.32	-31.75	-1.38	120
N ₂ F ₄	-2.4	-0.01	-5.0	-0.22	120
OF	--	--	29.1	1.26	b
OF ₂	6.40 ^a	0.28	5.86	0.25	121
O ₂ F	6.5	0.28	6.1	0.27	c
O ₂ F ₂	--	--	4.73	0.21	122
O ₃ F ₂	--	--	6.24	0.27	122

Table 19. Best Literature Values of Standard Heats of Formation
(Continued)

Species	ΔH_f° 0		ΔH_f° 298		Reference
	(kcal./mole)	(eV)	(kcal./mole)	(eV)	
ONF	-15.2 ^a	-0.66	-15.8	-0.68	22
NO ₂ F	-24.4 ^d	-1.06	-25.8	-1.12	40
NO ₃ F	-2.4 ^a	-0.10	-4.2	-0.18	53
	+4.3 ^a	+0.19	+2.5	+0.12	40,f
ONNF ₂	--	--	18.9	0.82	f
ONF ₃	--	--	-34.1	-1.48	71
	--	--	-69.6	-3.02	70
NF ⁺	--	--	343.1	14.88	70
OF ⁺	--	--	344.4	14.93	g
NO ₃ ⁻	--	--	-84.2	-3.65	123

^a Calculated using enthalpy difference for temperature from JANAF
Tables (1965)⁵⁴

^b Calculated from the data of O'Hare et al.¹¹⁷

^c Revised from value given by JANAF Tables (1967)¹²⁴ using more recent
value of ΔH_f° 298(F)

^d Calculated using enthalpy difference for temperature from JANAF
Tables (1966)¹¹⁰

^e Accepted as the better value by JANAF Tables (1965)⁵⁴

^f Recalculated from the data of Johnson and Colburn⁵⁷

^g Calculated from the data of Dibeler et al.¹¹⁵

Table 20. Best Literature Values of Ionization Potentials

Species	Ionization Potential (eV)	Reference
N	14.53	118
O	13.61	118
F	17.42	118
Ar	15.76	118
O ₃	12.80	108
NO	9.25	82
NO ₂	9.78, 9.80, 10.2 11.1, 10.97, 11.0 ^a	82
NF	11.7 ^b	70
NF ₂	11.73 12.0 ^a	70 82
NF ₃	13.00	70
ONF ₃	13.26	70
OF	13.15	c

^aTaken as the best value for this work

^bAssumed

^cRecalculated from the data of Dibeler, et al.¹¹⁵

Table 21. Best Literature Values of Electron Affinities

Species	Electron Affinity (eV)	Reference
F	3.448	110
O	1.465	110
O ₃	2.88	109
NO	0.87	125
	0.91 ^a	126
	1.62	109
	2.34	127
NO ₂	3.10	128
	3.99 ^{a,b}	126
	3.88	109
NO ₃	3.99	127
	4.39 ^a	c

^aTaken as the best value for this work

^bAccepted by the JANAF Tables (1966)¹¹⁰

^cDerived from $\Delta H_f^\circ(\text{NO}_3)$ and $\Delta H_f^\circ(\text{NO}_3^-)$ from Table 19

APPENDIX B

ELECTRONIC STRUCTURES OF N-O-F COMPOUNDS
USING LINNETT'S DOUBLE QUARTET MODELIntroduction

In recent years Linnett^{113,114} has developed an interesting and workable empirical model to describe the electronic structures of molecules consisting of atoms from the First Short Period. This model, called the Double Quartet, is a modification of the Lewis-Langmuir Octet Rule which emphasized the pairing of electrons to form an octet around the nucleus. Linnett's approach, however, deemphasizes the importance of the pairing of electrons and treats the octet as consisting of two groups of four electrons, or a double-quartet, each group having opposite electron spins.

The purpose of this appendix is to provide a systematic study of the electronic structures of N-O-F compounds using Linnett's Double Quartet Model. The structures of the known N-O-F compounds and several selected ions are adequately described using this approach. Also, most probable structures for several postulated N-O-F compounds are proposed. Based upon these structures, conclusions are drawn as to the likely existence and stability of these postulated compounds.

A detailed explanation of the Double Quartet Model can be found elsewhere^{113,114}. In general, Linnett's model is based upon the premise that the local disposition of electrons around each nucleus is determined

by Pauli Principle and inter-electron repulsion. The Pauli Principle leads to the conclusion that electrons of like spin tend to repel each other, while those of opposite spin tend to come together. These are known as "spin correlation" effects. Inter-electron repulsion, or "charge correlation," results from the fact that all electrons have the same negative charge and thus repel each other.

The determination of the Linnett structures is also guided by the formal charge distribution in the atoms. The formal charge for a particular atom is calculated by algebraically summing the charges associated with the atom according to the following simple rules: the nuclear charge and the charges on the inner-shell and unshared electrons are treated as being fully associated with the atom; and the charges on electrons shared in a bond with another atom are assigned half to each atom. Based upon experience Linnett¹¹⁴ has suggested the formal charge limitations shown in Table 22 for nitrogen, oxygen, and fluorine. The

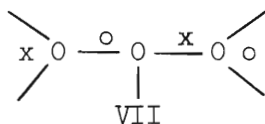
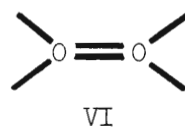
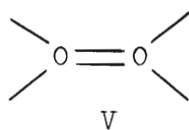
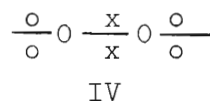
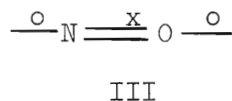
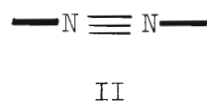
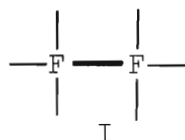
Table 22. Formal Charge Limitations

Atom	Satisfactory	Possible
N	$-\frac{1}{2}$ to +1	-1 (just)
O	$-\frac{1}{2}$ to $+\frac{1}{2}$	-1 and +1
F	-1 to $+1/3$	$+\frac{1}{2}$

formal charges designated satisfactory result in structures of considerable importance, whereas those labeled possible result in structures of only minor importance. The most probable structures are also determined in light of Pauling's Adjacent Charge Rule which states:⁴⁷

"In general, structures in which adjacent atoms have electrical charges of the same spin are much less important than other structures, the diminution in importance resulting from the increase in coulomb energy corresponding to the adjacent charges."

The formulae used in representing the Linnett structures are as follows. Crosses (x) and circles (o) each represent electrons, but of opposite spins. A heavy line represents two electrons of opposite spins occupying the same spatial orbital, i.e. a close pair, and a light line represents two electrons of opposite spins on the same atom or between the same pair of atoms, but not occupying the same spatial orbital. A few simple examples demonstrating the notation are given below, where I-VII represent F_2 , N_2 , NO, the ground state of O_2 , the first and second excited states of O_2 , and O_3 , respectively.



ONF and ONF⁻

Linnett¹¹⁴ has discussed the structure of nitrosyl fluoride according to the five following structures, where the formal charges and number of close pairs are given in Table 23. Structures XI and XII

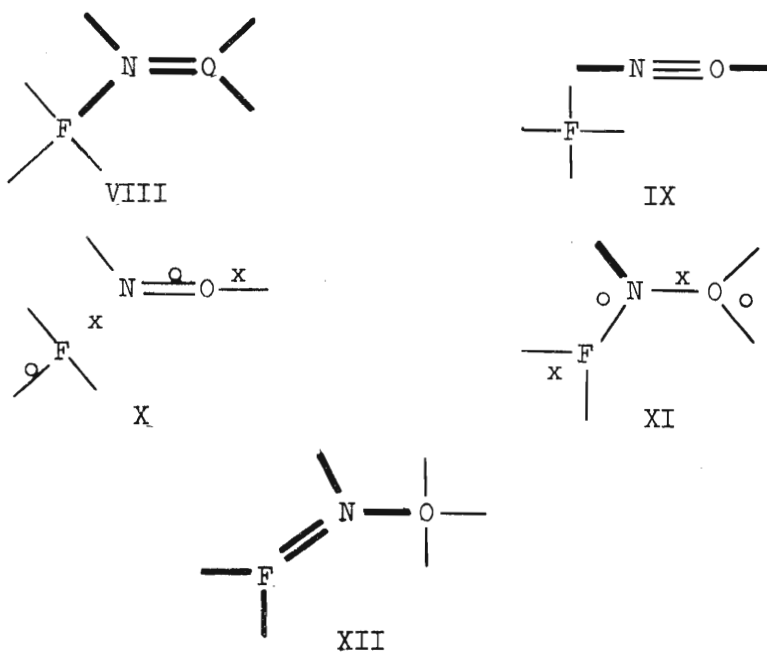


Table 23. Formal Charges in ONF

	F	N	O	No. of Close Pairs
VIII	0	0	0	6
IX	-1	0	+1	2
X	$-\frac{1}{2}$	0	$+\frac{1}{2}$	0
XI	$+\frac{1}{2}$	0	$-\frac{1}{2}$	1
XII	+1	0	-1	6

are excluded because of the positive formal charges on the F atom. The isoelectronic molecule ozone has structure XI, but in O_3 the formal charges are all zero and thus more favorable. Structure IX is expected to be of minor importance compared to VII and X due to the +1 formal charge on the O atom. Both VII and X have permissible charge distributions. However, X is clearly more favorable since it has no close pairs, whereas VIII has six pairs of electrons in which both electrons occupy the same spatial orbital. Since the repulsion forces of VIII are much greater than those in X, then X should be the most stable configuration.

Structure X predicts that the N-F bond length should be abnormally long. This is indeed the case, since the N-F bond is 1.512 \AA in ONF° compared to the single bond length of 1.371 in NF_3^{54} . Structure X also predicts that FNO has the same five electron N-O bond as in nitric oxide. Once again, the bond lengths, 1.136 \AA for N-O in FNO and 1.15 \AA in NO^{54} , confirm this prediction.

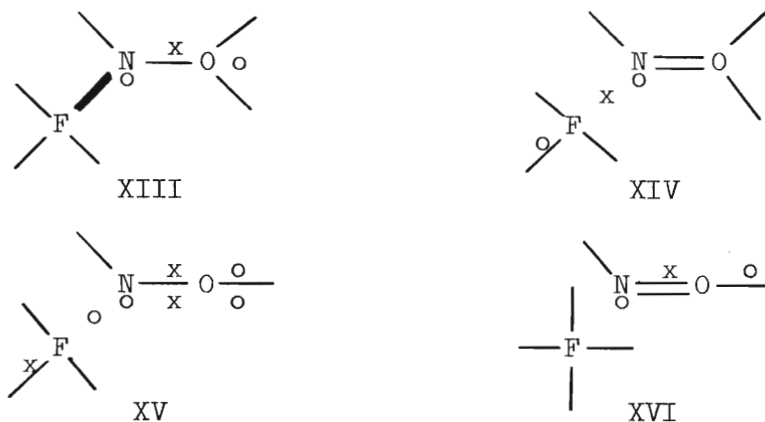
Jones et al.¹⁹ have discussed the bonding in nitrosyl fluoride in terms of three valence-bond representations, which are, in fact, equivalent to the Linnett structures VII, IX, and XII. They maintained that the major contribution is from VIII and explain the ONF° angle as follows. The NO sigma bond is considered to involve a nitrogen sp hybrid orbital with the lone pair on N occupying the other sp orbital. The second NO bond is a p π bond leaving the third p orbital for sigma bonding to fluorine. The resulting ONF° angle should be 90° , but they contend that this is increased to the actual value of 110° by the repulsion between the O and F atoms. This repulsion and distortion also is said to

lead to a longer and weaker NF bond than in NF_3 . Also, Pauling¹²⁹ and Buckton et al.²¹ have suggested that the structure of ONF^- is a combination of the Lewis structures VIII, IX, and XII.

From the above discussion it is evident that the Linnett model gives a far superior description of the electronic structure of ONF^- than does the traditional valence-bond approach. Whereas the valence-bond approach suggests a combination of several unsatisfactory structures, the Double Quartet model shows that one structure adequately accounts for the properties of the ONF^- molecule. Furthermore, the discussion by Jones et al.¹⁹ of the bonding in ONF^- seems rather nebulous. In the representation given by VIII, one usually considers the nitrogen orbitals to consist of three sp^2 and one p orbital rather than two sp and two p orbitals. This, in fact, would predict an ONF^- angle of 120° , which, if anything, would be increased by repulsion between the F and O atoms.

There are four likely structures, shown below, for the ONF^- ion. None of these violate the rules established for formal charge distributions, nor do they contain a large number of close pairs (see Table 24). Structure XIII is the least likely since no negative charge is assigned to the fluorine atom. Structure XVI, which consists of F^- loosely bonded to NO, is somewhat questionable due to the adjacent negative charges on F and N. Of the remaining two structures, XV is the more likely since it allows the larger separation of electrons, i.e. decreased inter-electron repulsion.

Structure XV predicts that the ONF^- ion should have a stable configuration. Thus, it is not surprising that the electron affinity

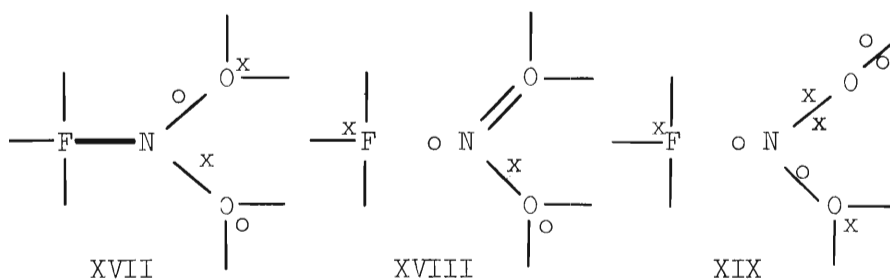
Table 24. Formal Charges in ONF^-

	F	N	O	No. of Close Pairs
XIII	0	$-\frac{1}{2}$	$-\frac{1}{2}$	1
XIV	$-\frac{1}{2}$	$-\frac{1}{2}$	0	0
XV	$-\frac{1}{2}$	$-\frac{1}{2}$	0	0
XVI	-1	$-\frac{1}{2}$	$+\frac{1}{2}$	0

of ONF^- was derived in the text to be a rather large 2.69 eV, even though ONF^- contains an odd number of electrons. Furthermore, XV predicts a rather weak ON-F^- bond. This is indeed the case, as the value for $D(\text{ON-F}^-)$ was derived in the text to be 1.77 eV as compared to an average $D(\text{N-F})$ of about 2.5 eV.



There are three structures for nitrosyl fluoride, shown below, which give reasonable representations of the electronic distribution. These are, in fact, identical to the structures proposed by Linnett^{113,114}

Table 25. Formal Charges in NO_2F

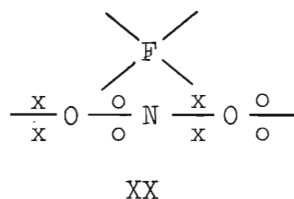
	F	N	O	O	No. of Close Pairs
XVII	0	+1	$-\frac{1}{2}$	$-\frac{1}{2}$	1
XVIII	$-\frac{1}{2}$	+1	0	$-\frac{1}{2}$	0
XIX	$-\frac{1}{2}$	+1	0	$-\frac{1}{2}$	0

for nitryl chloride. Structure XVII suffers from the disadvantage of having one close pair of electrons and not having any negative charge on the F atom. Structure XIX has a greater separation of electrons than XVIII, but suffers slightly from having electrons of one spin (the x's) favor a linear ONO group while the electrons of opposite spin (the o's) favor a bent ONO group. Thus, it is difficult to choose a priori between the three structures.

At the time Linnett wrote his book, the NF bond distance in NO_2F was believed to be 1.35 \AA^{29} . This influenced Linnett¹¹⁴ to conclude: ". . . it can be said, with complete certainty, that the FN bond is not abnormally long and so does not resemble the NF bond in FNO." This would suggest the importance of structure XVII, which is the major structure for NO_2Cl . However, recently Legon and Millen³⁰ (see Introduction)

found that the N-F bond in $\text{NO}_2\overset{\text{O}}{\text{F}}$ is 1.467 Å, which may not be quite as long as the 1.512 Å in $\text{ON}\overset{\text{O}}{\text{F}}$, but certainly is long compared to the 1.371 Å in NF_3 . They also found that the nitro-group parameters in $\text{NO}_2\overset{\text{O}}{\text{F}}$ differ considerably from those in HNO_2 and NO_2Cl . These facts strongly suggest that XVII is the least important of the three structures for $\text{NO}_2\overset{\text{O}}{\text{F}}$. The difference between the structures of $\text{NO}_2\overset{\text{O}}{\text{F}}$ and NO_2Cl is probably attributable to the greater electronegativity of F compared to Cl.

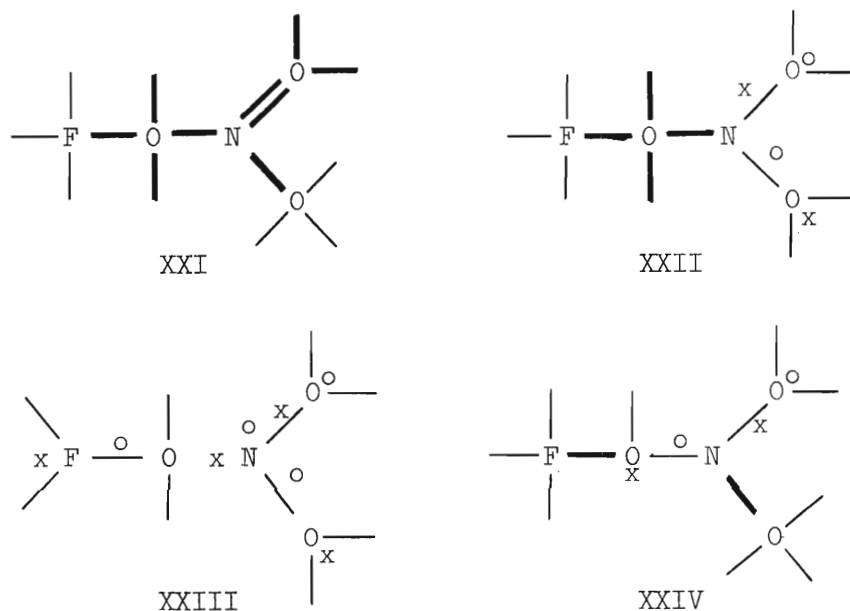
Legon and Millen³⁰ suggested that the above facts concerning the molecular parameters of $\text{NO}_2\overset{\text{O}}{\text{F}}$ could be interpreted on the basis of a greater contribution of an ionic structure $\text{O}_2\text{N}^+\text{F}^-$. The most stable double quartet representation of this would be



This places the allowed formal charges of -1 on F, +1 on N, and zero on both O atoms. This arrangement, however, strongly favors a linear ONO group. Since the actual ONO angle is 136° , the ionic structure XX is rather unlikely.



The structure of fluorine nitrate is known to be planar, with the nitro group bonded to an OF group through an O-N bond. Four possible double quartet structures for NO_3F are shown below. Of these structures

Table 26. Formal Charges in NO_3F

	F	O'	N	O	O	No. of Close Pairs
XXI	0	0	+1	0	-1	9
XXII	0	0	+1	$-\frac{1}{2}$	$-\frac{1}{2}$	4
XXIII	$+\frac{1}{2}$	0	$+\frac{1}{2}$	$-\frac{1}{2}$	$-\frac{1}{2}$	0
XXIV	0	$+\frac{1}{2}$	+1	$-\frac{1}{2}$	-1	2

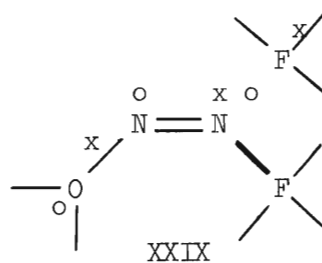
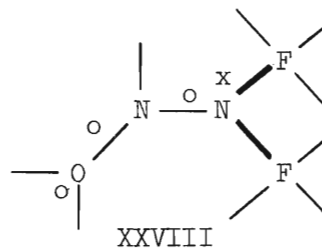
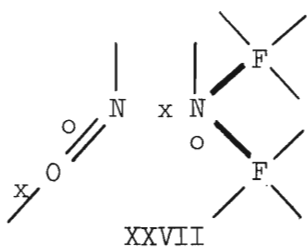
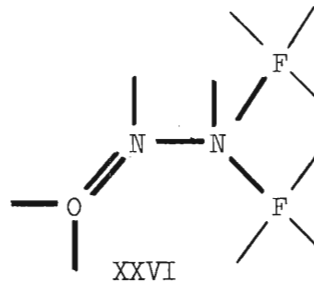
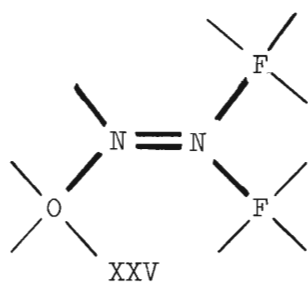
XXI, which is actually the simple valence-bond representation, is most unsatisfactory due to the high charge correlation from nine close pairs of electrons. Structure XXIII is rather unlikely because of the $+\frac{1}{2}$ formal charge on the F atom. The remaining two structures are reasonable, but both contain slight disadvantages. Structure XXII has the more favorable charge distribution, but contains four close pairs. Structure XXIV, and its mirror image, has only two close pairs, but it gives a borderline

formal charge of -1 to one of the O atoms. It also suffers slightly from the disadvantage of having positive formal charges on the adjacent O and N atoms. All four structures predict the NO_3 group to be planar and allow for the O-F bond also to lie in the same plane.

The fact that fluorine nitrate is unstable and even explodes at liquid air temperature indicates that structures normally thought to be of only minor importance may actually be the most important in this molecule. From Table 3 the bond lengths in NO_3F are 1.42, 1.39, and 1.29 Å for F-O', O'-N, and N-O respectively. These are compared to the single F-O bond of 1.412 Å in OF_2 , the single O'-N bond of 1.46 Å in $\text{O}_2\text{NO}'\text{NO}_2$, and the three-electron N-O bond of 1.18 Å in the nitro group of N_2O_3 ⁵⁴. This suggests that the F-O' in NO_3F is indeed a single bond, whereas the O'-N bond is slightly stronger than the normal N-O single bond and the N-O bond (nitro group) is in between a normal single and three electron bond. Furthermore, the slow thermal decomposition of NO_3F (see Introduction) is initiated by cleavage of the F-O' bond, suggesting that this is the weakest bond in the molecule. From the above discussion it is evident that the structure of NO_3F is adequately explained by a combination of XXII and XXIV.



The actual structure of ONNF_2 is unknown, but it is generally believed to consist of a nitric oxide and difluoramine radical joined through a N-N bond. Five possible double quartet structures for this arrangement are shown below with the formal charge distributions given in Table 27. The valence-bond structure XXV is eliminated because of

Table 27. Formal Charges in ONNF_2

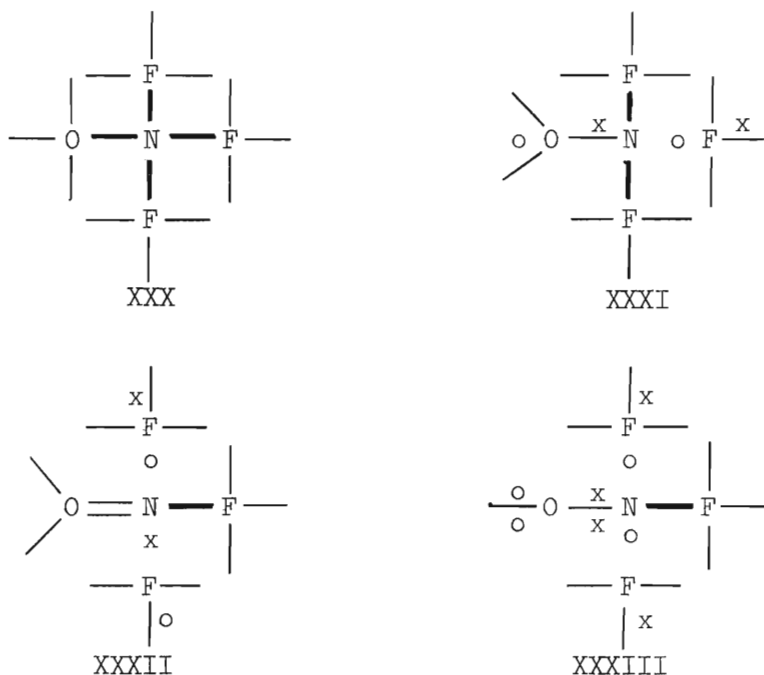
	O	N	N	F	F	No. of Close Pairs
XXV	-1	0	+1	0	0	6
XXVI	0	0	0	0	0	9
XXVII	$+\frac{1}{2}$	0	$-\frac{1}{2}$	0	0	2
XXVIII	$-\frac{1}{2}$	0	$+\frac{1}{2}$	0	0	2
XXIX	$-\frac{1}{2}$	$+\frac{1}{2}$	$+\frac{1}{2}$	$-\frac{1}{2}$	0	1

the high number of close pairs (6) and the -1 formal charge on the O atom. Structure XXVI, although it has a favorable formal charge distribution, suffers from high inter-electron repulsion due to nine close pairs. The remaining three structures have very few close pairs, but they have the slight disadvantage of requiring some of the electrons to be distorted from their tetrahedral arrangement in the quartet, thus increasing the absolute energy in the molecule. However, XXVIII is favored over XXVII since the negative charge resides on the O atom and the positive charge on the N atom in XXVIII, whereas the opposite is the case for XXVII. Structure XXIX suffers from the added disadvantage of having positive formal charges on adjacent N atoms. From the above discussion it seems that the most probable structure would be XXVIII with possibly some contributions from XXVII and XXIX.

If the nitric oxide and difluoramine radicals were joined by an O-N rather than N-N bond, then structures XXV-XXIX (with the O and N interchanged) would yield the following respective formal charge distributions for the N (nitroso group) and O atoms: (-2,+1), (-1,+1), $(-\frac{1}{2},+1)$, $(-\frac{3}{2},+1)$, and $(-\frac{3}{2},+\frac{3}{2})$. All of these distributions are prohibitive and indicate that the two radicals are definitely joined by a N-N bond.

ONF₃, ONF₂⁺, and ONF₂ Radical

The trifluoramine oxide molecule, ONF₃, is very nearly tetrahedral, with N as the central atom. Four likely structures for this configuration are shown below. The simple valence bond structure XXX is the least likely since it contains four close pairs of electrons and

Table 28. Formal Charges In ONF_3

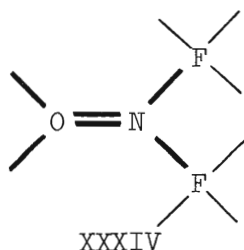
	O	N	F	F	F	No. of Close Pairs
XXX	-1	+1	0	0	0	4
XXXI	$-\frac{1}{2}$	+1	0	$-\frac{1}{2}$	0	2
XXXII	0	+1	$-\frac{1}{2}$	0	$-\frac{1}{2}$	1
XXXIII	0	+1	$-\frac{1}{2}$	0	$-\frac{1}{2}$	1

a -1 formal charge on the O atom. The remaining three structures and their mirror images all have permissible charge distributions and fewer close pairs. Structures XXXII and XXXIII are quite similar, but inter-electron repulsion favors XXXIII. Structure XXXIII has a slight advantage over XXXI in having one fewer close pair and $-\frac{1}{2}$ formal charge shifted

from the O to another F atom. However, XXXI has slightly less distortion of the electrons from their tetrahedral arrangement. Thus, it seems likely that the structure of ONF_3 is a combination of XXXI and XXXIII.

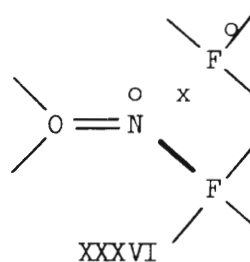
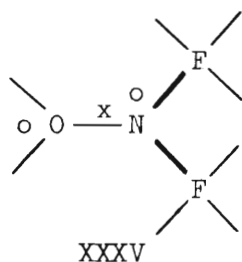
Bartlett et al.⁶⁵ suggested that the bonding in ONF_3 could be formulated in a conventional way, with the O atom joined to NF_3 by a semi-ionic bond $\equiv \text{N}^+ - \text{O}^-$, which is equivalent to XXX. From the above discussion this seems rather unlikely. More recently Fox and coworkers,⁶⁶ on the basis of the observed infrared spectrum of ONF_3 , concluded that the N-O bond has nearly 75 percent double bond character. The combination of the Linnett structures XXXI and XXXIII is compatible with this conclusion. Also, it is obvious from XXXI and XXXIII why ONF_3 never decomposes to NF_3 and why it acts as a fluorinating rather than oxygenating agent, i.e. the weak link in the molecule is a one electron N-F bond.

The most likely structure for the ONF_2^+ ion is



in which there are a relatively high number of close pairs (6) and the formal charges are zero on the O and F atoms and +1 on the N atom. The arrangement of the electrons in XXXIV predicts a planar configuration for ONF_2^+ . This is indeed the case, since the ionic complexes $\text{NF}_2\text{O}^+\text{SbF}_6^-$, $\text{NF}_2\text{O}^+\text{AsF}_6^-$, $\text{NF}_2\text{O}^+\text{BF}_4^-$, and $\text{NF}_2\text{O}^+\text{B}_2\text{F}_7^-$ have recently been prepared^{111,112} in which the ONF_2^+ cation is planar.

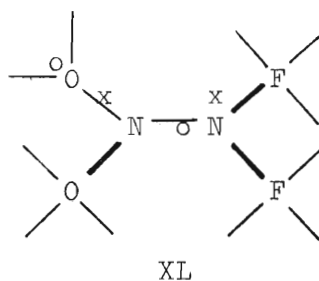
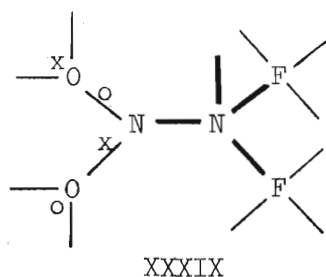
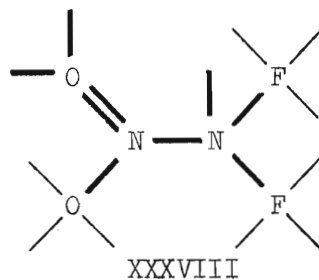
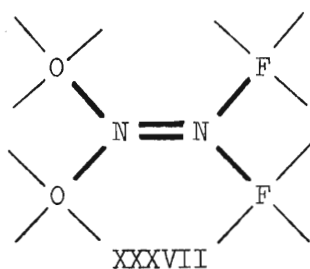
Two possible structures for the ONF_2 free radical are



in which the formal charges on the O, N and two F atoms are $(-\frac{1}{2}, +\frac{1}{2}, 0, 0)$ and $(0, +\frac{1}{2}, 0, -\frac{1}{2})$, respectively. Both structures have permissible charge distributions, but XXXVI and its mirror image are favored slightly over XXXV since it has one fewer close pair and the formal charge of $-\frac{1}{2}$ is on a F atom rather than the O atom. However, both structures suffer from the disadvantage that the electrons of one spin favor a planar arrangement while those of the opposite spin do not. The above double quartet structures suggest that the ONF_2 radical might possess a stable structure. Fox et al.⁶⁰ claimed to have produced the relatively stable ONF_2 radical by photolysis of ONF_3 at -196°C .



Four likely configurations for the new compound, O_2NNF_2 , claimed to have been prepared and identified in this work, are shown below in XXXVII-XL. Structure XXXVII is highly unlikely since it has six close pairs and formal charges of -1 on both O atoms and +1 on adjacent N atoms. Structure XXVIII is equally unlikely due to the high repulsion forces from nine close pairs and the -1 formal charge on one of the O atoms. Structure XL has the fewest number of close pairs (3), but it is also unsatisfactory due to the -1 charge on one O atom and the positive formal charges on adjacent N atoms. The remaining structure, XXXIX, has an

Table 29. Formal Charges In O_2NNF_2

	O	O	N	N	F	F	No. of Close Pairs
XXXVII	-1	-1	+1	+1	0	0	6
XXXVIII	-1	0	+1	0	0	0	9
XXXIX	$-\frac{1}{2}$	$-\frac{1}{2}$	+1	0	0	0	4
XL	-1	$-\frac{1}{2}$	+1	$+\frac{1}{2}$	0	0	3

excellent charge distribution and four close pairs. The bonding in the NO_2 and NF_2 groups of XXXIX is identical to that in N_2O_4 and N_2F_4 , respectively. (These are not shown for sake of brevity.) Thus, structure XXXIX predicts that O_2NNF_2 should exist, and that the bond lengths should be similar to the N-F bond of 1.37 Å in NF_3 and the N-N and N-O bonds of 1.75 and 1.18 Å, respectively, in N_2O_4 .

ONNF₂ Dimer and F₂NONNF₂

Two possibilities for the unidentified red-brown substance observed in the condensation of NO and N₂F₄ are an ONNF₂ dimer and the molecule F₂NONNF₂ (see text). In Linnett's discussion of the dimerization of nitroso-compounds,¹¹⁴ he suggests that organic nitroso-compounds dimerize readily in order to reduce their high inter-electron repulsion. Linnett proposed four possible structures for (RNO)₂, R being alkyl or aryl. The two expected to give a major contribution are

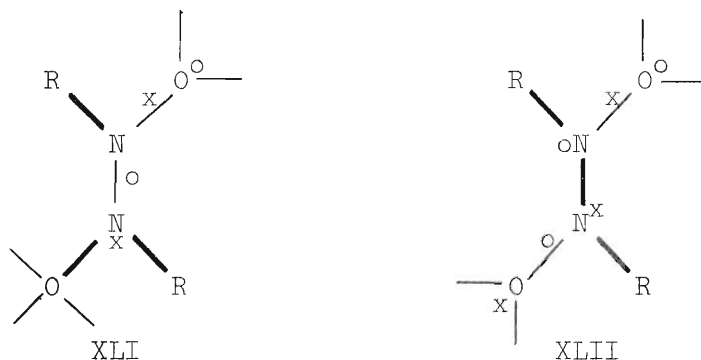


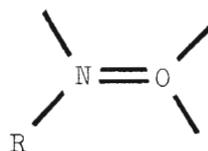
Table 30. Formal Charges in (RNO)₂

	R	N	O	O	N	R	No. of Close Pairs
XLI	0	+1	- $\frac{1}{2}$	-1	+ $\frac{1}{2}$	0	3
XLII	0	+ $\frac{1}{2}$	- $\frac{1}{2}$	- $\frac{1}{2}$	+ $\frac{1}{2}$	0	3

Formal charge distributions favor XLII over XLI (and its mirror image), but XLI has the slight advantage that in XLII the electrons of different spins favor different shapes at both N atoms, whereas in XLI both sets

favor a planar arrangement at the upper N atom but at the other N atom one set favors a non-planar arrangement (x's) while the other set (o's) favors a planar arrangement. However, both sets suffer slightly from having positive formal charges on adjacent N atoms. Linnett concluded that the actual structure of $(\text{RNO})_2$ is due to equal contributions from XLI and XLII.

Since organic nitroso-compounds have the normal Lewis-structures, such as



XLIII

it is easy to understand why dimerization readily occurs. The $(\text{RNO})_2$ would be more stable than two RNO 's since the number of close pairs of electrons would be reduced from twelve in the latter to only three in the former, and the total bond order would remain constant. The nitrosyl halides (XNO), on the other hand, do not dimerize since they have no close pairs which would result in high inter-electron repulsion.

If ONNF_2 had the structure XXVI, then the dimer of ONNF_2 should be more stable than the monomer. However, as explained earlier, the structure of ONNF_2 consists of contributions from XXVII, XXVIII, and XXIX. Therefore, dimerization is not favored because there is no net decrease in inter-electron repulsion and no net increase in bond order. This suggests that the existence of $(\text{ONNF}_2)_2$ is rather doubtful, since ONNF_2 , itself, is stable only at cryogenic temperatures.

Three possible double quartet structures for the F_2NONNF_2 molecule are shown below in XLIV-XLVI. The most likely structure is XLVI

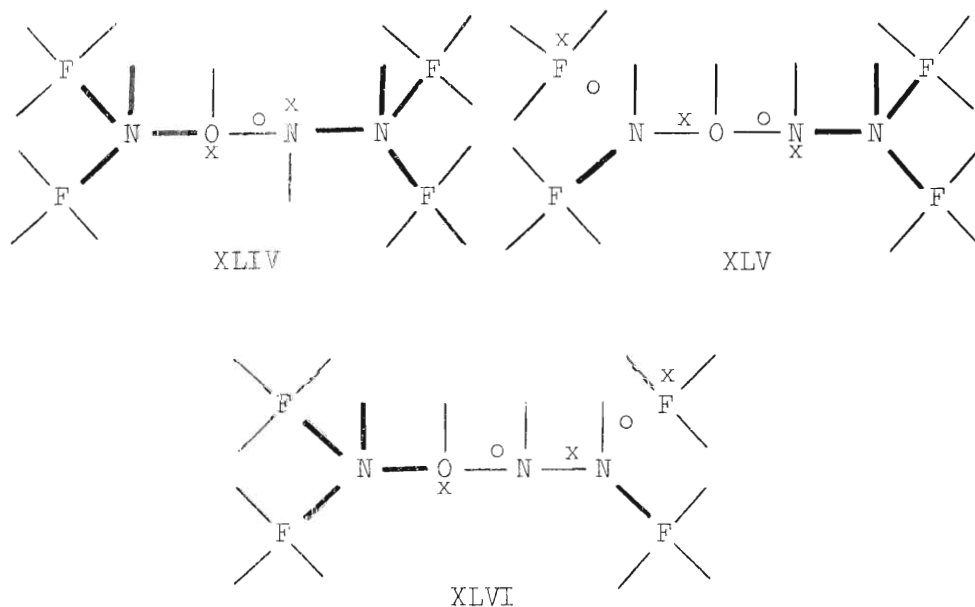


Table 31. Formal Charges In F_2NONNF_2

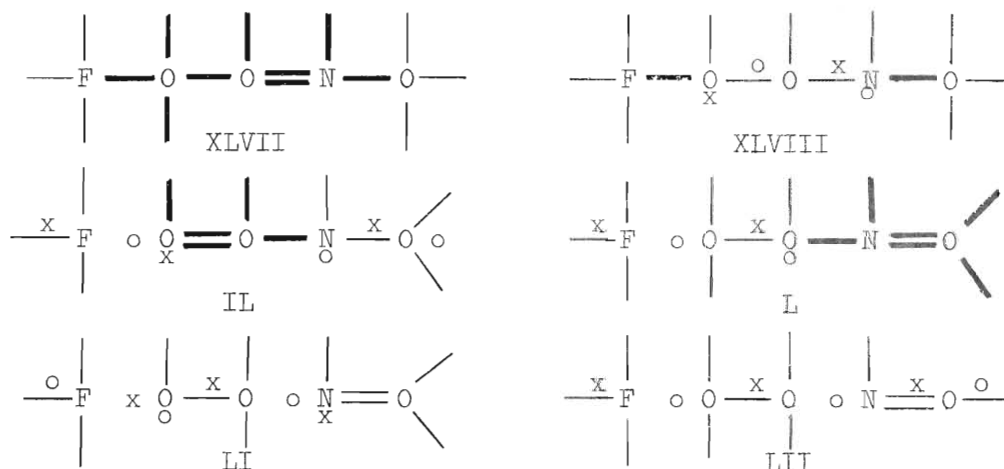
	F	F	N	O	N	N	F	F	No. of Close Pairs
XLIV	0	0	0	$+\frac{1}{2}$	$-\frac{1}{2}$	0	0	0	8
XLV	0	$-\frac{1}{2}$	0	+1	$-\frac{1}{2}$	0	0	0	5
XLVI	0	0	0	$+\frac{1}{2}$	0	0	$-\frac{1}{2}$	0	5

because charge correlation effects favor XLV and XLVI over XLIV, and formal charge distribution favors XLVI. The double quartet structure XLVI suggests the F_2NONNF_2 may be somewhat stable because the net change on going from $N_2F_4 + NO$ to F_2NONNF_2 would be a decrease from seven to five close pairs of electrons with no change in the bond order.

$F(O_2)_n NO$ and $FO(O_2)_n NO$

This section is concerned with the double quartet representation of two families of compounds, $F(O_2)_n NO$ and $FO(O_2)_n NO$, postulated by Spratley and Pimentel⁷⁴ (see Introduction). Only the first two members ($n = 0, 1$) of each family are considered due to the increasing complexity of the larger molecules.

The first member ($n = 0$) of the family $F(O_2)_n NO$ is nitrosyl fluoride, ONF, which has already been discussed in an earlier section. Six possible structures for the $n = 1$ member of $F(O_2)_n NO$, which is a structural isomer of fluorine nitrate, are shown in XLVII-LII. Structures



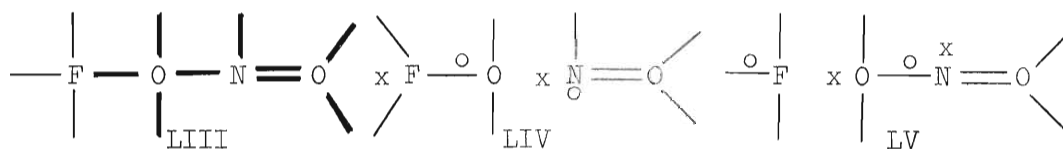
XLVII, IL and L are eliminated because of their unsatisfactory charge distributions and high charge correlation (see Table 32). Structures XLVIII and LI are of minor importance at most due to the +1 or -1 formal charges on one or more O atoms. The remaining structure, LII, not only has zero close pairs but also has excellent charge distribution. However, LII suffers from the slight disadvantage that the sets of electrons of opposite spin favor different arrangements, i.e. linear and bent. How

Table 32. Formal Charges In FO_2NO

	F	O	O	N	O	No. of Close Pairs
XLVII	0	0	+1	0	-1	9
XLVIII	0	$+\frac{1}{2}$	+1	$-\frac{1}{2}$	-1	2
IL	$-\frac{1}{2}$	$+\frac{1}{2}$	+1	$-\frac{1}{2}$	$-\frac{1}{2}$	5
L	$-\frac{1}{2}$	0	$+\frac{1}{2}$	0	0	6
LI	$-\frac{1}{2}$	+1	0	$-\frac{1}{2}$	0	0
LII	$-\frac{1}{2}$	0	0	0	$+\frac{1}{2}$	0

adversely this would affect the stability of FO_2NO is difficult to say, but it seems that LII would be at least as stable as the two structures proposed for NO_3F , XXII and XXIV. Structure LII, furthermore, is consistent with Spratley and Pimentel's postulation that FO_2NO would have very weak F-O and $\text{FO}_2\text{-NO}$ bonds and strong O-O and $\text{FO}_2\text{N-O}$ bonds.

The first member ($n = 0$) in the $\text{FO}(\text{O}_2)_n\text{NO}$ family is a structural isomer of nitryl fluoride, FNO_2 . Three possible structures for the FONO molecule are shown in LIII-LV. Structure LII is eliminated due to



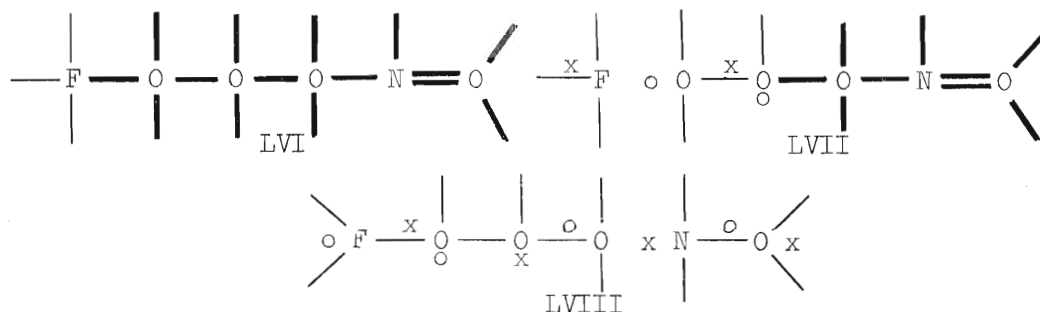
very high inter-electron repulsion, whereas LIV is unlikely due to the $+\frac{1}{2}$ formal charge on the F atom (see Table 33). The remaining structure, LV, is the most likely since it has no close pairs and an excellent

Table 33. Formal Charges In FONO

	F	O	N	O	No. of Close Pairs
LIII	0	0	0	0	9
LIV	$+\frac{1}{2}$	0	$-\frac{1}{2}$	0	0
LV	$-\frac{1}{2}$	0	$+\frac{1}{2}$	0	0

charge distribution. However, it does suffer slightly from having one set of electrons (o's) favor a linear arrangement whereas the other set (x's) favor a bent arrangement. Once again, this fact makes the stability of the FONO molecule somewhat doubtful. Spratley and Pimentel's model predicts a fairly strong F-O bond and weak FO-NO bond. This would correspond to LIV which was ruled out due to its unfavorable charge distribution. The most probable double quartet structure (LV), on the other hand, predicts a weak F-O bond and fairly strong FO-NO bond.

Three of the more probable structures for the second member ($n = 1$) of the $\text{FO}(\text{O}_2)_n\text{NO}$ family are shown in LVI-LVIII. Both LVI and LVII would

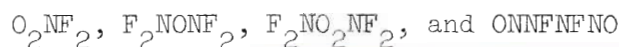


be extremely unstable due to the high charge correlation (see Table 34). Structure LVIII has no close pairs, but it is eliminated due to

Table 34. Formal Charges In FOO_2NO

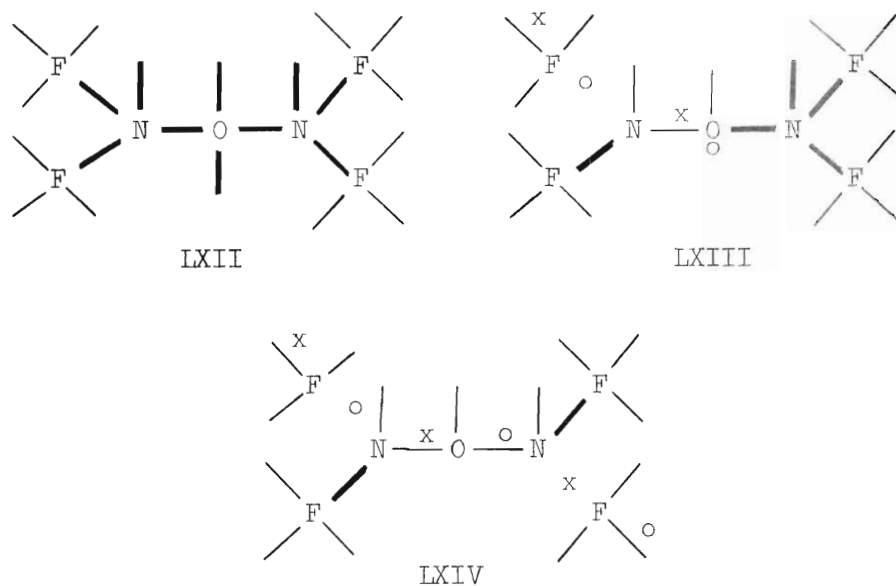
	F	O	O	O	N	O	No. of Close Pairs
LVI	0	0	0	0	0	0	15
LVII	$-\frac{1}{2}$	0	$+\frac{1}{2}$	0	0	0	9
LVIII	$+\frac{1}{2}$	$+\frac{1}{2}$	$+\frac{1}{2}$	0	-1	$-\frac{1}{2}$	0

a most unfavorable charge distribution ($+\frac{1}{2}$ on F and -1 on N; $+\frac{1}{2}$ charges on three adjacent atoms; and -1 and $-\frac{1}{2}$ charges on two adjacent atoms). Furthermore, it is impossible to construct a double quartet structure for FOO_2NO which would correspond to the model proposed by Spratley and Pimentel (see Table IV). In fact, this is true for all the members of the $\text{FO}(\text{O}_2)_n\text{NO}$ family, because a strong F-O bond (three or more electrons) would require a prohibitive positive formal charge on the fluorine atom.



This section is concerned with the doublet quartet representation of possible products occurring from the reaction of NF_2 radicals (from N_2F_4) with O , O_2 , or O_3 . These compounds include O_2NF_2 , F_2NONF_2 , $\text{F}_2\text{NO}_2\text{NF}_2$, and the unstable intermediate postulated by Martinez et al.,⁵⁸ ONNFNFNO (see Introduction). Some of these compounds are quite complex and would require a large number of possible Linnett structures. However, only the more representative structures are shown here.

Three possibilities for the O_2NF_2 molecule are shown below in LIX-LXI. Structures LX and LXI are eliminated due to the +1 charge on an O atom in each. This leaves LIX, which has four close pairs of electrons

Table 36. Formal Charges In F_2NONF_2

	F	F	N	O	N	F	F	No. of Close Pairs
LXII	0	0	0	0	0	0	0	10
LXIII	0	$-\frac{1}{2}$	0	$+\frac{1}{2}$	0	0	0	5
LXIV	0	$-\frac{1}{2}$	0	+1	0	0	$-\frac{1}{2}$	2

is eliminated due to the +1 formal charge on the O atom. This leaves LXIII, which has an excellent charge distribution, but a fairly high number of close pairs (five). Based upon LXIII it is expected that F_2NONF_2 would be slightly unstable with respect to FNO and NF_3 , since the net change from one F_2NONF_2 molecule to one FNO and one NF_3 is a decrease in number of close pairs (five to four) whereas the bond order remains constant at six.

Three possible structures for the $\text{F}_2\text{NO}_2\text{NF}_2$ molecule are shown below in LXV-LXVII. The two structures LXV and LXVI are unlikely due

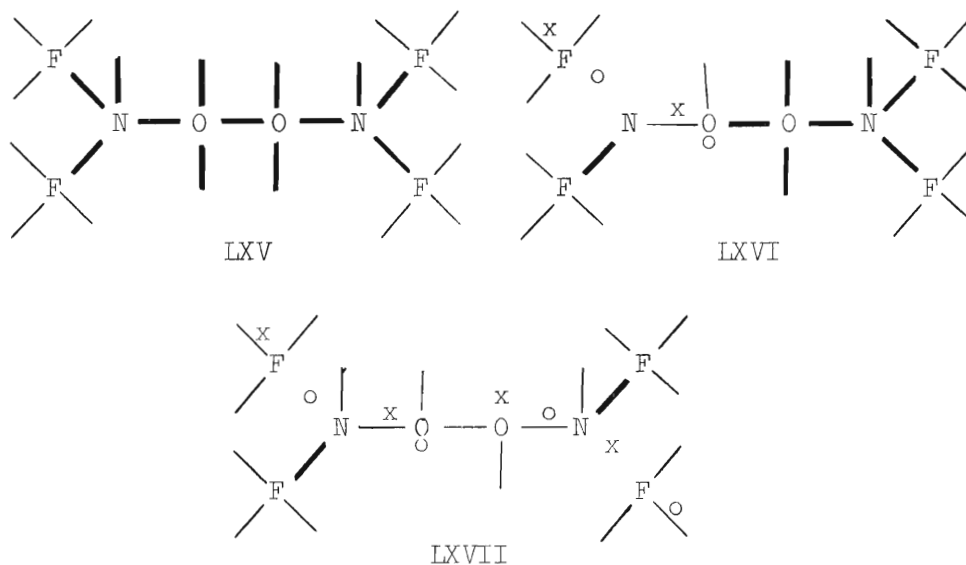


Table 37. Formal Charges In $\text{F}_2\text{NO}_2\text{NF}_2$

	F	F	N	O	O	N	F	F	No. of Close Pairs
LXV	0	0	0	0	0	0	0	0	13
LXVI	0	$-\frac{1}{2}$	0	$+\frac{1}{2}$	0	0	0	0	8
LXVII	0	$-\frac{1}{2}$	0	$+\frac{1}{2}$	$+\frac{1}{2}$	0	0	$-\frac{1}{2}$	2

to the high number of close pairs (see Table 37). Structure LXVII has only two close pairs, but it suffers somewhat from having a $+\frac{1}{2}$ formal charge on adjacent O atoms. By comparing LXVII with XXXVI, it seems that $\text{F}_2\text{NO}_2\text{NF}_2$ would decompose to two ONF_2 radicals because the net change in bond order and number of close pairs would be zero while the breaking of

the O-O bond would eliminate the disadvantage of having positive charges on adjacent O atoms.

Two possible structures for the ONNFNFNO molecule are shown below in LXVIII and LXIX. Structure LXVIII is eliminated due to a prohibitive

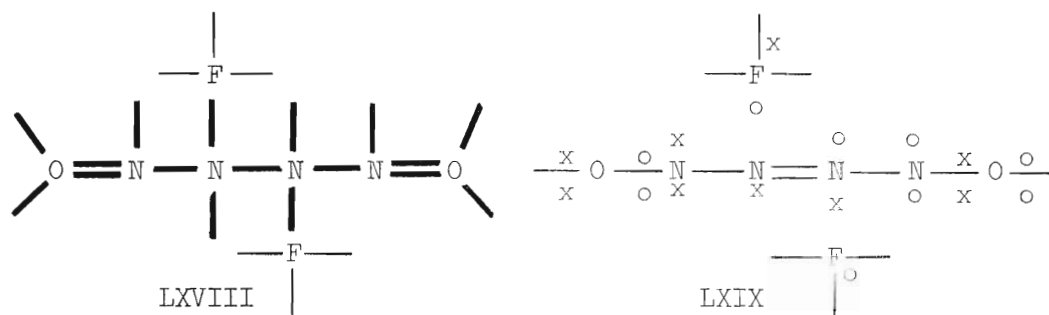


Table 38. Formal Charges In ONNFNFNO

	O	N	N	F	N	F	N	O	No. of Close Pairs
LXVIII	0	0	0	0	0	0	0	0	17
LXIX	0	0	$+\frac{1}{2}$	$-\frac{1}{2}$	$+\frac{1}{2}$	$-\frac{1}{2}$	0	0	0

number of close pairs (seventeen). Structure LXIX has no close pairs and only the slight disadvantage of having $+\frac{1}{2}$ formal charges on two adjacent N atoms. Furthermore, LXIX contains very weak one-electron N-F bonds and single ON-N bonds. Thus, it would appear to support the postulation of Martinez and coworkers⁵⁸ that the intermediate which decomposes to F, N₂, and NO in the ratio of 2:1:2 might be ONNFNFNO. However, the double quartet approach predicts that this intermediate might be stable with respect to F₂ + N₂ + 2 NO since decomposition of ONNFNFNO would result in an increase in the number of close pairs from zero to one whereas the bond order remains constant at nine.

F_2NOF , $FN(OF)_2$ and $N(OF)_3$

Substitution of an OF radical for one or more fluorine atoms in nitrogen trifluoride would result in the presently unknown compounds F_2NOF , $FN(OF)_2$, and $N(OF)_3$. Three possible structures for the F_2NOF molecule, which is a structural isomer of trifluoramine oxide, ONF_3 , are shown below in LXX-LXXII. Structure LXX is unlikely due to the seven

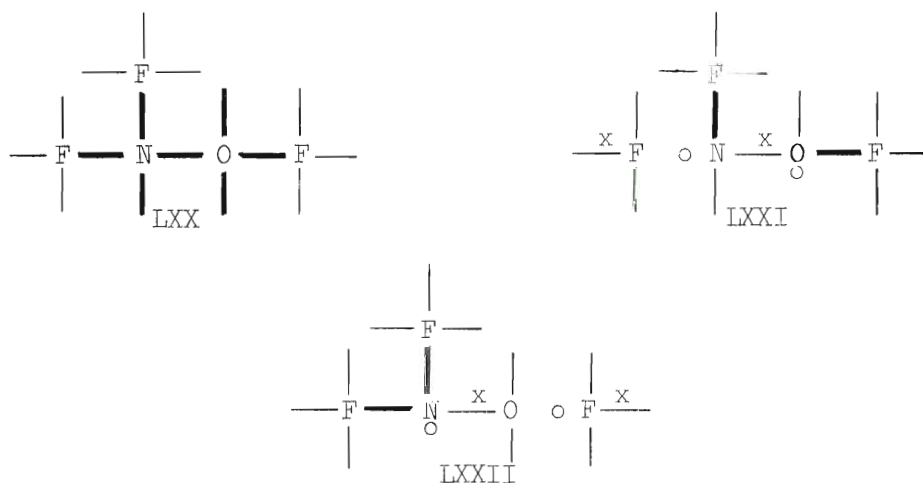


Table 39. Formal Charges In F_2NOF

	F	F	N	O	F	No. of Close Pairs
LXX	0	0	0	0	0	7
LXXI	$-\frac{1}{2}$	0	0	$+\frac{1}{2}$	0	2
LXXII	0	0	$+\frac{1}{2}$	0	$-\frac{1}{2}$	2

close pairs of electrons. Structures LXXI and LXXII both have favorable charge distributions and only two close pairs, but LXXII has the slight disadvantage of having the $+\frac{1}{2}$ formal charge on the N rather than the O

atom. Structure LXXI predicts that the F_2NOF molecule should be slightly unstable with respect to F_2 and ONF since decomposition of F_2NOF would result in a decrease in the number of close pairs from two to one whereas the bond order would remain constant at four.

Four possible structures for $FN(OF)_2$ are shown below in LXXIII-LXXVI. All four structures have permissible formal charge distributions.

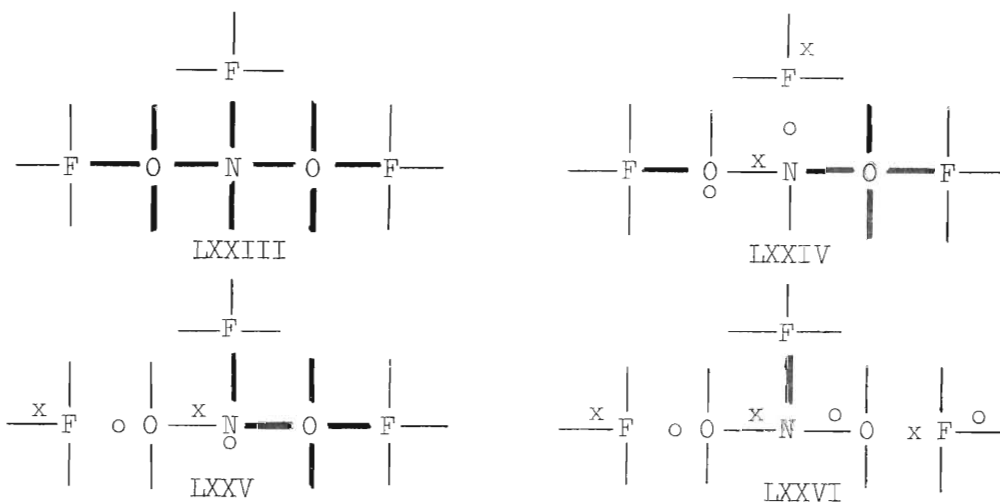


Table 40. Formal Charges In $FN(OF)_2$

	F	O	N	F	O	F	No. of Close Pairs
LXXIII	0	0	0	0	0	0	10
LXXIV	0	$+\frac{1}{2}$	0	$-\frac{1}{2}$	0	0	5
LXXV	$-\frac{1}{2}$	0	$+\frac{1}{2}$	0	0	0	5
LXXVI	$-\frac{1}{2}$	0	+1	0	0	$-\frac{1}{2}$	1

However, inter-electron repulsion strongly favors LXXVI over the other three (see Table 40). It is difficult to say whether LXXVI would actually

be stable since the two one-electron O-F bonds suggest that $\text{FN}(\text{OF})_2$ might readily dissociate to form FNO_2 and F_2 with no net change in the bond order or number of close pairs.

Three possible structures for $\text{N}(\text{OF})_3$ are shown below in LXXVII-LXXIX. Once again, all three structures have permissible charge distributions, but charge correlation effects favor XXIX. Thus, $\text{N}(\text{OF})_3$

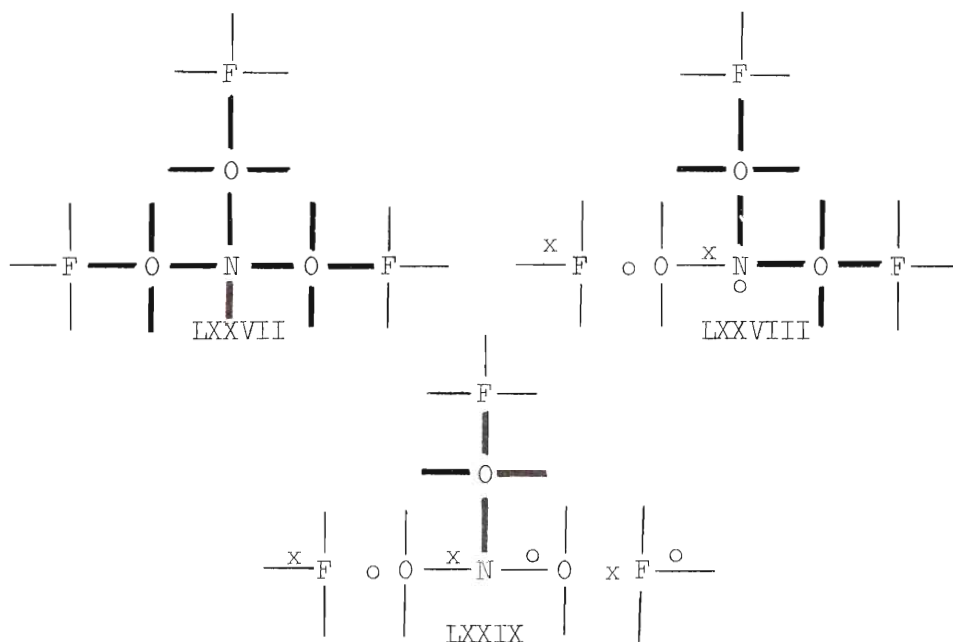
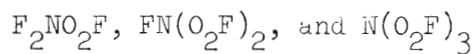


Table 41. Formal Charges In $\text{N}(\text{OF})_3$

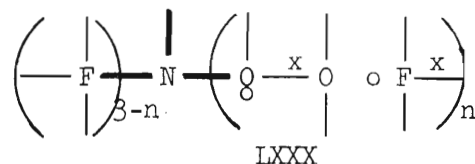
	F	O	N	O	F	O	F	No. of Close Pairs
LXXVII	0	0	0	0	0	0	0	13
LXXVIII	$-\frac{1}{2}$	0	$+\frac{1}{2}$	0	0	0	0	8
LXXIX	$-\frac{1}{2}$	0	+1	0	0	0	$-\frac{1}{2}$	4

also has two weak one-electron O-F bonds, which indicates that it may decompose to NO_3F and F_2 even though the bond order and number of close pairs would remain constant.

From the above double quartet discussion, it appears that the three molecules F_2NOF , $\text{FN}(\text{OF})_2$, and $\text{N}(\text{OF})_3$ would be of marginal stability. All three would be susceptible to decomposition by losing two F atoms each to form ONF , NO_2F , and NO_3F , respectively.



Substitution of an O_2F radical for one or more F atoms in NF_3 would result in the molecules $\text{F}_2\text{NO}_2\text{F}$, $\text{FN}(\text{O}_2\text{F})_2$, and $\text{N}(\text{O}_2\text{F})_3$. The electronic structure of a substituted O_2F group was discussed by this author with respect to the FO_2NO molecule (XLVII-LII) and also by Linnett¹¹⁴ in regard to O_2F_2 . From these discussions it appears that the only reasonable structures for the family of compounds $\text{F}_{3-n}\text{N}(\text{O}_2\text{F})_n$, where $n = 1, 2, 3$, would have a zero formal charge on the N atom and a net formal charge of zero on the three substituted groups. (This conclusion is not evident from this discussion alone, but it can be arrived at by considering the numerous combinations of possible electronic structures for the O_2F grouping in $\text{F}_{3-n}\text{N}(\text{O}_2\text{F})_n$.) The most probable structure for this family of compounds is shown below in LXXX, which is analogous



to structure XLIX for FO_2NO . For $n = 0$ LXXX reduces to the correct

structure for NF_3 . The number of close pairs in this family of compounds will always be four, and the formal charges (from left to right in LXXX) on F, N, O, O, and F will be 0, 0, $+\frac{1}{2}$, 0, and $-\frac{1}{2}$. Due to the high number of close pairs of electrons, it is probable that this entire family of compounds would be unstable since decomposition could be easily initiated by cleavage of the weak one-electron O-F bond.



This section is concerned with the discussion of the compounds NF_5 and F_3NNF_3 which have been suggested by Miller et al.⁷⁵ (see Introduction).

The well known compound PF_5 (P being in the same group of the Periodic Table as N) has a structure in which the central P atom is surrounded by a trigonal bipyramid of five F atoms. This expansion of the double quartet, in this case to a double sextet in N, is possible in elements of the third period and higher due to the availability of d orbitals to allow for sp^3d or sp^3d^2 hybridization. However, this is not possible for nitrogen since it has no 2d orbitals.

It is impossible to construct any plausible structures for NF_5 or F_3NNF_3 using the Linnett model in which the bonding is considered to be covalent. However, an ionic structure $(\text{NF}_4)^+\text{F}^-$ can be postulated for NF_5 in which the cation consists of four F atoms (zero formal charge on each) at the four corners of a tetrahedron in which is enclosed a nitrogen atom having a +1 formal charge.

Summary and Conclusions

The preceding discussion has shown that Linnett's Double Quartet Model can adequately describe the electronic structures of the known compounds ONF , NO_2F , NO_3F , ONNF_2 , and ONF_3 , the ONF_2 radical, and the ONF^- and ONF_2^+ ions. This model also predicts a stable structure for O_2NNF_2 , a new compound claimed to have been isolated and identified in this work. The Double Quartet Model was also used to propose the most likely structures of a wide variety of postulated N-O-F species and to draw approximate conclusions regarding their likely existence (see Table 42). The compounds F_2NONNF_2 (proposed to be the unidentified red-brown substance described in the text), FO_2NO and FONO (proposed by Spratley and Pimentel⁷⁴), ONNFNFNO (an intermediate postulated by Martinez et al.⁵⁸), and $\text{F}_{3-n}\text{N}(\text{OF})_n$ ($n = 1, 2, 3$) were shown to have marginal stabilities, which suggests the possible isolation of these species in the future.

It should be emphasized that the Double Quartet Model is highly empirical in nature. However, the principles behind this model, i.e. the fundamental properties of electrons, are easy to understand and apply. Some of the larger molecules presented herein have been treated rather superficially since a complete description would require an inordinate number of structures.

Certainly the Double Quartet Model works well in describing the existing N-O-F species. Only time will tell how accurate are the predictions of the stabilities of the postulated N-O-F compounds. It is quite obvious, however, that this method is far superior to the traditional valence bond method using Lewis structures.

Table 42. Summary of Predicted Existences of Postulated N-O-F Species Based Upon Linnett's Double Quartet Model

Molecule	Most Likely Structure(s)	Predicted Existence
$(\text{ONNF})_2$	XLI & XLII	unlikely
F_2NONNF_2	XLVI	marginal
FO_2NO	LII	marginal
FONO	LV	marginal
FO_3NO	LVIII	unlikely
O_2NF_2	LIX	unlikely
F_2NONF_2	LXIII	unlikely
$\text{F}_2\text{NO}_2\text{NF}_2$	LXVII	unlikely
ONNFNFNO	LXIX	marginal
F_2NOF	LXXII	marginal
$\text{FN}(\text{OF})_2$	LXXVI	marginal
$\text{N}(\text{OF})_3$	LXXVIII	marginal
$\text{F}_2\text{NO}_2\text{F}$	LXXX	unlikely
$\text{FN}(\text{O}_2\text{F})_2$	LXXX	unlikely
$\text{N}(\text{O}_2\text{F})_3$	LXXX	unlikely
NF_5	no covalent structure plausible	
F_3NNF_3	no covalent structure plausible	

APPENDIX C

SELECTED IONIZATION EFFICIENCY DATA AND APPEARANCE

POTENTIAL DETERMINATIONS BY EVD

In this appendix are presented the ionization efficiency curves for several selected ions of N-O-F compounds and their appearance potential determinations by the extrapolated voltage difference (EVD) method. The appearance potentials are given the qualitative ratings of excellent, good, fair, or poor depending upon the nature of the IE curve and quality of the EVD fit. In all cases Ar was used as the calibrating gas.

Figures 7 and 8 show the IE curves for NO_2F^+ from NO_2F and NO_2^+ from O_2NNF_2 , respectively. Figure 9 shows the determination of $A(\text{NO}_2\text{F}^+)$ and $A(\text{NO}_2^+)$ from the IE curves in Figures 7 and 8, respectively, using the EVD method. Both of these AP's are rated excellent since their IE curves had very little noise and their EVD data fell in a straight line.

Figures 10 and 11 show the IE curves for ONF_2^+ from ONF_3 and NO^+ from ONNF_2 , respectively. Figure 12 shows the resulting EVD determination of the appearance potentials of these two ions. The data on $A(\text{ONF}_2^+)$ is rated as excellent. However, $A(\text{NO}^+)$ is rated only as good since the EVD data drift away from a straight line as the intensity approaches zero.

Figure 13 shows the IE curve for NF^+ from ONNF_2 . This is a typical example of a high intensity ion peak in which more than one ion-source process is occurring. Figure 14 shows the EVD data for the AP determination of the higher energy process for NF^+ , i.e. $A_2(\text{NF}^+)$. Even though the IE curve for NF^+ had very little noise and the resulting EVD curve

for the higher energy process gave a straight line, the data on $A_2(\text{NF}^+)$ is rated only as good due to the method of subtracting the contribution of the lower energy process in the IE curve of NF^+ .

Figure 15 shows the IE data for O^+ from NO_2F . This curve has a relatively high noise/signal ratio, which is typical of a low intensity ion (<10%) which has more than one ion-source process occurring. Figure 16 shows the EVD determinations of $A_1(\text{O}^+)$ and $A_2(\text{O}^+)$ from the IE data of Figure 15. $A_1(\text{O}^+)$ is rated as poor due to the high noise/signal ratio in the IE curve and the poor EVD fit. $A_2(\text{O}^+)$ is rated as fair since the EVD data fall approximately along a straight line even though the IE curve has a high noise/signal ratio.

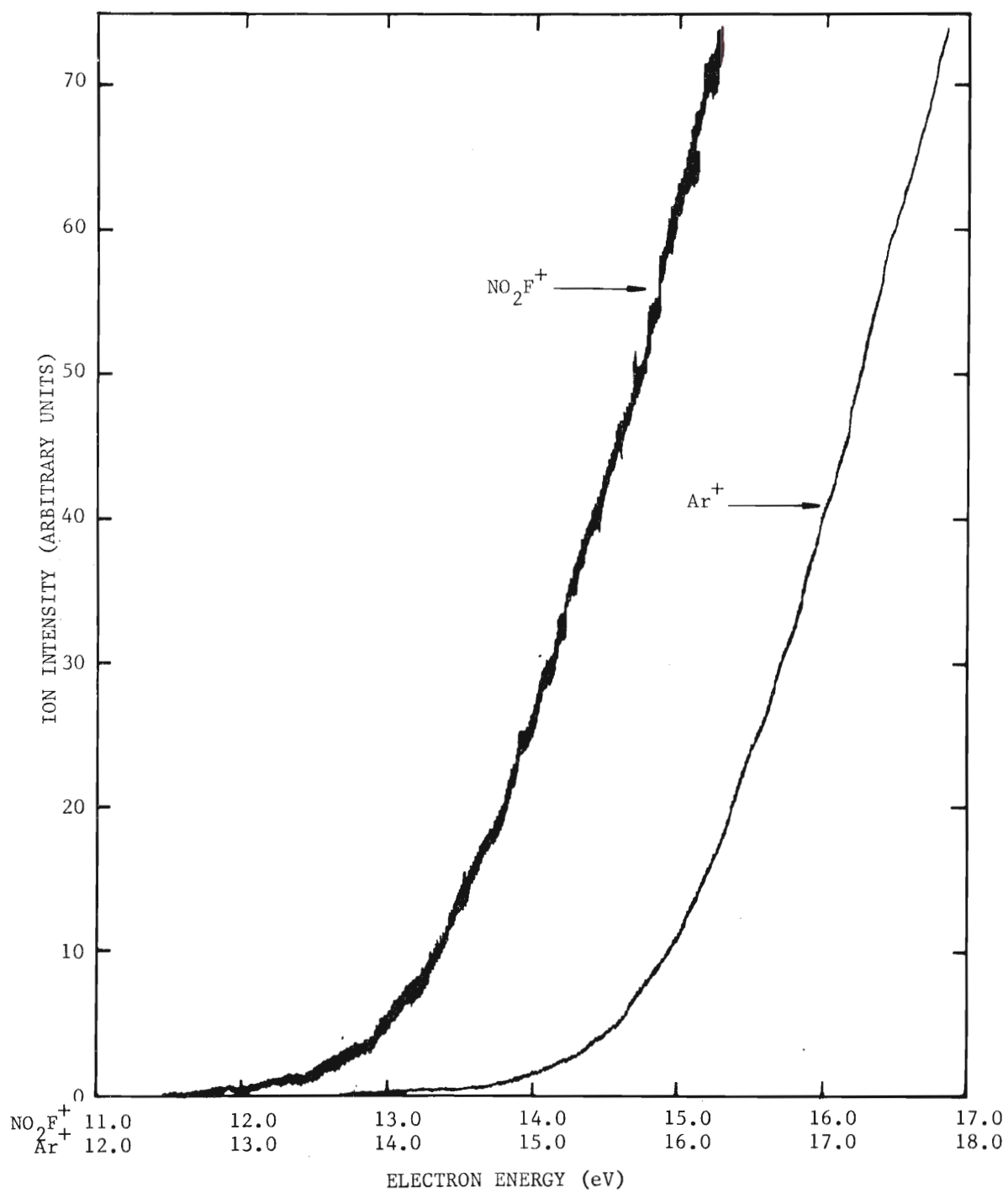


Figure 7. Ionization Efficiency Data
For NO_2F^+ From NO_2F With Argon As Standard

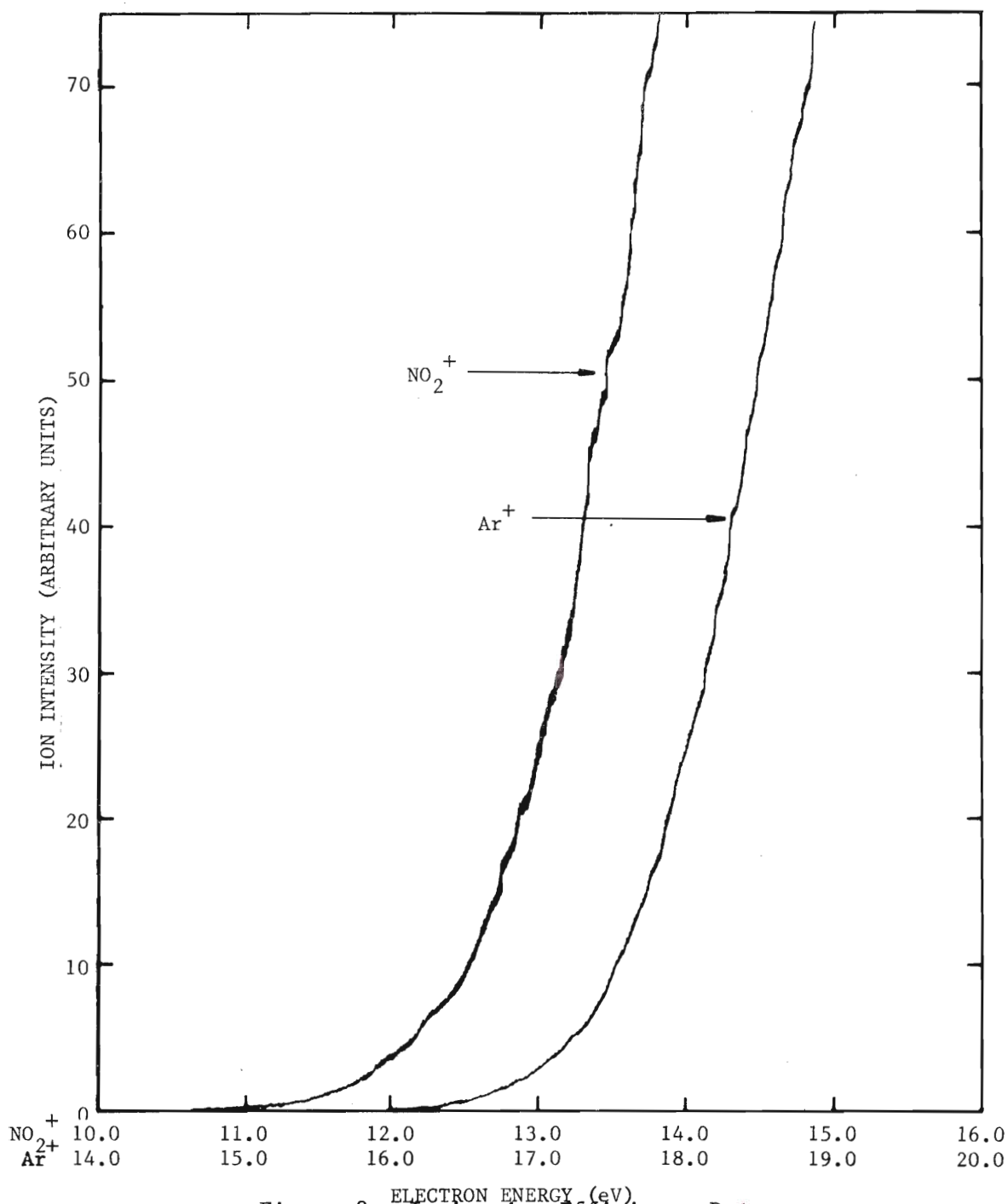


Figure 8. Ionization Efficiency Data
For NO₂⁺ From O₂NNF₂ With Argon As Standard

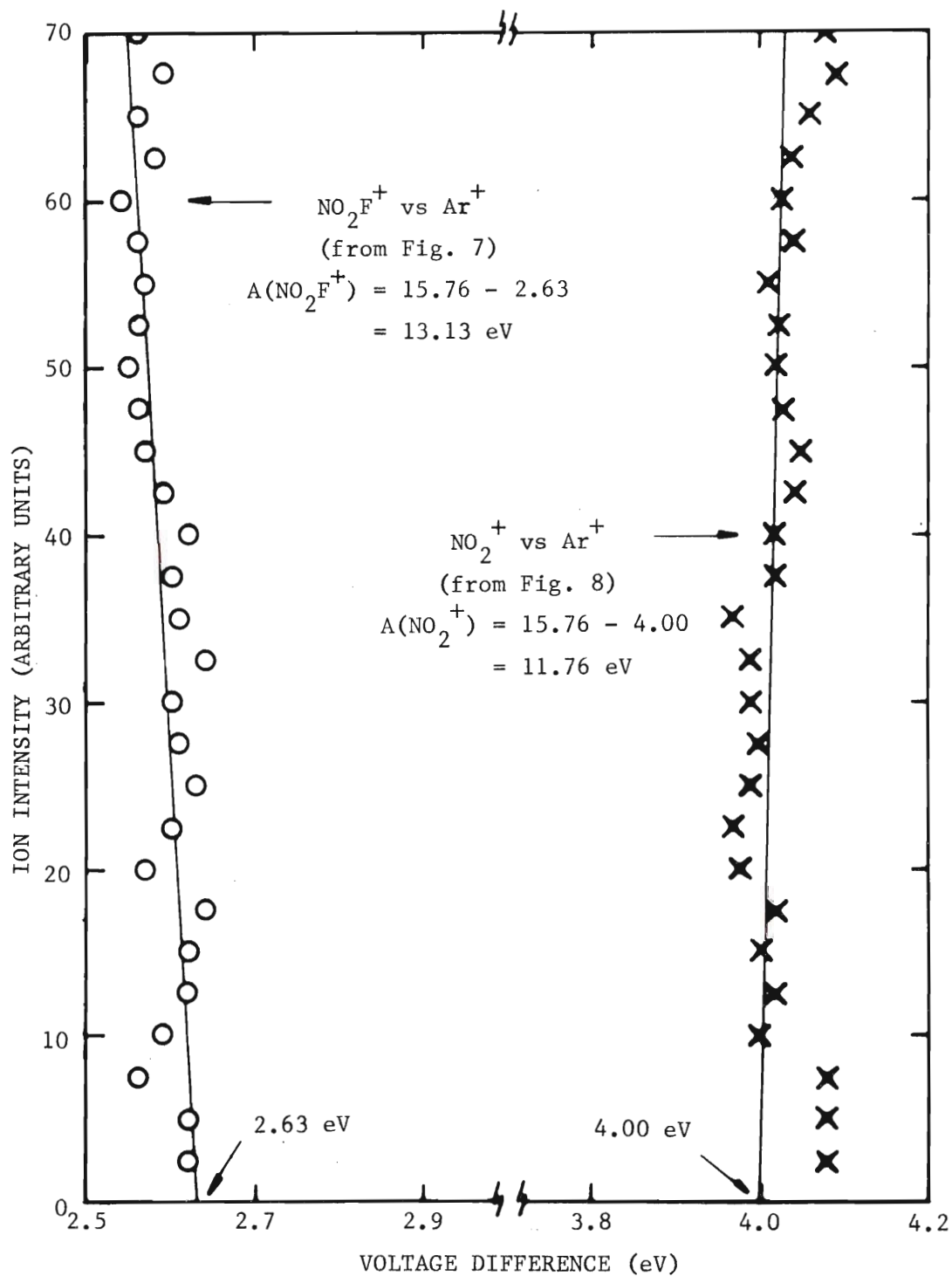


Figure 9. Appearance Potential Determination
Of NO_2F^+ From NO_2F And NO_2^+ From O_2NNF_2 By EVD

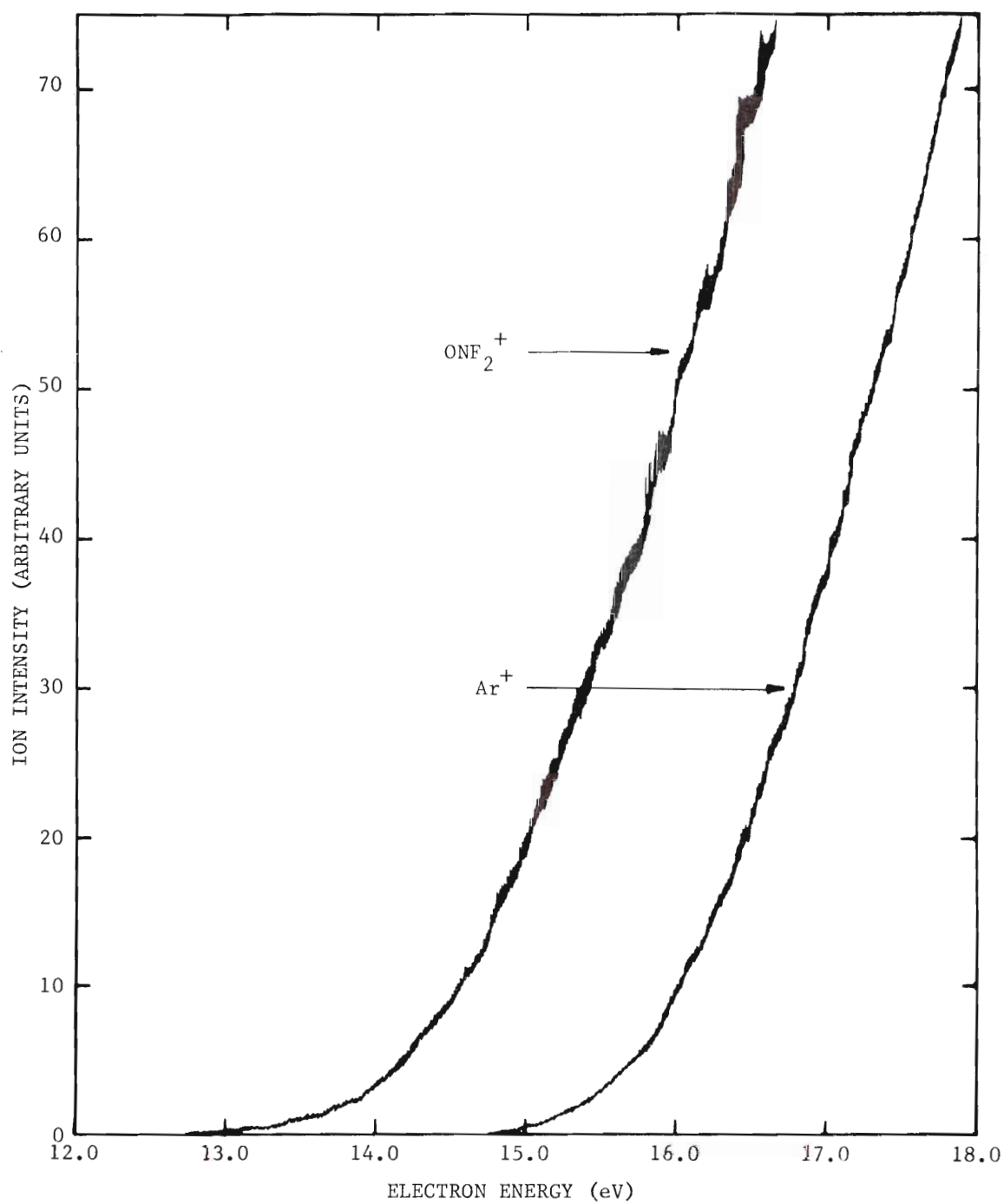


Figure 10. Ionization Efficiency Data
For ONF_2^+ From ONF_3 With Argon As Standard

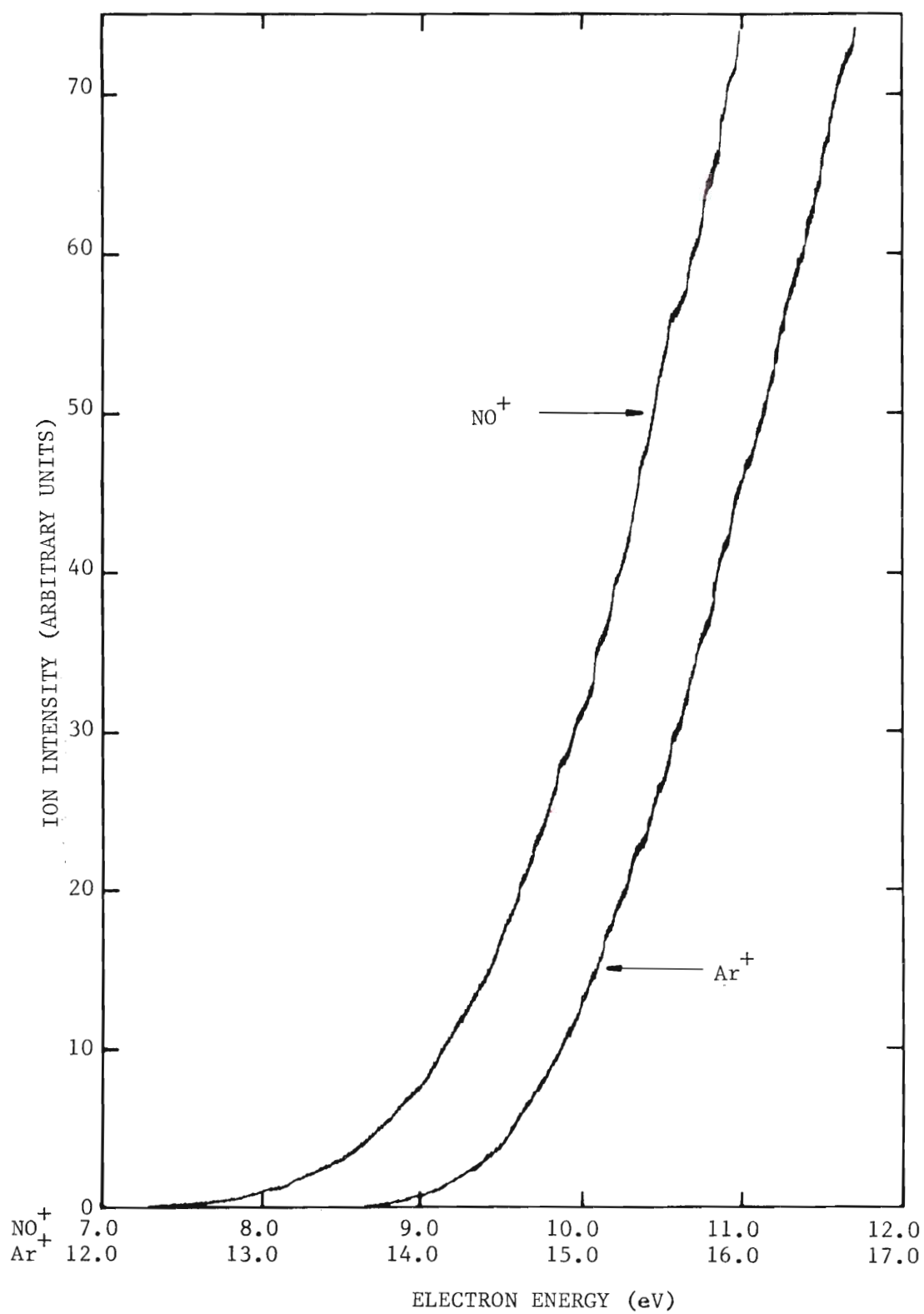


Figure 11. Ionization Efficiency Data
For NO^+ From ONNF_2 With Argon As Standard

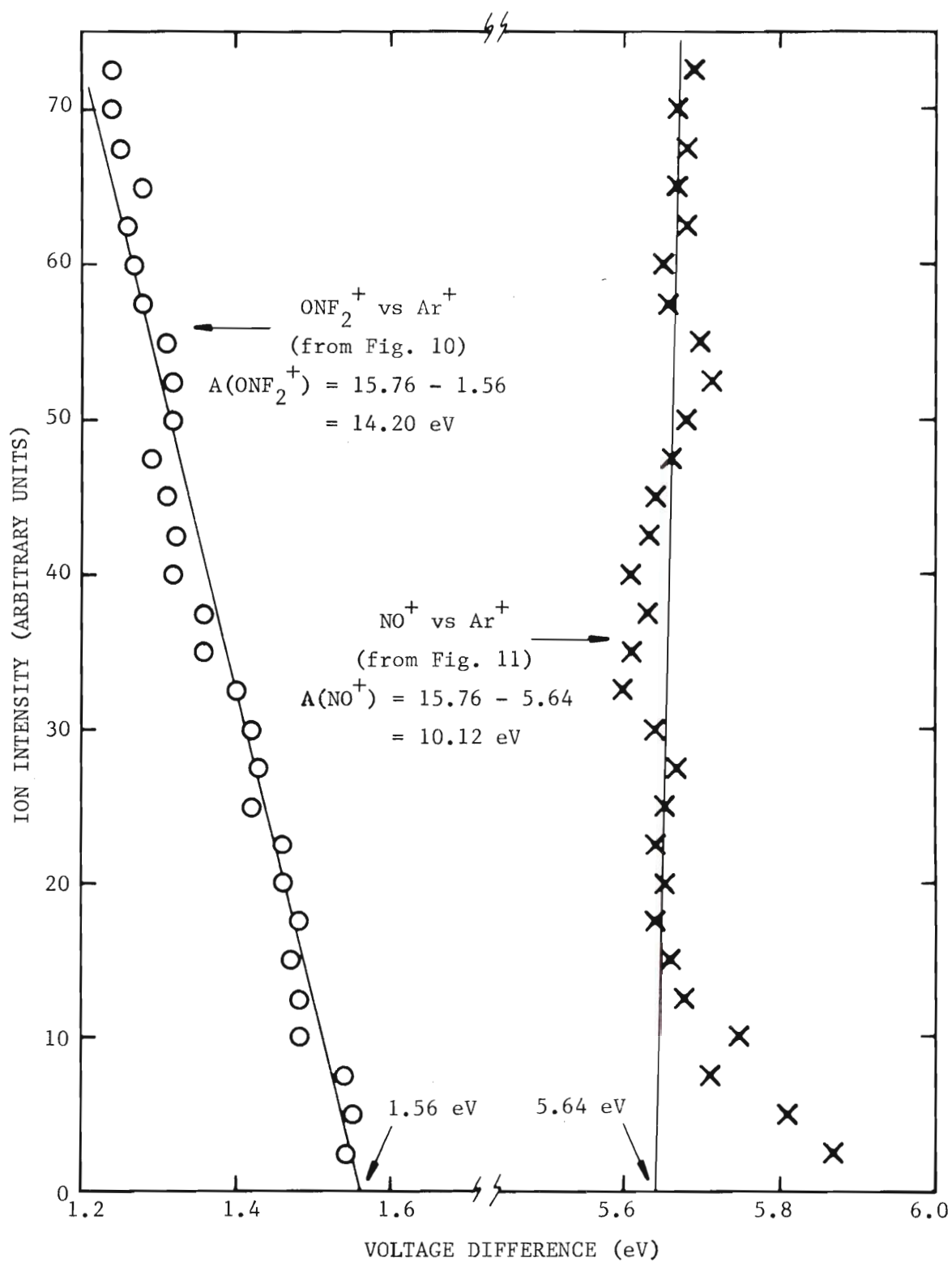


Figure 12. Appearance Potential Determination Of
ONF₂⁺ From ONF₃ And NO⁺ From ONNF₂ By EVD

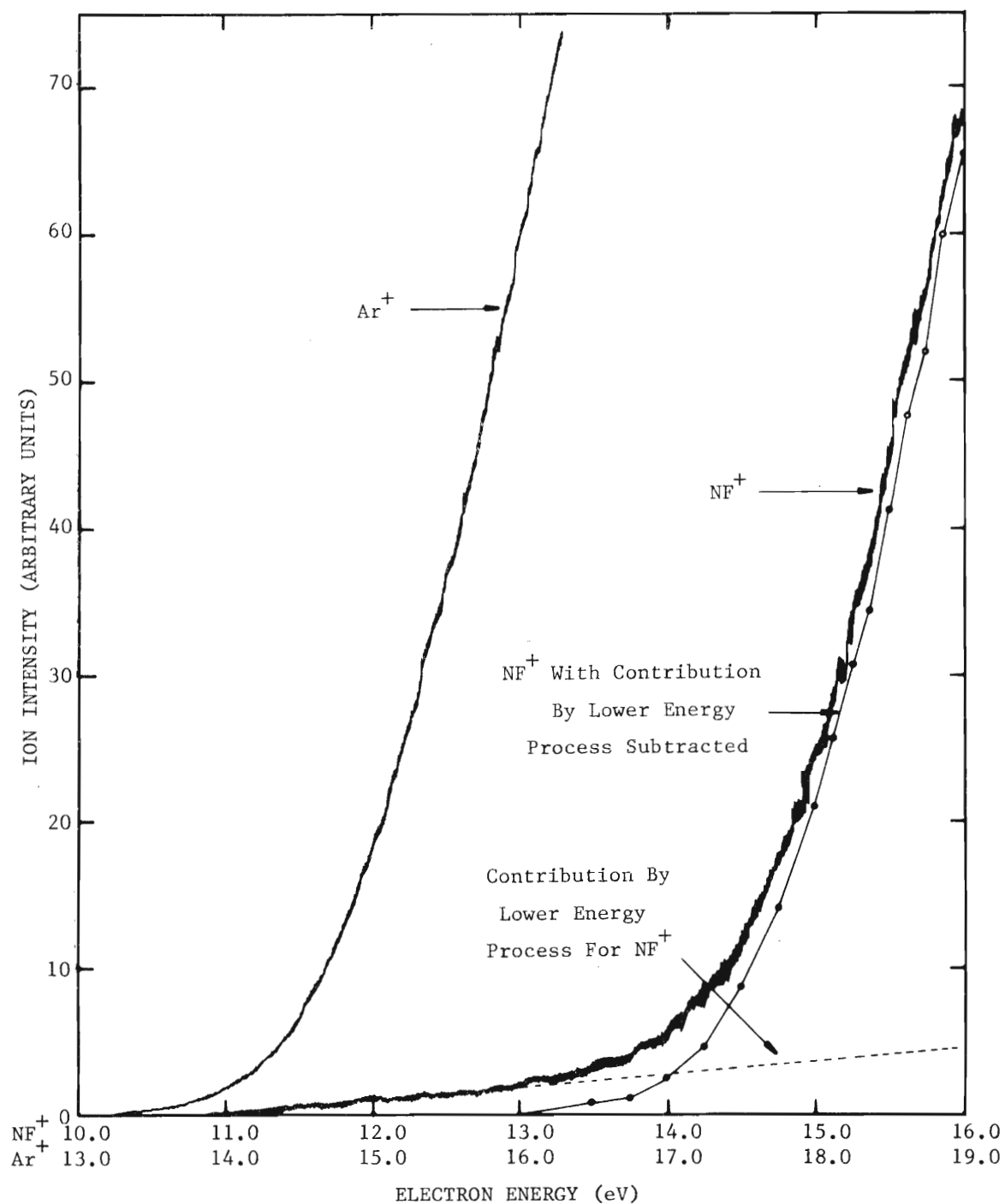


Figure 13. Ionization Efficiency Data
For NF⁺ From ONNF₂ With Argon As Standard

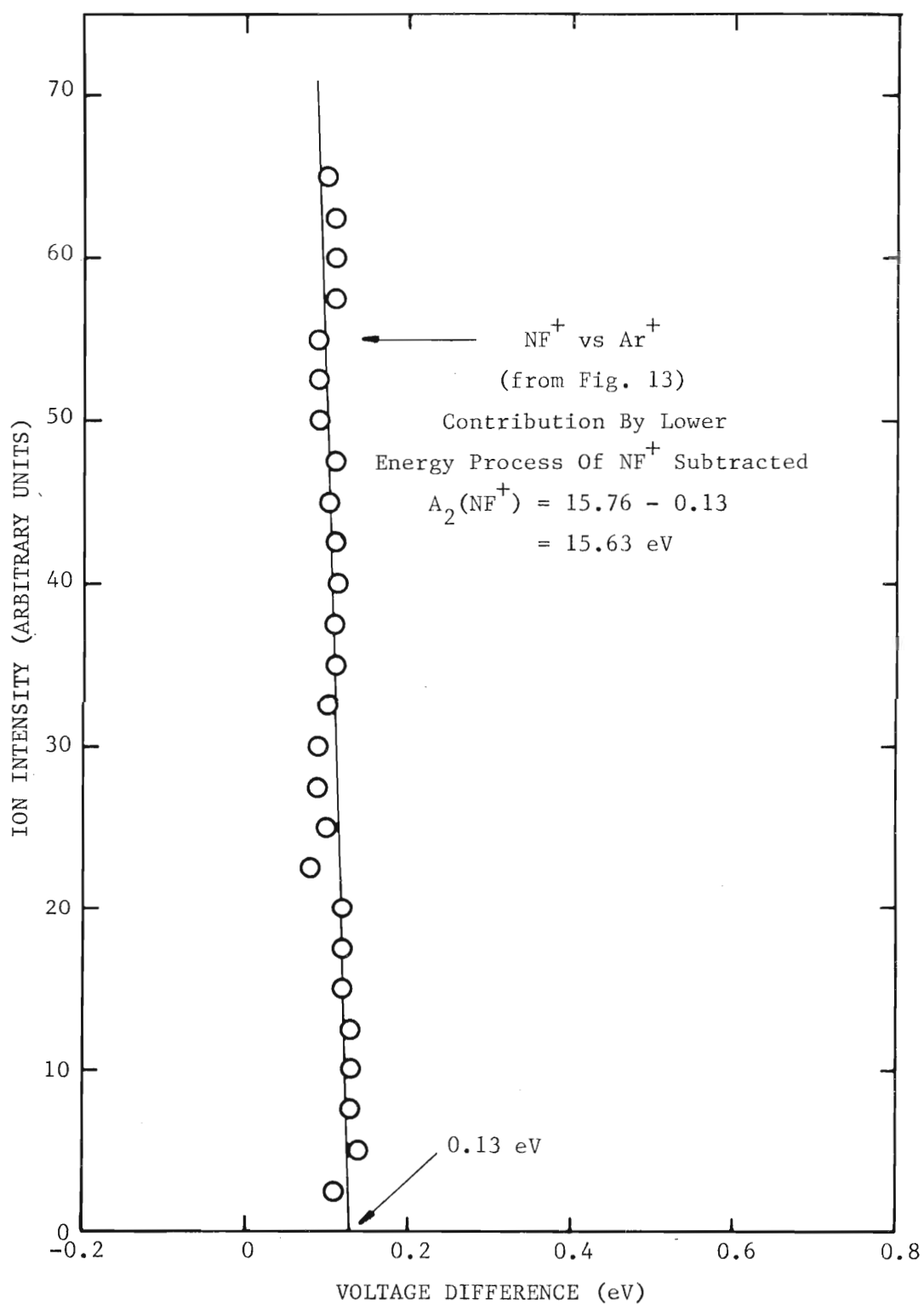


Figure 14. Appearance Potential Determination
 Of NF^+ From ONNF_2 By EVD

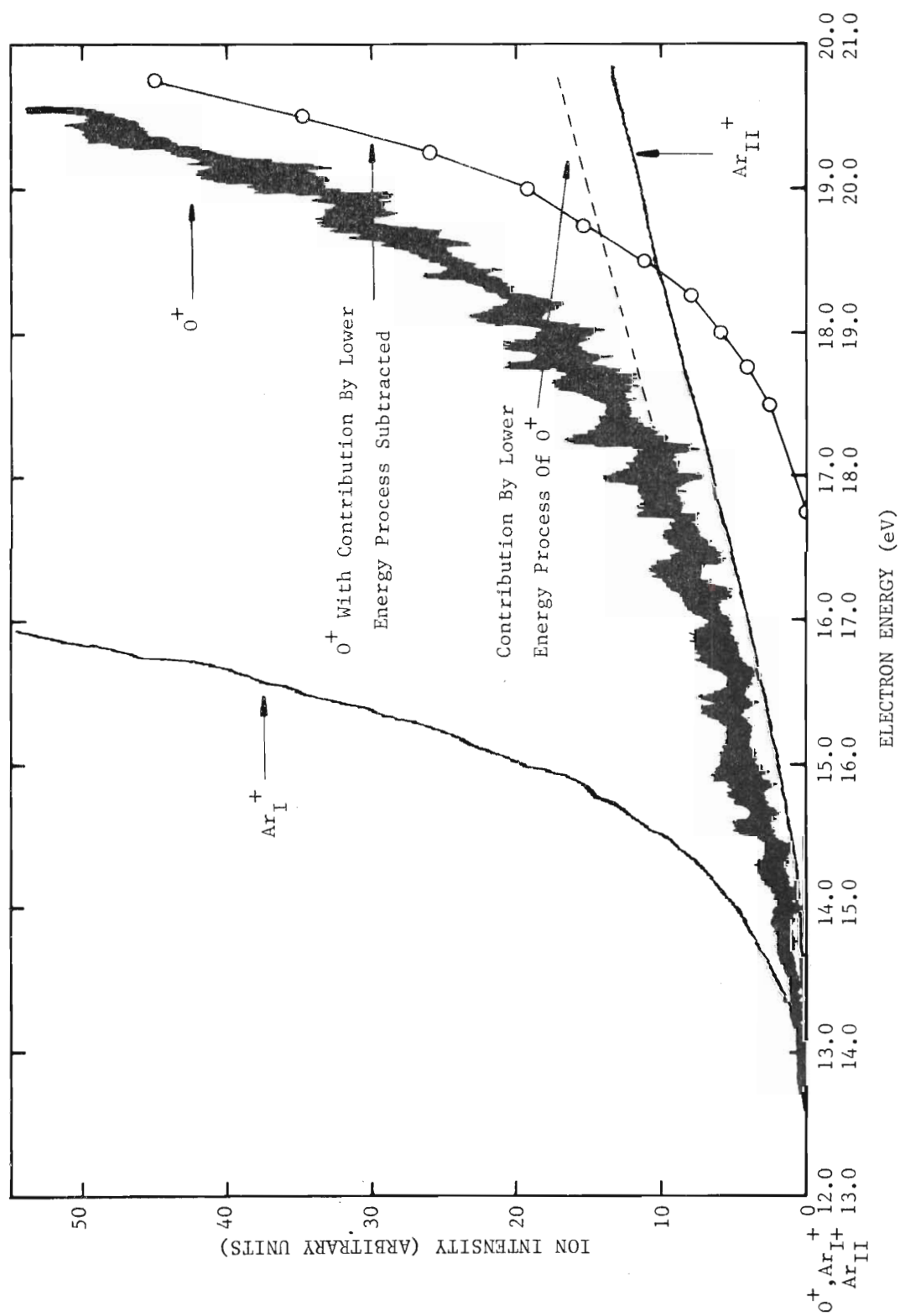


Figure 15. Ionization Efficiency Data For O^+ From NO_2F With Argon As Standard

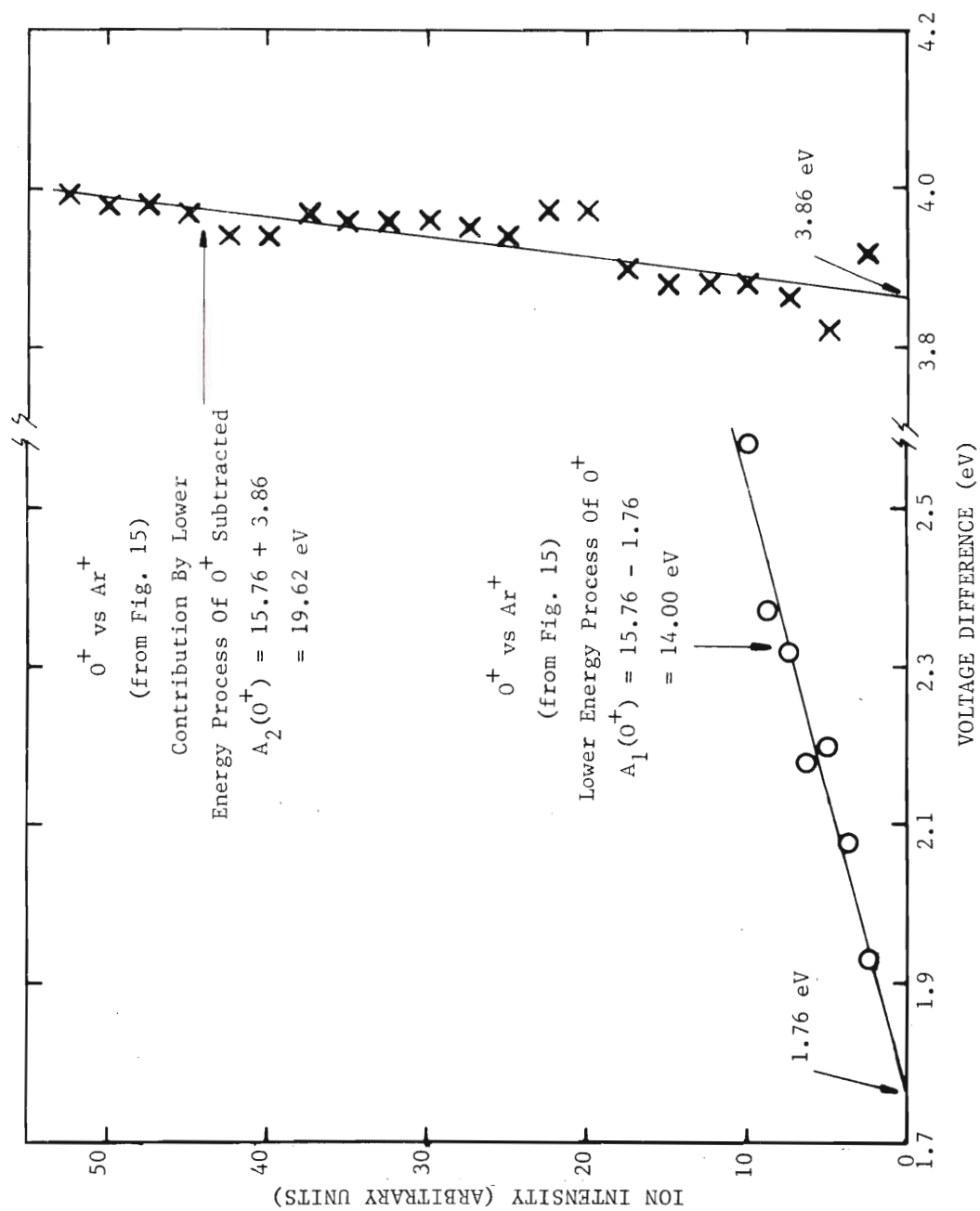


Figure 16. Appearance Potential Determination of O^+ From NO_2F By EVD

APPENDIX D

MISCELLANEOUS DATA

In the appendix are presented relative vapor pressure data and mass spectra of compounds observed in the N-O-F experiments. Table 43 lists the temperatures corresponding to vapor pressures of one torr for most of the compounds observed in the N-O-F experiments. The compounds in the table are arranged in order of decreasing volatility. Tables 44-47 show the positive ion mass spectra of NO, NO₂, N₂O, N₂F₂, NF₃, N₂F₄, OF₂, O₂F₂, SiF₄, NH₃, SF₆, and CF₃Cl. These spectra were observed in this thesis research except for N₂O (Colburn et al.¹³⁰), N₂F₂ (Selected Mass Spectral Data¹³¹), and SiF₄ (Malone⁷⁹).

Table 43. Temperature Corresponding to Vapor Pressures of One Torr
For Compounds Observed in N-O-F Experiments

Compound	Temp. at Vap. Press. of 1 Torr ($^{\circ}\text{C}$)	Reference
N_2	-226	118
F_2	-223	118
O_2	-219	118
Ar	-218	118
OF_2	-196	132
CF_4	-185	118
NO	-185	118
NF_3	-184	9
O_3	-180	118
N_2F_2 -trans	-174	9
N_2F_2 -cis	-169	9
C_2F_6	-168	133
N_2F_4	-164	9
O_3F_2	-162	134
ONF_3	-157	66
SiF_4	-144	118
NO_2F	-144	13
N_2O	-143	118
ONNF_2	-141	This work
O_2F_2	-140	135

Table 43. Temperature Corresponding to Vapor Pressures of One Torr For Compounds Observed in N-O-F Experiments (Continued)

Compound	Temp. at Vap. Press. of 1 Torr ($^{\circ}\text{C}$)	Reference
SF_6	-133	118
NO_3F	-133	43
ONF	-132	13
O_2NNF_2	-118	This work
Cl_2	-118	118
NH_3	-109	118
N_2O_3	-106	107 ^a
SO_2	-96	118
HF	-95	132
NO_2 (N_2O_4)	-56	118
H_2O	-17	118

^a Solid composition assumed to be $\text{NO}_{1.525}$; resulting vapor composition is $\text{NO}_{1.03}$.

Table 44. Positive Ion Mass Spectra of NO, NO₂, N₂O, and N₂F₂

^a NO			^a NO ₂		
m/e	Ion	Rel. Inten.	m/e	Ion	Rel. Inten.
14	N ⁺	9.6	14	N ⁺	7.8
16	O ⁺	3.4	16	O ⁺	20.2
30	NO ⁺	100.0	30	NO ⁺	100.0
			46	NO ₂ ⁺	27.2

^b N ₂ O			^c N ₂ F ₂			
m/e	Ion	Rel. Inten.	m/e	Ion	Rel. Inten.	
					trans.	cis.
14	N ⁺	12.9	14	N ⁺	11.6	10.5
16	O ⁺	5.0	19	F ⁺	1.8	5.3
28	N ₂ ⁺	10.8	23.5	N ₂ F ⁺⁺	-	1.4
30	NO ⁺	31.1	28	N ₂ ⁺	100.0	84.5
31	NO ⁺ (i)	0.1	33	NF ⁺	5.0	6.0
44	N ₂ O	100.0	47	N ₂ F ⁺	43.4	100.0
45	N ₂ O(i)	0.7	66	N ₂ F ₂ ⁺	25.3	0.5

^a This Work^b Data by Colburn et al.¹³⁰^c From Selected Mass Spectral Data¹³¹

(i) isotopic species

Table 45. Positive Ion Mass Spectra of NF_3 , N_2F_4 , OF_2 , and O_2F_2

NF_3^a			N_2F_4^a		
m/e	Ion	Rel. Inten.	m/e	Ion	Rel. Inten.
14	N^+	5.2	14	N^+	8.6
19	F^+	6.7	19	F^+	4.1
33	NF^+	36.2	28	N_2^+	18.4
52	NF_2^+	100.0	33	NF^+	46.0
71	NF_3^+	27.2	47	N_2F^+	16.9
			52	NF_2^+	100.0
			66	N_2F_2^+	9.2
			85	N_2F_3^+	12.8
			104	N_2F_4^+	2.9
OF_2^a			$\text{O}_2\text{F}_2^{a,b}$		
m/e	Ion	Rel. Inten.	m/e	Ion	Rel. Inten.
16	O^+	29.4	16	O^+	14.2
19	F^+	8.3	19	F^+	5.4
35	OF^+	100.0	32	O_2^+	100.0
54	OF_2^+	65.3	35	OF^+	1.5
			38	F_2^+	0.8
			48	O_3^+	0.4
			51	O_2F^+	18.0

^aThis work^bData taken at -140°C

Table 46. Positive Ion Mass Spectra of SiF_4 and NH_3

m/e	Ion	SiF_4^a	m/e	Ion	NH_3^b
		Rel. Inten.			Rel. Inten.
19	F^+	?	14	N^+	1.8
28	Si^+	?	15	NH^+	6.8
29	$\text{Si}^+(\text{i})$	0.6	16	NH_2^+	81.5
47	SiF^+	9.0	17	NH_3^+	100.0
48	$\text{SiF}^+(\text{i})$	0.6			
49	$\text{SiF}^+(\text{i})$	0.4			
66	SiF_2^+	1.6			
85	SiF_3^+	100.0			
86	$\text{SiF}_3^+(\text{i})$	1.5			
104	SiF_4^+	2.7			
105	$\text{SiF}_4^+(\text{i})$	1.1			

^aData by Malone⁷⁹^bThis work

(i) isotopic species

Table 47. Positive Ion Mass Spectra of SF_6 and CF_3Cl

SF_6^a			CF_3Cl^a		
m/e	Ion	Rel. Inten.	m/e	Ion	Rel. Inten.
19	F^+	2.8	12	C^+	2.2
32	S^+	2.6	19	F^+	2.2
34	$\text{S}^+(\text{i})$	-	31	CF^+	12.2
51	SF^+	12.3	35	Cl^+	16.0
53	$\text{SF}^+(\text{i})$	0.5	37	$\text{Cl}^+(\text{i})$	5.0
70	SF_2^+	12.1	42.5	$\text{CF}_2\text{Cl}^{++}$	1.0
72	$\text{SF}_2^+(\text{i})$	0.4	43.5	$\text{CF}_2\text{Cl}^{++}(\text{i})$	0.6
89	SF_3^+	39.6	47	CCl^+	2.1
91	$\text{SF}_3^+(\text{i})$	1.7	49	$\text{CCl}^+(\text{i})$	0.6
108	SF_4^+	10.7	50	CF_2^+	18.3
110	$\text{SF}_4^+(\text{i})$	0.2	66	CFCl^+	0.4
127	SF_5^+	100.0	68	$\text{CFCl}^+(\text{i})$	-
129	$\text{SF}_5^+(\text{i})$	5.0	69	CF_3^+	100.0
			85	CF_2Cl^+	23.0
			87	$\text{CF}_2\text{Cl}^+(\text{i})$	7.1
			104	CF_3Cl^+	0.7
			106	$\text{CF}_3\text{Cl}^+(\text{i})$	0.2

^aThis Work

(i) isotopic species

NOMENCLATURE

The following symbols and abbreviations are so defined unless specified otherwise in the text.

\AA	= angstrom
ac	= alternating current
adiab.	= adiabatic
AP	= appearance potential
atm	= atmosphere
$A(X^+)$	= appearance potential of X^+ , eV
$A_i(X^+)$	= appearance potential of X^+ corresponding to the i th lowest threshold energy process in the ionization efficiency curve of X^+ , eV
c	= constant in equation
calc.	= calculated
cc	= cubic centimeter
cm	= centimeter
contd.	= continued
D	= bond dissociation energy, kcal./mole or eV
dc	= direct current
$D(X-Y)$	= bond dissociation energy of X-Y, kcal./mole or eV
e	= electron
E	= internal energy, kcal./mole
E^*	= total excess energy, kcal./mole
EA	= electron affinity, eV

epr	= electron paramagnetic resonance analysis
Eq.	= equation
\bar{e}_t	= excess translational energy of fragments from collision with electron, kcal./mole
eV	= electron volt, 1 eV = 23.06 kcal./mole
EVD	= extrapolated voltage difference method
exptl.	= experimental
h	= Planck's constant, 6.624×10^{-27} erg seconds
ΔH_f	= heat of formation, kcal./mole
$\Delta H_f^{\circ T}(X)$	= standard heat of formation of X at temperature T, reactants and products in ideal gas state, kcal./mole
ΔH_r	= heat of reaction, kcal./mole
I.D.	= inside diameter, inches
IE	= ionization efficiency
in.	= inch
IP	= ionization potential
ir	= infrared analysis
I_{sp}	= specific impulse, pounds-force per pound mass per second or seconds
$I(X)$	= ionization potential of X, eV
kcal.	= kilocalorie
LI	= linear intercept method
M	= molecular weight
mamp	= milliampere
m/e	= mass-to-charge ratio
min.	= minute
ml	= milliliter
mm	= millimeter

mmole	= millimole
N	= number of classical oscillators in a molecule
nmr	= nuclear magnetic resonance analysis
O.D.	= outside diameter, inches
psia	= pounds per square inch absolute
psig	= pounds per square inch gage
PV	= pressure times volume
ref.	= reference
Rel. Abund.	= relative abundance, %
RPD	= retarding potential difference method
S.C.F.M.	= standard cubic feet per minute
T	= temperature, °C or °K
temp.	= temperature, °C or °K
TOF	= time-of-flight
vac.	= vacuum
vap. press.	= vapor pressure
vert.	= vertical
α	= arbitrary parameter
Δ	= the temperature at which the vapor pressure is known to be one torr minus the median of the temperature range of the observed vapor pressure of 0.1-0.2 torr, °C
π^*	= antibonding π orbital
μ	= micron of Hg pressure
ν	= frequency

BIBLIOGRAPHY*

1. R. L. Wilkens, Theoretical Evaluation of Chemical Propellants, Prentice-Hall, Inc. (1963)
2. B. Siegel and L. Schieler, Energetics of Propellant Chemistry, John Wiley & Sons, Inc. (1964)
3. S. F. Sarnier, Propellant Chemistry, Reinhold Publishing Corp. (1966)
4. R. T. Holzmann, Adv. Chem. Ser. 54, 1 (1966)
5. M. W. Windsor, "Trapped Radicals in Propulsion" in Formation and Trapping of Free Radicals, A. M. Bass and H. P. Broida, eds., Academic Press (1960)
6. N. Bowman, J. Space Flight 2, 1 (1950)
7. J. F. Gall, Amer. Rocket Soc. J. 29, 95 (1959)
8. E. W. Lawless and I. C. Smith, Inorganic High-Energy Oxidizers, Marcel Dekker, Inc. (1968)
9. C. J. Hoffman and R. G. Neville, Chem. Revs. 62, 1 (1962)
10. C. Woolf, Adv. Fluorine Chem. 5, 1 (1965)
11. R. Schmutzler, Angew. Chem. Int. Ed. Engl. 7, 440 (1968)
12. O. Ruff and K. Stauber, Z. anorg. allg. Chem. 47, 190 (1905)
13. O. Ruff, W. Menzel and W. Neumann, Z. anorg. allg. Chem. 208, 293 (1932)
14. C. T. Ratcliffe and J. M. Shreeve, Chem. Commun. 19, 674 (1966)
15. E. A. Jones and P. Woltz, J. Chem. Phys. 18, 1516 (1950)
16. D. W. Magnuson, Phys. Rev. 83, 485 (1951)
17. P. Woltz, E. A. Jones and A. H. Nielsen, J. Chem. Phys. 20, 378 (1952)

*Abbreviations in this Bibliography follow the form used by Chemical Abstracts (1965).

18. D. W. Magnuson, J. Chem. Phys. 20, 380 (1952)
19. L. H. Jones, L. B. Asprey, and R. R. Ryan, J. Chem. Phys. 47, 3371 (1967)
20. D. W. Magnuson, J. Chem. Phys. 19, 1071 (1951)
21. K. S. Buckton, A. C. Legon and D. J. Millen, Trans. Faraday Soc. 65, 1975 (1969)
22. H. S. Johnston and H. T. Bertin, Jr., J. Am. Chem. Soc. 81, 6402 (1959)
23. C. V. Stephenson and E. A. Jones, J. Chem. Phys. 20, 135 (1950)
24. R. P. Nielsen, C. D. Wagner, V. A. Campanile, J. N. Wilson, Adv. Chem. Ser. 54, 168 (1966)
25. O. Ruff, Z. angew. Chem. 42, 807 (1929)
26. E. E. Aynsley, G. Hetherington and P. L. Robinson, J. Chem. Soc. 1954, 1119
27. R. A. Davis and D. A. Rausch, Inorg. Chem. 2, 1300 (1963)
28. R. A. Ogg and J. D. Ray, J. Chem. Phys. 25, 797 (1956)
29. D. F. Smith and D. W. Magnuson, Phys. Rev. 87, 226 (1952)
30. A. C. Legon and D. J. Millen, J. Chem. Soc. A 1968, 1736
31. T. Tanaka and Y. Morino, J. Mol. Spectrosc. 32, 430 (1969)
32. R. E. Dodd, J. A. Rolfe and L. A. Woodward, Trans. Faraday Soc. 52, 146 (1956)
33. D. L. Bernitt, R. H. Miller and I. C. Hisatsune, Spectrochim. Acta 23A, 237 (1967)
34. L. Clayton, Q. Williams and T. L. Weatherly, J. Chem. Phys. 30, 1328 (1959)
35. M. G. Pillai, Z. Physik. Chem. 218, 334 (1961)
36. P. G. Puranik and E. V. Rao, Indian J. Phys. 35, 177 (1961)
37. E. Tschuikow-Roux, J. Phys. Chem. 66, 1636 (1962)
38. G. Hetherington and P. L. Robinson, "Spec. Pub. #10," Chem. Soc., London, 23 (1957)

39. R. Anderson and R. O. MacLaren, United Technology Corp., Quarterly Technical Summary Report No. 4, UTC-2002-QT4, Contract No. Nonr. 3433(00), February 28, 1962
40. J. D. Breazeale and R. O. MacLaren, United Technology Corp, Final Technical Summary Report, UTC-2002-FR, Contract No. Nonr. 3433(00), February 28, 1963
41. R. Anderson and R. O. MacLaren, United Technology Corp., Quarterly Technical Summary Report No. 2, UTC-2002-QT2, Contract No. Nonr. 3433(00), October 1961
42. G. H. Cady, J. Am. Chem. Soc. 56, 2635 (1934)
43. O. Ruff and W. Kwasnick, Angewandte Chemie 48, 238 (1935)
44. D. M. Yost and A. Beerbower, J. Am. Chem. Soc. 57, 782 (1935)
45. E. R. DeStaricco, J. E. Sicre, and H. J. Schumacher, Z. physik. Chem. N. F. 39, 337 (1963)
46. D. H. Hill and L. A. Bigelow, J. Am. Chem. Soc. 59, 2127, (1937)
47. L. Pauling and L. O. Brockway, J. Am. Chem. Soc. 59, 13 (1937)
48. W. B. Dixon and E. B. Wilson, Jr., J. Chem. Phys. 35, 191 (1961)
49. A. P. Cox and J. M. Riveros, J. Chem. Phys. 42, 3106 (1965)
50. R. H. Miller, D. Bernitt and I. C. Hisatsune, Spectrochim. Acta 23A, 223, (1967)
51. W. E. Skiens and G. H. Cady, J. Am. Chem. Soc. 80, 5640 (1958)
52. A. J. Arvia, L. F. R. Cafferata and H. J. Schumacher, Chem. Ber. 96, 1187 (1963)
53. O. G. Talakin, L. A. Akhanshchikova, E. N. Sosnovskii, A. V. Pankratov and A. N. Zercheninov, Russ. J. Phys. Chem. 36, 561 (1962)
54. "JANAF Thermodynamic Data," The Dow Chemical Co., Midland, Mich., 1965
55. C. B. Colburn and F. A. Johnson, Inorg. Chem. 1, 715 (1962)
56. F. A. Johnson, Adv. Chem. Ser. 36, 123 (1962)
57. F. A. Johnson and C. B. Colburn, Inorg. Chem. 2, 24 (1963)
58. F. Martinez, J. A. Mojtoicz and H. D. Smith, Air Force Office of Scientific Research Technical Report, AFOSR/DRA-61-7, Contract No. AF29(600)-2695, December 1961

59. E. C. Curtis, D. Pilipovich and H. W. Moberly, J. Chem. Phys. 46, 2905 (1967)
60. W. B. Fox, J. S. MacKenzie, N. Vanderkooi, B. Bukornich, C. A. Wamser, J. R. Holmes, R. E. Eibeck and B. B. Stewart, J. Am. Chem. Soc. 88, 2604 (1966)
61. W. B. Fox and J. S. MacKenzie, U. S. Pat. 3,323,866 (Allied Chem. Corp.) June 6, 1967
62. A. F. Maxwell and D. H. Kelly, U. S. Pat. 3,341,293 (Allied Chem. Corp.), September 12, 1967
63. N. Bartlett and S. P. Beaton, Chem. Commun. (6), 167 (1966)
64. N. Bartlett, S. P. Beaton and K. Jha, Chem. Commun. (6), 168 (1966)
65. N. Bartlett, J. Passmore and E. J. Wells, Chem. Commun. (7), 213 (1966)
66. W. B. Fox, J. S. MacKenzie, E. R. McCarthy, J. R. Holmes, R. F. Stahl and R. Juurik, Inorg. Chem. 7, 2064 (1968)
67. J. Mason and W. Van Bronswijk, J. Chem. Soc. D (7), 357 (1969)
68. S. Abramowitz and I. W. Levin, J. Chem. Phys. 51, 463 (1969)
69. W. H. Kirchhoff and D. R. Lide, J. Chem. Phys. 51, 467 (1969)
70. V. H. Dibeler and J. A. Walker, Inorg. Chem. 8, 1728 (1969)
71. R. Bougon, J. Chatelet, J. P. Desmonlin and P. Plurien, Compt. Rend. C266, 1761 (1968)
72. W. B. Fox, J. S. MacKenzie and R. K. Vitek, Brit. Pat. 1,054,330 (Allied Chem. Corp.), January 11, 1967
73. W. B. Fox, J. S. MacKenzie and R. K. Vitek, Brit. Pat. 1,066,679 (Allied Chem. Corp.), April 26, 1967
74. R. D. Spartley and G. C. Pimentel, J. Am. Chem. Soc. 88, 2394 (1966)
75. A. R. Miller, R. R. Tsukimura and R. Velten, Sci. 155, 688 (1967)
76. I. J. Solomon, A. J. Kacmarek and J. Raney, Inorg. Chem. 7, 1221 (1968)
77. I. J. Solomon, A. J. Kacmarek, J. N. Keith and J. Raney, J. Am. Chem. Soc. 90, 6557 (1968)

78. J. N. Keith, I. J. Solomon, I. Sheft and H. H. Hyman, Inorg. Chem. 7, 230 (1968)
79. T. J. Malone, "Mass Spectrometric Studies of the Synthesis, Reactivity, and Energetics of the Oxygen Fluorides at Cryogenic Temperatures," Ph.D. Thesis, Georgia Institute of Technology (1966)
80. J. K. Holzhauer and H. A. McGee, Jr., Analytical Chem. 41, 24A (1969)
81. D. B. Bivens, "Mass Spectrometric Study of the Products Obtained From Fast Cryogenic Quenching of Several Reactions Involving Atomic Hydrogen or Atomic Oxygen," Ph.D. Thesis, Georgia Institute of Technology (1966)
82. J. L. Franklin, J. G. Dillard, H. M. Rosenstock, J. T. Herron, K. Draxl and F. H. Field, "Ionization Potentials, Appearance Potentials, and Heats of Formation of Gaseous Positive Ions," NSRDS-NBS 26, June 1969
83. F. H. Field and J. L. Franklin, Electron Impact Phenomena and the Properties of Gaseous Ions, Academic Press, New York, 1957
84. M. Krauss and V. H. Dibeler, "Appearance Potential Data of Organic Molecules" in Mass Spectrometry of Organic Ions, F. W. McLafferty, ed., Academic Press, New York, 1963
85. C. A. McDowell, Mass Spectrometry, McGraw-Hill Book Co., Inc. New York, 1963
86. J. W. Warren, Nature 165, 810 (1950)
87. W. J. Martin, "Mass Spectrometric Studies and Cryogenic Reactivity of CF_2 and Cl_2 ," Ph.D. Thesis, Georgia Institute of Technology (1965)
88. G. Herzberg, Molecular Spectra and Molecular Structure, Vol. 3, D. Van Nostrand Co., Inc., Princeton, N. J., 1966
89. H. Hurzeler, M. G. Inghram and J. D. Morrison, J. Chem. Phys. 28, 76 (1958)
90. V. H. Dibeler and R. M. Reese, J. Res. NBS A68 (Phys. & Chem.) No. 4, 409 (1964)
91. P. Marmet and L. Kerwin, Can. J. Phys. 38, 787 (1960)
92. C. E. Brion, D. C. Frost and C. A. McDowell, J. Chem. Phys. 44, 1034 (1966)
93. R. E. Fox, W. M. Hickam, D. J. Grove and T. Kjeldaas, Rev. Sci. Instr. 26, 1101 (1955)

94. R. E. Fox, W. M. Hickam and T. Kjeldaas, Phys. Rev. 89, 555 (1953)
95. M. I. Al-Joboury and D. W. Turner, J. Chem. Soc. 4434 (1964)
96. I. N. Bakulina and N. I. Ionov, Zh. Eksperim i Teor. Fiz. 36, 1001 (1959)
97. R. W. Kiser, Introduction to Mass Spectrometry and Its Applications, Prentice-Hall, Inc., Englewood Cliffs, N. J., 1965
98. A. L. Wahrhaftig, "The Theory of Mass Spectra and the Interpretation of Ionization Efficiency Curves," in Application of Mass Spectrometry to Organic Chemistry, R. I. Reed, ed., Academic Press, New York, 1966
99. F. P. Lossing, A. W. Tickner and W. A. Bryce, J. Chem. Phys. 19, 1254 (1951)
100. J. D. Morrison, J. Chem. Phys. 21, 1767 (1953)
101. R. W. Kiser, and E. J. Gallegos, J. Phys. Chem. 66, 947 (1962)
102. D. P. Stevenson, Disc. Faraday Soc. 10, 35 (1951)
103. J. L. Franklin, P. M. Hierl and D. A. Whan, J. Chem. Phys. 47, 3148 (1967)
104. M. A. Haney and J. L. Franklin, J. Chem. Phys. 48, 4093 (1968)
105. R. J. Holt, "The Preparation of Some Highly Reactive, Three Membered Ring Organic Compounds as Cryochemical Reagents, and the Low Temperature Mass Spectrometric Study of Their Stability and Molecular Energetics," Ph.D. Thesis, Georgia Institute of Technology (1969)
106. A. G. Streng, Chem. Revs. 607 (1963)
107. I. R. Bente, Prog. Inorg. Chem. 5, 1 (1963)
108. J. T. Herron and H. I. Schiff, J. Chem. Phys. 24, 1266 (1956)
109. H. O. Prichard, Chem. Revs. 52, 529 (1953)
110. "JANAF Thermodynamic Data, 1st Addendum," The Dow Chemical Co., Midland, Mich., 1966
111. C. A. Wamser, W. B. Fox, B. Sukornick, J. R. Holmes, B. B. Stewart, R. Juurik, N. Vanderkooi, Jr., and D. Gould, Inorg. Chem. 8, 1249 (1969)
112. K. O. Christe and W. Maya, Inorg. Chem. 8, 1253 (1969)

- 113. J. W. Linnett, J. Am. Chem. Soc. 83, 2643 (1961)
- 114. J. W. Linnett, The Electronic Structure of Molecules, Spottiswoode Ballantyne & Co. Ltd., London & Colchester, 1964
- 115. V. H. Dibeler, R. M. Reese and J. L. Franklin, J. Chem. Phys. 27, 1296 (1957)
- 116. J. Troe, H. G. Wagner and G. Weden, Zeits. Physik. Chem. 56, 238 (1967)
- 117. P.A.G. O'Hare and A. C. Wahl, J. Chem. Phys. 53, 2469 (1970)
- 118. R. C. Weast, ed., Handbook of Chemistry and Physics, 49th Ed., The Chemical Rubber Co., 1968
- 119. V. H. Dibeler, J. A. Walker and K. E. McCulloh, J. Chem. Phys. 51, 4230 (1969)
- 120. L. C. Walker, J. Phys. Chem. 71, 361 (1967)
- 121. R. C. King and G. T. Armstrong, J. Res. Natl. Bur. Stds. U.S. 72A, 113 (1968)
- 122. A. D. Kirshenbaum, A. V. Grosse and J. G. Aston, J. Am. Chem. Soc. 81, 6398 (1959)
- 123. M. F. Ladd and W. H. Lee, J. Inorg. Nucl. Chem. 13, 218 (1960)
- 124. "JANAF Thermodynamic Data, 2nd Addendum," The Dow Chemical Co., Midland, Mich., 1967
- 125. J. Jortner and U. Sokolov, Nature 190, 1003 (1961)
- 126. A. L. Farragher, F. M. Page and R. C. Wheeler, Disc. Faraday Soc. No. 37, 203 (1964)
- 127. D. F. C. Morris, J. Inorg. Nucl. Chem. 6, 295 (1958)
- 128. P. Warneck, Chem. Phys. Lett. 3 (7), 532 (1969)
- 129. L. Pauling, The Nature of the Chemical Bond, Cornell Univ. Press, Ithaca, New York, 1960
- 130. C. B. Colburn, F. A. Johnson, A. Kennedy, K. McCallum, L. C. Metzger and C. O. Parker, J. Am. Chem. Soc. 81, 6397 (1959)
- 131. "Selected Mass Spectral Data," American Petroleum Institute Research Project No. 44
- 132. J. H. Perry, ed., Chemical Engineers' Handbook, 4th Ed., McGraw-Hill (1963)

- 133. O. Ruff and O. Bretschneider, Z. anorg. allgem. Chem. 210, 173 (1933)
- 134. A. D. Kirshenbaum and A. V. Grosse, J. Am. Chem. Soc. 81, 1277 (1959)
- 135. O. Ruff and W. Menzel, Z. anorg. allgem. Chem. 198, 375 (1931)

VITA

Paul Anthony Sessa was born in Stamford, Connecticut on January 24, 1945. He attended Stamford public elementary and junior high schools and Stamford Catholic High. Upon graduation from high school in 1962 he received the Thomas E. Saxe Scholarship Award. He entered the University of Notre Dame in the fall of 1962, and was awarded a Bachelor of Science in Chemical Engineering, Cum Laude, in June 1966. He received the Walsh-Hudson-Cavanaugh and U. S. Rubber Company Scholarships while at Notre Dame.

During the summer of 1965 he was employed by American Cyanamid Company in Stamford, Connecticut. He was employed by the Monsanto Company in Springfield, Massachusetts during the summer of 1966.

In September 1966 he enrolled at the Georgia Institute of Technology as a predoctoral student and was awarded a National Defense Education Act Title IV Fellowship for three years. He received a Master of Science Degree in Chemical Engineering in June 1968. He also received graduate fellowships from the Air Force Office of Scientific Research and the Union Carbide Corporation.

He is a member of Tau Beta Pi and the Society of Sigma Xi.

In 1966 he was married to the former Marie Martino of Providence, Rhode Island. They have one daughter, Jacqueline Marie. They plan to live in the Summit, New Jersey area where he will be employed by Celanese Research Company.